

WISCONSIN HIGHWAY RESEARCH PROGRAM #0092-05-08

**DETERMINATION OF SHEAR STRENGTH VALUES FOR GRANULAR
BACKFILL MATERIAL USED BY THE WISCONSIN DEPARTMENT OF
TRANSPORTATION**

A REVISED DRAFT REPORT

Principal Investigators: Tuncer B. Edil and Craig H. Benson

Graduate Research Assistants: Christopher A. Bareither

Geo Engineering Program
Department of Civil and Environmental Engineering
University of Wisconsin-Madison

SUBMITTED TO THE WISCONSIN
DEPARTMENT OF TRANSPORTATION

June 29, 2007

ACKNOWLEDGEMENT

Financial support for this study was provided by the Wisconsin Department of Transportation (WisDOT) through the Wisconsin Highway Research Program (WHRP). Xiaodong Wang assisted with the project in the laboratory.

DISCLAIMER

This research was funded through the Wisconsin Highway Research Program by the Wisconsin Department of Transportation and the Federal Highway Administration under Project # 0092-05-08. The contents of this report reflect the views of the authors who are responsible for the facts and accuracy of the data presented herein. The contents do not necessarily reflect the official views of the Wisconsin Department of Transportation or the Federal Highway Administration at the time of publication.

This document is disseminated under the sponsorship of the Department of Transportation in the interest of information exchange. The United States Government assumes no liability for its contents or use thereof. This report does not constitute a standard, specification or regulation.

The United States Government does not endorse products or manufacturers. Trade and manufacturers' names appear in this report only because they are considered essential to the object of the document.

Technical Report Documentation Page

1. Report No. WHRP 07-09	2. Government Accession No	3. Recipient's Catalog No	
4. Title and Subtitle DETERMINATION OF SHEAR STRENGTH VALUES FOR GRANULAR BACKFILL MATERIAL USED BY THE WISCONSIN DEPARTMENT OF TRANSPORTATION		5. Report Date <u>August 2007</u>	6. Performing Organization Code University of Wisconsin-Madison
7. Authors Tuncer B. Edil, Craig H. Benson, Christopher A. Bareither		8. Performing Organization Report No.	
9. Performing Organization Name and Address Geological Engineering Program, Department of Civil and Environmental Engineering University of Wisconsin-Madison 1415 Engineering Drive Madison, WI 53706		10. Work Unit No. (TRAIS)	11. Contract or Grant No. WisDOT SPR# 0092-05-08
12. Sponsoring Agency Name and Address Wisconsin Department of Transportation Division of Business services Research Coordination Section 4802 Sheboygan Avenue Room 104 Madison, WI 53707-7965		13. Type of Report and Period Covered Final report, 2004-2007	14. Sponsoring Agency Code
15. Supplementary Notes			
16. Abstract This study evaluated the effects of physical characteristics and geologic factors on the shear strength of compacted sands from Wisconsin that are used as granular backfill for mechanically stabilized earth walls and reinforced soil slopes. Physical properties and shear strength were determined for 30 compacted sands collected from a broad range of geological deposits. Relationships between strength-deformation behavior, geologic origin, and physical properties were used to categorize the sands into four friction angle groups. Sands with the lowest friction angle are derived from weathering of underlying sandstones, and tend to be medium-fine, well-rounded, and poorly-graded sands. Sands with the highest friction angle are from recent glacial activity and tend to be coarser grained, well-graded, and/or angular. A multiple regression model was developed that can be used to predict friction angle (ϕ') of the compacted sands based on effective particle size (D_{10}), maximum dry unit weight (γ_{dmax}), and Krumbein roundness. The model predicts ϕ' within $\pm 2^\circ$ of the measured ϕ' .			
17. Key Words Granular backfill, sand, shear strength, direct shear test, large-scale direct shear test, friction angle, geological origin, particle characteristics		18. Distribution Statement No restriction. This document is available to the public through the National Technical Information Service 5285 Port Royal Road Springfield VA 22161	
19. Security Classif.(of this report) Unclassified	19. Security Classif. (of this page) Unclassified	20. No. of Pages	21. Price

TABLE OF CONTENTS

ACKNOWLEDGEMENT.....	i
DISCLAIMER.....	ii
TECHNICAL DOCUMENT PAGE.....	iii
LIST OF FIGURES.....	vii
LIST OF TABLES.....	x
1. EXECUTIVE SUMMARY.....	13
1.1. INTRODUCTION.....	13
1.2. MAJOR FINDINGS.....	13
1.3. REFERENCES	16
2. INTRODUCTION.....	17
3. SOURCES OF SANDS	19
3.1. WEATHERED SANDSTONE DEPOSITS	20
3.2. FLUVIAL OUTWASH DEPOSITS	20
3.3. GLACIAL OUTWASH DEPOSITS.....	21
3.4. ICE CONTACT STRATIFIED DEPOSITS	21
3.5. MISCELLANEOUS GLACIAL DEPOSITS.....	21
4. PHYSICAL CHARACTERISTICS	23
4.1. INDEX PROPERTIES.....	23
4.2. PARTICLE ROUNDNESS	23
4.3. MINIMUM AND MAXIMUM VOID RATIOS.....	25
4.4. STANDARD PROCTOR COMPACTION	25
4.5. MINERALOGY AND CHEMICAL PROPERTIES	27
5. SHEAR STRENGTH TESTING.....	28
5.1. DIRECT SHEAR TESTS	28
5.2. COMPARISON TESTS.....	29
6. SHEAR STRENGTH BEHAVIOR.....	31
6.1. FRICTION ANGLE GROUPS	32
6.2. ESTIMATING SHEAR STRENGTH BASED ON PHYSICAL PROPERTIES..	36
7. SUMMARY AND CONCLUSIONS.....	39

8. REFERENCES.....	41
9. TABLES AND FIGURES	44
APPENDIX A - COMPARISON OF SHEAR STRENGTH OF GRANULAR BACKFILL MEASURED IN SMALL-SCALE AND LARGE-SCALE DIRECT SHEAR TESTS	67
ABSTRACT.....	67
A-1. INTRODUCTION.....	68
A-2. BACKGROUND.....	69
A-3. MATERIALS AND METHODS.....	71
A-3.1. SANDS	71
A-3.2. SMALL-SCALE DIRECT SHEAR TESTS	71
A-3.3. LARGE-SCALE DIRECT SHEAR TESTS.....	73
A-3.4. REPEATABILITY OF DIRECT SHEAR METHODS	75
A-3.5. TRIAXIAL COMPRESSION TESTS.....	76
A-4. SHEAR BEHAVIOR IN DIRECT SHEAR TESTING	77
A-5. SMALL-SCALE VERSUS LARGE-SCALE SHEAR STRENGTH.....	79
A-6. COMPARISON OF TRIAXIAL COMPRESSION, SMALL-SCALE DIRECT SHEAR AND LARGE-SCALE DIRECT SHEAR	81
A-7. CONCLUSIONS.....	82
A-8. REFERENCES.....	83
A-9. TABLES AND FIGURES	85
A1. NORMAL FORCE TRANSFER	100
A2. BOX FRICTION CORRECTION PROCEDURE.....	104
A2.1 Box Interface Friction	104
A2.2 Box Friction Equations	104
A2.3 Box Friction Method Comparison	107
A3. LARGE-SCALE DIRECT SHEAR SPECIMEN DENSITY	113
APPENDIX B - REPRODUCIBILITY OF DIRECT SHEAR TESTS CONDUCTED ON GRANULAR BACKFILL MATERIALS	116

B-1. INTRODUCTION	116
B-2. DEFINITIONS, MATERIALS, AND METHODS	118
B-2.1.DEFINITIONS	118
B-2.2.SANDS.....	118
B-2.3.TEST METHODS	119
B-2.4.INTRA-LABORATORY DIRECT SHEAR TESTS.....	119
B-2.5.INTER-LABORATORY DIRECT SHEAR TESTS.....	121
B-2.6.TRIAXIAL COMPRESSION TESTS	123
B-3. RESULTS	124
B-3.1. INTRA-LABORATORY TESTS	124
B-3.2. INTER-LABORATORY DIRECT SHEAR TESTING	125
<i>B-3.2.1. Failure Envelopes and Friction Angles.....</i>	<i>125</i>
<i>B-3.2.2. Shear Deformation and Volume Change</i>	<i>127</i>
<i>B-3.2.3. Bias and Reporducibility.....</i>	<i>129</i>
B-4. CONCLUSIONS.....	130
B-5. ACKNOWLEDGEMENTS.....	131
REFERENCES	132

LIST OF FIGURES

Fig. 1.	Sample location and geologic origin of the sands.	51
Fig. 2	Particle-size distribution curves: (a) P1-S1 through P2-S8, (b) P2-S9 through P5-S1.	52
Fig. 3.	Influence of geologic deposit type on physical characteristics of sands: (a) median particle size, (b) coefficient of uniformity, (c) particle roundness.	53
Fig. 4.	Relationship between maximum void ratio and minimum void ratio and comparison to trend line for clean sands (< 5% fines) reported by Cubrinovski and Ishihara (2002).	54
Fig. 5.	Relationships between minimum and maximum void ratio and (a) median grain size (D_{50}) and (b) roundness.	55
Fig. 6.	Minimum void ratio at maximum dry density from standard compaction vs. minimum void ratio from vibratory table (a) and influence of geologic origin on maximum dry unit weight (b).	56
Fig. 7.	Percentages of mineralogical components in sands for different geologic deposits.	57
Fig. 8.	Comparison of ϕ' and dilatancy factor (a) and comparison of ϕ' and relative horizontal displacement at failure (%) (b).	58
Fig. 9.	Relationship between friction angle and roundness for fine sand ($D_{50} < 0.425$ mm) and medium sand ($D_{50} > 0.425$ mm).	59
Fig. 10.	Influence of quartz content (%) on ϕ' (a) and roundness (b).	60
Fig. 11.	Representative behavior of sands: (a) shear stress vs. relative horizontal displacement (RHD) and (b) vertical displacement vs. RHD in each strength group at normal stress of 99 kPa. Group 1 (P1-S4), Group 2 (P3-S7), Group 3 (P5-S1) and Group 4 (P2-S5).	61
Fig. 12.	Relationships between shear stress and relative horizontal displacement (RHD) (a) and vertical displacement and RHD (b) at normal stress of 99 kPa for sands P2-S3, P2-S4, and P3-S2.	62
Fig. 13.	Wisconsin state map with friction angles superimposed on sample locations.	63

		viii
Fig. 14.	Relationships of friction angle and density as reported in NAVFAC D 7.01 (1986) with friction angle vs. compacted density for the present study superimposed.	64
Fig. 15.	Comparison between ϕ' predicted using regression model and ϕ' measured in direct shear (a) and ϕ' predicted using regression model with average roundness and ϕ' measured in direct shear (b).	65
Fig. A-1	Particle size distribution curves for backfill materials used in study.	90
Fig. A-2	Schematic of large-scale direct shear machine.	91
Fig. A-3.	Failure envelopes for repeatability tests: (a) small-scale direct shear and (b) large-scale direct shear. All tests conducted with Sand TS while inundated using displacement rate of 0.24 mm/min.	92
Fig. A-4.	Shear stress versus relative horizontal displacement measured in small-scale direct shear with failure stress defined by (a) peak stress (Sand P2-S6) and (b) initial horizontal tangent (Sand P3-S2).	93
Fig. A-5.	Shear-displacement curves for LS-DS tests showing failure stress for cases with (a) initial horizontal tangent followed by plowing (Sand P3-S1) and (b) shear stress increase at the same rate with additional horizontal displacement (Sand P3-S2).	94
Fig. A-6.	Relative horizontal displacement at failure in large-scale direct shear (LS-DS) vs. relative horizontal displacement at failure in small-scale direct shear (SS-DS) for sands exhibiting a peak stress.	95
Fig. A-7.	Vertical displacement at front and rear of the large-scale direct shear box vs. relative horizontal displacement for Sand P2-S4, which exhibited “plowing” behavior for normal stresses between 62 and 184 kPa inclusive.	96
Fig. A-8.	Schematic of particle movements during shearing in large-scale direct shear.	97
Fig. A-9.	Friction angles obtained from large-scale direct shear (LS-DS) tests versus friction angles obtained from small-scale direct shear (SS-DS) tests.	98
Fig. A-10.	Failure envelopes obtained from small-scale direct shear (SS-DS), large-scale direct shear (LS-DS), and triaxial compression (TC) tests: (a) Sand P1-S1, (b) Sand P1-S6, (c) Sand P2-S9, and (d) Sand TS.	99
Fig. A1-1.	Setup of load transfer test for large-scale direct-shear tests.	102

Fig. A1-2.	Comparison of normal force measured on the shear plane to normal force applied on the surface: (a) large-scale direct shear and (b) small-scale direct shear.	103
Fig. A2-1.	Relationship of box interface frictional force and relative horizontal displacement for tests at interface normal forces of 0.32, 0.55, 0.81, 1.28, and 1.48 kN.	109
Fig. A2-2.	Relationship of box interface frictional force and normal force.	110
Fig. A2-3.	Schematic of large-scale direct shear box identifying the corrected area of the shear box interface (A_{CB}), corrected area of soil (A_{CS}), contact area of upper shear box and soil (A_{CS}), horizontal displacement (Δ_h), specimen width (W), and thickness of front of upper shear box (t).	111
Fig. A2-4.	Friction angles obtained from large-scale direct shear tests (ϕ'_{LS-DS}) versus friction angles obtained from small-scale direct shear tests (ϕ'_{SS-DS}): (a) no box friction correction applies, (b) box friction Method 1, (c) box friction Method 2, (d) box friction Method 3, and (e) box friction Method 4.	112
Fig. B-1.	Particle size distribution curves for backfill materials used in this study.	140
Fig. B-2.	p'-q diagram for Sand TS in triaxial compression with failure envelope.	141
Fig. B-3.	Mohr-Coulomb failure envelopes and friction angles for triaxial compression tests on P1-S1, P1-S6, P2-S9, and TS.	142
Fig. B-4.	Failure envelopes for Sand TS obtained from intra-laboratory direct shear tests.	143
Fig. B-5.	(a) Shear stress versus relative horizontal displacement and (b) vertical displacement versus relative horizontal displacement for intra-laboratory direct shear tests on Sand TS at a normal stress of 147 kPa.	144
Fig. B-6.	Failure envelopes from inter-laboratory direct shear tests: (a) Sand P1-S1, (b) Sand P1-S6, (c) Sand P2-S9, and (d) Sand TS.	145
Fig. B-7.	Friction angles from inter-laboratory direct shear tests (a) P1-S1, (b) P1-S6, (c) P2-S9, and (d) TS.	146
Fig. B-8.	Shear stress vs. relative horizontal displacement (a) and vertical displacement vs. relative horizontal displacement (b) for Sand P1-S1 at normal stress (σ_n) of 184 kPa. Data reported for all laboratories except Lab D (tests conducted at $\sigma_n = 177$ kPa) and Lab I (tests conducted at $\sigma_n = 192$ kPa).	147

- Fig. B-9. Shear stress vs. relative horizontal displacement for Sand P2-S9 at a normal as reported by Laboratories A,B,E,G and J and (a) hypothetical relationship between shear stress and relative horizontal displacement for continuous and discrete sampling. 148
- Fig. B-10. Comparison of friction angles from inter-laboratory direct shear tests with and without area correction. 149

LIST OF TABLES

Table 1.	Index properties of the sands.	44
Table 2.	Physical properties and geological origins of the sands.	45
Table 3.	Mineralogical percentages of select sands from X-Ray diffraction.	47
Table 4.	Friction angle groups with respective range of friction angles and geologic origin.	48
Table 5.	Average and standard deviation of independent variables in Eq. 2 for strength groups, ϕ' predicted with Eq. 2 using average independent variables, and range of ϕ' predicted with Eq. 2 using independent variables unique to each sand.	49
Table 6.	Roundness categories including Krumbein images, range of roundness, and average roundness.	50
Table A-1.	Physical parameters of sands used for shear strength testing.	85
Table A-1.	Physical parameters of sands used for shear strength testing (Continued).	86
Table A-2.	Shear strength parameters for repeatability tests conducted on Sand TS using small-scale (SS) and large-scale (LS) direct shear tests.	87
Table A-3.	Shear strength parameters for small-scale direct shear and large-scale direct shear tests.	88
Table A-4.	Friction Angles and ANCOVA Statistics for Sands P1-S1, P1-S6, P2-S2, and P2-S6 for Small-Scale Direct Shear (SS-DS), Large-Scale Direct Shear (LS-DS), and Triaxial Compression (TC).	89
Table A2-1.	Comparison of Large-Scale Direct Shear Friction Angle (ϕ'_{LS-DS}) and Small-Scale Direct Shear Friction Angle (ϕ'_{SS-DS}) without Any Box Friction Correction and with Corrections for Methods 1-4.	108
Table B-1.	Summary of shear strength testing on 20-30 dry Ottawa sand (Converse 1952).	133
Table B-2.	Physical characteristics of backfill materials used.	134
Table B-3.	Summary of differences between ASTM D 3080 and AASHTO T 236 standards for direct shear testing.	135

Table B-4.	Friction angles and cohesion intercepts reported by laboratories and determined by authors.	136
Table B-5.	ANCOVA summary for inter-laboratory failure envelopes, omitting Lab G.....	137
Table B-6.	Box shape and dimensions, specimen thickness, displacement rate, and gap spacing used by laboratories in inter-laboratory direct shear testing.	138
Table B-7.	Inter-Laboratory Direct Shear Statistics.....	139

SECTION 1

1. EXECUTIVE SUMMARY

1.1. INTRODUCTION

Granular materials are preferred for structural fill because they are strong, drain water rapidly, and settle relatively little. An important application of granular materials is backfill in mechanically stabilized earth (MSE) walls and reinforced soil (RS) slopes. For these applications, the friction angle of the sand (ϕ') generally is the most important property.

Design of MSE walls and RS slopes by the Wisconsin Department of Transportation (WisDOT) is generally conducted following recommendations in a design document distributed by the Federal Highway Administration (Elias et. al. 2001). WisDOT initially adopted $\phi' = 34^\circ$ for MSE wall design provided that a backfill met the criteria for particle size distribution, plasticity index, and electrochemical characteristics stipulated in Elias et. al. (2001). However, in the early 2000's, direct shear tests were conducted on several backfill materials meeting the requirements in Elias et. al. (2001). These tests, which were performed by the WisDOT, yielded ϕ' ranging from 29-32°. Since then, WisDOT has since reduced the ϕ' used for MSE wall design to 30° for backfill materials meeting the requirements in Elias et. al. (2001), but permits friction angles greater than 30° if the friction angle can be confirmed by direct shear testing.

1.2. MAJOR FINDINGS

In the research program described herein, the primary objective was to identify geologic origin and physical characteristics contributing to the shear strength of granular backfill materials in Wisconsin. Additional work included the following: (1) develop a direct shear test procedure that is capable of providing a repeatable, reliable estimate of ϕ' , and (2) assess inter-laboratory bias and reproducibility of the direct shear test method commonly used in commercial

and state soil testing laboratories. The research is presented in three papers, of which the additional work is included as appendices to the main document.

The main document discusses the shear strength of naturally occurring sands in Wisconsin that are used as granular backfill. Thirty sands were sampled throughout Wisconsin to represent an assortment of potential backfill materials. Geologic origin, physical characteristics, and ϕ' were determined for all sands. Direct shear tests were conducted in a square box 64 mm wide to determine ϕ' . Relationships between strength and deformation behavior, geologic origin, and physical characteristics were used to divide the sands into four friction angle groups. Sands with the lowest friction angle are derived from weathering of underlying sandstones, and tend to be medium-fine, well-rounded, and poorly-graded sands. Sands with the highest friction angle are from recent glacial activity and tend to be coarser grained, well-graded, and/or angular.

Isolating the physical characteristics that affect ϕ' was difficult because several variables affected the shear strength of the sands. Therefore, a multiple regression analysis was performed to develop a model to predict ϕ' of the compacted sands based on readily obtained physical characteristics. The model predicts ϕ' based on effective grain size (D_{10}), maximum dry unit weight (γ_{dmax}) determined by standard compaction, and particle roundness (Krumbein 1941) and is capable of predicting ϕ' of compacted sands in Wisconsin within $\pm 2^\circ$ of the ϕ' measured in direct shear.

Appendix A, "Comparison of shear strength of granular backfill measured in small-scale and large-scale direct shear tests," examines scale effects in direct shear testing. Many backfill materials include particles too large to include in a standard direct shear box. To test these materials in direct shear, the large particles must be removed or a large shear box used. Direct shear tests were performed on the 30 sand samples in a 64-mm square small-scale direct shear (SS-DS) box containing a specimen 31 mm thick and also in a 305-mm large-scale direct shear

(LS-DS) box containing a specimen 152 mm thick. The SS-DS tests were conducted on material passing a No. 4 sieve (4.75 mm) (P4), whereas the LS-DS tests included P4 material as well as material retained on the No. 4 sieve (R4) but smaller than 25.4 mm. SS-DS and LS-DS tests were conducted following similar methods as outlined in AASHTO T 236-92, with test specimens prepared to identical P4 densities. The objective was to compare ϕ' measured in SS-DS and LS-DS and to assess the influence of R4 material on ϕ' . SS-DS and LS-DS tests on the 30 sands, including between 0 to 30% R4 material, showed that ϕ' determined in SS-DS and LS-DS differed by $\leq 4^\circ$. Triaxial compression (TC) tests were also performed on four of the sands. Analysis of the failure envelopes obtained in TC, SS-DS, and LS-DS for these 4 sands showed that the envelopes obtained by different test methods were not statistically different.

Assuming that TC provides a valid estimate of the ϕ' for a given backfill material, both SS-DS and LS-DS were shown to be comparable to TC. Comparisons between SS-DS and LS-DS revealed that including R4 material, up to 30%, did not affect ϕ' . Thus, scalping the R4 material and measuring ϕ' in SS-DS, provides a reasonable estimate of the actual ϕ' of a given backfill material.

Appendix B, "Reproducibility of Direct Shear Tests Conducted on Granular Backfill Materials," presents the findings of direct shear tests performed on four backfill materials by 10 independent laboratories. The four granular backfill materials were tested by the 10 laboratories following the method in AASHTO T 236-92, along with additional stipulations intended to limit the variability between laboratories. Even though a standard was to be followed and stipulations were provided, the test conditions used by the laboratories differed, including box shape, box size, displacement rate, and gap spacing. Data from the 10 laboratories showed high variability in the failure envelopes and friction angles, varying by as much as 18° for a given backfill material. Analysis of the data from the 10 laboratories showed that the reproducibility of direct shear tests on granular backfill is $\pm 8.8^\circ$. Tests were also conducted on the 4 backfill

materials in TC to define the bias in the direct shear test. The bias is -3.4° , on average, when an area correction is not applied to the direct shear data, and -2.1° when area corrections are applied.

The source of variability in failure envelopes and friction angles between the 10 laboratories could not be attributed to a single factor. Significant differences in the strength-deformation behavior indicated problems may have existed in specimen preparation. The wide variation in ϕ' indicates that efforts are needed to improve the consistency of direct shear testing in the US.

1.3. REFERENCES

- Elias, V., Christopher, B. R., and Berg, R. R. (2001) Mechanically Stabilized Earth Walls and Reinforced Soil Slopes Design and Construction Guidelines, *U. S. Department of Transportation Federal Highway Administration*, Publication No. FHWA-NHI-00-043.
- Krumbein, W. C. (1941) "Measurement and geological significance of shape and roundness of sedimentary particles," *Journal of Sedimentary Petrology*, 11(2), 64-72.

SECTION 2

2. INTRODUCTION

Design of mechanically stabilized earth (MSE) walls and reinforced soil (RS) slopes by many agencies, including the Wisconsin Department of Transportation (WisDOT), is generally conducted following the guidelines developed by Elias et al. (2001) for the Federal Highway Administration (FHWA). These guidelines indicate that the backfill can be assumed to have an internal angle of friction (ϕ') of 34° provided that specified criteria for particle size distribution, plasticity index, and electrochemical characteristics are satisfied.

In Wisconsin, natural sands meeting the criteria in Elias et al. (2001) generally are used for MSE wall backfill and for RS slopes. However, testing conducted by WisDOT in 2002-03 indicated that some compacted natural sands meeting the criteria in Elias et al. (2001) could have friction angles less than 34° . Sands having lower friction angles had similar geologic history, suggesting that geological factors should be considered when evaluating the suitability of sands for backfill. Accordingly, a statewide examination was undertaken to assess how geologic origin and physical properties influence the friction angle of naturally occurring sands in Wisconsin.

Thirty sands throughout Wisconsin were sampled to obtain a representative assortment of potential granular backfill materials. Although all of the samples were collected in Wisconsin, they represent a reasonably wide range of geological origins and physical characteristics, and therefore are likely to be representative of the northern Midwest and other geographic regions where glaciation has occurred. Physical properties and geological origin of each sand were studied, and the friction angle of each sand was measured in direct shear test as is commonly done by WisDOT and other transportation agencies when evaluating the shear strength of compacted backfill materials for MSE walls and RS slopes (Bareither et al. 2006a). Relationships between shear strength, physical properties, and regional geology were

established and a regression model was developed that can be used to estimate ϕ' based on commonly measured physical characteristics.

SECTION 3

3. SOURCES OF SANDS

Thirty backfill samples were collected from the locations shown in Fig. 1. These sources represent the sand deposits typically found in Wisconsin (weathered sandstone, fluvial outwash, glacial outwash, ice-contact stratified deposits, and other deposits of glacial origin). Sampling was conducted at greater density near major metropolitan areas, where there is a greater need for granular backfill materials. When possible, samples were selected from an in situ layer at each site so that a precise geologic origin could be established. At three locations, however, samples were collected from sieved and washed backfill material. For these sands, the geologic origin was generalized for the entire location. Approximately 0.1 m³ of material was collected at each site. Each sample was blended together thoroughly and allowed to air-dry. After air-drying, each sample was blended again and placed uniformly in a large (0.12 m³) sealed container.

The five geological/geographical provinces shown in Fig. 1 were established by Martin (1965). Province 1 (P1) is referred to as the “western uplands” and also as the “driftless area” due to the absence of glacially deposited material. Province 2 (P2), referred to as the “eastern ridges and lowlands,” encompasses the youngest bedrock in Wisconsin and also the broadest range of glacial deposits. Province 3 (P3), referred to as the “central plains,” is completely underlain by Cambrian Sandstone. Province 4 (P4), referred to as the “northern highlands,” is underlain by metamorphic and igneous bedrock, forming the southern portion of the Canadian Shield. Province 5 (P5), referred to as the “Lake Superior lowlands,” primarily contains glaciolacustrine deposits associated with fluctuations of Glacial Lake Duluth. The sample names used in this study reflect the province in which they were sampled (P#) combined with the sample number from the respective province (S#) combined as (P#-S#).

3.1. WEATHERED SANDSTONE DEPOSITS

Four samples were obtained from deposits derived from eolian and fluvial weathering of underlying Cambrian and St. Peter sandstones (Fig.1). The sand particles in these sandstones had been exposed to more than 100 million years of eolian and fluvial abrasion before consolidation into sandstone (Dott and Attig 2004). These weathering processes resulted in sandstones comprised of well-rounded medium-to-fine sand-size particles. These particles are comprised predominantly of quartz because of its resistance to disintegration and decomposition (Prothero and Schwab 2004).

The sand deposits derived from fluvial and eolian weathering of the Cambrian and St. Peter sandstones have the same characteristics as the sand particles in the parent rocks (Dott and Attig 2004). These sand deposits are also free from direct glacial activity, which is unusual in Wisconsin and many other upper tier states in the US. The majority of Wisconsin was glaciated during the past 2.5 million years, and more significantly during the Wisconsin Glaciation (25,000 and 10,000 bp) (Clayton et al, 1991).

3.2. FLUVIAL OUTWASH DEPOSITS

Fluvial outwash deposits (Fig. 1) were sampled at six locations. The fluvial outwash deposits consist of poorly-graded stratified sand with layers of fine sediment deposited during periods of decreased flow in the Wisconsin, Mississippi, Black, and Chippewa Rivers. All of the fluvial outwash deposits lie in regions underlain by Cambrian Sandstone, which is a primary source of sediment input during erosion. However, all of these fluvial deposits also contain glacial outwash sediments from large river systems that acted as outlets for glacial meltwater during the Wisconsin Glaciation. Thus, sands derived from fluvial outwash deposits contain particles having a broader distribution of size, shape, and mineralogy compared to the sands derived solely from weathered sandstone.

3.3. GLACIAL OUTWASH DEPOSITS

Ten samples were obtained from glacial outwash deposits (Fig. 1) formed during the Wisconsin Glaciation from glaciers overlying non-sandstone bedrock. These deposits were sampled at the highest frequency because of their abundance and broad geographic availability. Sediments contained in the glacial outwash samples were deposited closer to the glacier margin compared to those of the fluvial outwash deposits. Outwash sediment near the glacier margin is often deposited rapidly during flood events, resulting in very well-graded sands and gravels that are more angular and coarser grained compared to fluvial outwash deposits (Church and Gilbert 1975, Werrity 1992, Bennett and Glasser 1996, Maizels 2002).

3.4. ICE CONTACT STRATIFIED DEPOSITS

Four samples were obtained from ice-contact stratified (ICS) deposits (Fig. 1) that formed during the Wisconsin Glaciation. ICS deposits are water-laid sediments formed in contact with glacial ice that consist of more angular particles due to short transport distances. They vary in particle size and gradation due to fluctuations in meltwater discharge and sediment concentration.

3.5. MISCELLANEOUS GLACIAL DEPOSITS

Five samples were obtained from miscellaneous glacial deposits, including drumlin, esker, and glaciolacustrine (lake) sand deposits (Fig. 1). The composition and physical properties of drumlins depend on the material present during glacial advance (Bennett and Glasser 1996). The drumlin that was sampled contained outwash sands and gravels deposited during an earlier glacial advance. Eskers can be composed of sediments ranging from sorted silt to broadly graded and matrix-supported gravel (Benn and Evans 1998) that typically have

traveled less than 15 km from the outcrop source (Lee 1965; Price 1973). The esker deposit in this study varied from poorly graded fine sand to well-graded gravel. The sample collected was from a poorly graded medium-fine sand layer. Glaciolacustrine sands were obtained from deposits related to Glacial Lake Oshkosh and Glacial Lake Wisconsin that consist of poorly-graded fine sands characteristic of selective deposition in waters having low turbulence. Sample P2-S3 may have been reworked post glaciation due to fluvial and eolian weathering.

SECTION 4

4. PHYSICAL CHARACTERISTICS

4.1. INDEX PROPERTIES

Index properties of the samples are summarized in Table 1 and the particle size distribution curves are shown in Fig. 2. The samples vary from uniformly to broadly graded, with median particle size (D_{50}) ranging from 0.15 to 3.50 mm, coefficient of uniformity (C_u) ranging from 1.8 to 34.1, and fines content ranging from 0.1% to 14.4%. The gravel content of the samples ranges from 0.0% to 47.8%. All of the samples classify as sands in the Unified Soil Classification System in ASTM D 2487, with the majority (24 of 30) classifying as poorly graded sand (SP). All of the sands classify as A-1, A-2 or A-3, i.e., “granular” according to the AASHTO soil classification system.

The variations of D_{50} and C_u with respect to geologic deposit type are shown in Fig. 3. Sands designated as weathered sandstone are all poorly graded ($2.35 \leq C_u \leq 3.00$) medium to fine cleans sands with similar specific gravity of solids (2.63 – 2.66). Sands designated as fluvial outwash are more uniformly graded ($1.86 \leq C_u \leq 2.86$) compared to weathered sandstone, but have a broader range of median particle size ($0.29 \text{ mm} \leq D_{50} \leq 0.70 \text{ mm}$). Sands designated as glacial outwash contain the coarsest particles and sands designated as glacial outwash and ICS represent the broadest distributions in particle size (Fig. 3). The miscellaneous glacial deposits are poorly graded with the smallest median particle size compared to all other materials.

4.2. PARTICLE ROUNDNESS

Particle shape can be described in terms of roundness, sphericity, and surface texture. Sphericity generally falls within a narrow range for naturally occurring sands (Zelasko 1966; Edil et. al. 1975) and surface texture is a second order feature that is cumbersome to measure and

highly variable (Cho et. al. 2006). Hence, for this study, particle shape was characterized by roundness using a visual procedure conducted with an optical microscope and charts developed by Krumbein (1941). Digital image analysis techniques are currently available for determination of particle shape (Janoo 1998; Jensen et. al. 2001; Cho et. al. 2006). However, the Krumbein method was adopted based on access to readily available equipment and its established use in previous research (Zelasko 1966; Edil et. al. 1975; Zelasko et. al. 1975). The Krumbein method can also be implemented by laboratories with little specialized equipment.

Particles from each sample were partitioned into four size fractions: gravel (< 76.2 mm and > 4.75 mm), coarse sand (< 4.75 mm and > 2.0 mm), medium sand (< 2.0 mm and > 0.425 mm), and fine sand (< 0.425 mm and > 0.075 mm). Roundness was determined for each size fraction constituting at least 5% by weight of the total sample. Edil et al. (1975) determined roundness for sand particles based on charts in Krumbein (1941) and reported that viewing at least 25 particles yielded a reliable mean roundness. For this study, 50 particles were analyzed from each size fraction and a weighted whole sample roundness was calculated for each sand based on the average roundness and percentage (by weight) of the sample in each size fraction. The Krumbein roundness chart was kept at a constant scale and the particular size fraction was viewed at similar scale as the particles on the roundness chart.

The roundness measurements are summarized in Table 2. The roundness varies between a minimum of 0.22 (angular) to a maximum of 0.62 (rounded). The variation of roundness with respect to geologic deposit type is shown schematically in Fig. 3c. Roundness is highest and most uniform for weathered sandstone deposits due to the uniformity of rounded particles in the parent sandstones. Roundness decreases from fluvial outwash to glacial outwash to ICS deposits corresponding to a decrease in distance from the glacier margin. The roundness for the miscellaneous deposits is typically low, but varies with distance and method of transport.

4.3. MINIMUM AND MAXIMUM VOID RATIOS

Three minimum void ratio (e_{\min}) and three maximum void ratio (e_{\max}) tests were performed on each sand. The minimum or maximum void ratio reported for each sand is the minimum or maximum void ratio obtained from the three tests. Maximum void ratio was determined according to Method B of ASTM D 4254 using a tremie tube and a 2.83 L mold. Minimum void ratio was measured according to ASTM D 4253 (Method 2A) using air-dried soil in a 2.83 L mold. The mold was vertically vibrated for 12 min at a frequency of 50 Hz with a 25.6 kg surcharge.

The minimum and maximum void ratios are summarized in Table 2. The relationship between e_{\max} and e_{\min} for the clean sands (< 5% fines) and the sands with 5-15% fines is shown in Fig. 4. The relationship between e_{\max} and e_{\min} compares well with the trend line reported by Cubrinovski and Ishihara (2002) for natural clean sands (< 5% fines). The e_{\min} and e_{\max} also depend modestly on median grain size (D_{50}) (Fig. 5a) and roundness (Fig 5b). Cubrinovski and Ishihara (2002) also report that e_{\max} decreases with increasing D_{50} for clean sands and sands with some fines (5-15% fines), and Edil et al (1975) report that e_{\max} and e_{\min} decrease with increasing roundness.

4.4. STANDARD PROCTOR COMPACTION

The FHWA guidelines for MSE walls and RS slopes indicate that the backfill should be compacted to at least 95% of the maximum dry unit weight corresponding to standard Proctor compactive effort. Maximum dry unit weights obtained from compaction tests are also commonly used by transportation departments to control placement of coarse and fine-grained soils. Therefore, standard Proctor compactions tests were conducted on each sand following AASHTO T 99-Method A using the sample fraction passing the No. 4 sieve (4.75 mm). Method A was used for all sands for consistency, even though two sands had $R_4 > 20\%$

Maximum dry unit weights (γ_{dmax}) and the void ratios corresponding to the maximum dry unit weight ($e_{\gamma d}$) are summarized in Table 2. For samples containing > 5% R4 material, a unit weight correction was applied following ASTM D 4718 to adjust γ_{dmax} and $e_{\gamma d}$ to account for the removed material. For a majority of the sands (22 of 30), the γ_{dmax} was obtained at zero water content and the dry unit weight decreased with addition of water and consistently remained less than γ_{dmax} at higher water contents. Arcement and Wright (2001), who studied granular backfills in Texas, also indicate that γ_{dmax} for poorly graded sands typically occurs at zero water content. Of the remaining 8 sands, 4 had greater than 6% fines and exhibited a conventional bell-shaped compaction curve, whereas 4 had negligible fines and exhibited an increase in dry unit weight near saturation. Compaction tests performed on poorly-graded sands with silt and silty sands by Arcement and Wright (2001) also showed conventional bell-shaped compaction curves.

A graph of $e_{\gamma d}$ (compaction test) versus e_{min} (vibratory table) is shown in Fig. 6a. Good correspondence exists between both measures of maximum density, although the vibratory table typically resulted in a slightly denser packing ($e_{min} = 99\%$ of $e_{\gamma d}$, on average). The variation of γ_{dmax} with respect to geologic deposit type is shown in Fig. 6b. The maximum dry unit weight of a given granular material depends on a number of particle characteristics, including size, shape, and gradation. The variation in particle characteristics between sands of differing geologic deposit type (Fig. 3) results in a different median and range of γ_{dmax} for each geologic deposit type (Fig. 6b). For example, the coarser particles and broader particle distributions of glacial outwash deposits produce sands that achieve a greater γ_{dmax} for given compactive effort. However, for a given type of deposit, γ_{dmax} varies within a relatively narrow range ($\approx 2 \text{ kN/m}^3$).

4.5. MINERALOGY AND CHEMICAL PROPERTIES

Mineralogy was determined for 15 samples by X-ray diffraction (Table 3). Quartz constitutes the majority of each sand (Table 3), except for P2-S5, which only has 25% quartz. Plagioclase, dolomite, potassium-feldspar, and phyllosilicates (includes illite, mica, kaolinite and chlorite) were the other dominant minerals present along with quartz. The average mineralogical fractions of quartz, non-quartz, and phyllosilicates for weathered sandstone, fluvial outwash, glacial outwash, and ice contact stratified type deposits are shown in Fig. 7. X-ray diffraction was not performed on any miscellaneous glacial deposits. The large fraction of quartz for sands designated weathered sandstone and fluvial outwash is derived from the Cambrian and St. Peter Sandstones. Although quartz is the dominant mineral in all deposit types, there is an increase in non-quartz material for glacial outwash and ICS sands. These types of materials originate primarily from regions of non-sandstone bedrock.

The pH, chloride content, sulfate content, and resistivity of each sand were measured as indicated in Elias et al. (2001). pH was measured in accordance with AASHTO T 289-91 using a single electrode pH meter, chloride content was measured following AASHTO T 291-94, sulfate content was measured following T 290-95, and resistivity was measured following AASHTO T 288-91. All of the sands met the electrochemical requirements for steel and geosynthetic reinforcing elements, except for P1-S4, which has pH of 4.6 (Bareither 2006). Elias et al. (2001) also specifies a limiting organic content of 1% when using steel reinforcements. Visual inspection of the samples indicated that the organic content was negligible.

SECTION 5

5. SHEAR STRENGTH TESTING

5.1. DIRECT SHEAR TESTS

Friction angle of each sand was measured in direct shear following the procedure in AASHTO T 236-92. Tests were conducted in a 64-mm-wide square shear box that contained a specimen 31 mm thick. Small-scale direct shear tests were used in lieu of other methods because direct shear testing is viewed to be more common in practice when evaluating MSE and RS slope backfill materials.

Prior to testing, the sands were air dried and sieved past a No. 4 sieve (4.75 mm). The fraction passing No. 4 sieve was compacted air-dried in the shear box in three lifts of equal thickness by tamping the top of each lift with a wooden tamper. The number of tamps per layer was adjusted to achieve the target density for each specimen (95% of maximum dry density determined by standard Proctor compaction, which is the compaction criterion in Wisconsin for MSE backfill).

Inundation of the specimen followed immediately after the normal stress was applied. Drainage was permitted through 9-mm-thick perforated PVC plates placed on the top and bottom of the specimen. Separation was provided by a thin non-woven heat-bonded calendered geotextile placed between the sand and the plates. Compression of the PVC and geotextile was measured at each normal stress and volume change measurements on initial normal loading were corrected.

All tests were conducted using a constant rate of displacement of 0.24 mm/min. Normal stresses between 26 and 184 kPa were applied. The maximum stress is comparable to the stress expected at the bottom of a 10-m high MSE wall backfilled with dense granular fill having a unit weight of approximately 18 kN/m³. Measurements of horizontal displacement, vertical displacement, and shear force were recorded using a personal computer equipped with a

Validyne data acquisition card (UPC601-U) and LABView software. Two linear variable displacement transducers (LVDTs) (Schlumberger Industries Model AG/5, 5 ± 0.003 mm) were used to measure horizontal and vertical displacements, and a load cell (Revere Transducer Model 363-D3-500-20P1, 2.2 ± 0.00015 kN) was used to measure shear force.

Failure was defined at peak shear stress for all sands exhibiting a peak stress. For sands exhibiting only an ultimate stress, failure was defined as the shear stress corresponding to the initial horizontal tangent to the shear stress-displacement curve. Mohr-Coulomb failure envelopes were obtained by linear least-squares regression with a non-negative intercept. The failure envelopes exhibited a high degree of linearity, with coefficients of determination (R^2) ranging from 0.997 to 1.000. In all cases, the cohesion intercept (c') was small, ranging between 0.0 and 8.0 kPa. This cohesion intercept (c') represents friction in the shear box and machine components, and possibly non-linearity of the failure envelopes near the origin.

5.2. COMPARISON TESTS

Comparative tests were conducted on four of the sands using consolidated-drained triaxial compression tests. Triaxial tests were performed on the fraction passing the No. 4 sieve (< 4.75 mm) compacted in a similar manner and to the same density as specimens in direct shear. Effective confining pressures ranging from 21 to 83 kPa were used so that normal and shear stresses at failure on the estimated failure plane fell within the range of those used in the DS tests (Bareither et al. 2006b). Friction angles obtained from the direct shear and the triaxial tests fell within $\pm 3.3^\circ$.

To assess the effect of gravel fraction on friction angle, large-scale direct shear tests were conducted on the sands containing $> 5\%$ gravel. Large-scale direct shear tests were conducted in 305 mm square box (152 mm thick) on the fraction passing a 25.4 mm sieve. Test specimens were prepared so that the density of the fraction passing a No. 4 sieve was

consistent with specimen densities in small-scale direct shear. Large-scale direct shear tests were performed at similar normal stresses and at a similar rate of horizontal displacement to small-scale direct shear tests (Bareither et al. 2006a). Friction angles obtained from the large-scale tests typically were within $\pm 2.0^\circ$ of the small-scale direct shear tests in which material retained on a No. 4 sieve was removed.

The direct shear test procedure used in this study was also evaluated for repeatability (Bareither et al. 2006b). Comparison of five replicate tests on a single sand yielded ϕ' ranging from 41.5° to 41.8° , with an average of 41.6° and standard deviation of 0.12° . Thus, the failure envelopes and friction angles obtained with the direct shear testing procedure are highly repeatable when the test is conducted by a single operator.

SECTION 6

6. SHEAR STRENGTH BEHAVIOR

The 30 sands tested in direct shear exhibited a wide range of shear strength behavior. A strong correspondence exists between ϕ' and propensity for dilation. This correspondence is shown in Fig. 8a, where ϕ' is graphed vs. the dilatancy factor (ψ), which was defined as:

$$\psi = \frac{(\Delta H_f / H_o)}{(\Delta L_f / L_o)} \quad (1)$$

where ΔH_f is the change in thickness of the specimen at failure, H_o is the initial thickness after normal stress application and inundation, ΔL_f is the change in horizontal displacement at failure ($\Delta H_f / \Delta L_f$ is the slope of the vertical displacement versus horizontal displacement curve at failure), and L_o is the initial specimen length. A strong correspondence also exists between ϕ' and relative horizontal displacement (RHD) at failure (Fig. 8b). Sands with the larger ϕ' typically have large dilatancy factors (Fig. 8a) and reach failure at smaller RHD (Fig. 8b).

Friction angle is also affected by particle roundness and particle size as shown in Fig. 9. The data in Fig. 9 have been grouped into fine sands and medium sands based on median particle size ($D_{50} < \text{or} > 0.425 \text{ mm}$). Lower roundness or larger median particle size results in larger ϕ' . Hennes (1951), Koerner (1970), Zelasko et al. (1975), and Cho et al. (2006) report similar correspondence between ϕ' and particle size and roundness for laboratory mixtures of granular materials.

Friction angle is also affected by quartz content, as shown in Fig. 10a. The sands with less quartz contained greater amounts of potassium-feldspar, plagioclase, calcite, and/or dolomite (Table 3), and these minerals generally have higher sliding frictional resistance

compared to that of quartz (Horn and Deere 1962, Ohnaka 1975). Equally important, however, is that the predominantly quartz sands also have greater roundness (Fig. 10b), which results in lower friction angle (Fig. 9). Sands with a greater fraction of quartz particles tend to have undergone more cycles of transport, and therefore tend to be more rounded. (Pettijohn et al. 1965; Prothero and Schwab 2004). The well-rounded quartz sands of Wisconsin that have low ϕ' are primarily derived from the Cambrian and St. Peter sandstones, and the particles in these sandstones are some of the most physically weathered sand particles in Wisconsin (Dott and Attig 2004).

6.1. FRICTION ANGLE GROUPS

Friction angles of the sands are summarized in Table 2. The data are presented in four groups (1-4) corresponding to sands having similar friction angles (increasing group number corresponds to increasing friction angle). The ranges of friction angles and geologic origin of the sands in each group are summarized in Table 4. Sands in each group generally have similar stress-displacement behavior. Representative relationships of shear stress vs. relative horizontal displacement (RHD) and vertical displacement vs. RHD for each group are shown in Fig. 11 at normal stress of 99 kPa. Sands in Group 1 typically exhibit contractive behavior and an ultimate strength, whereas sands in the other three groups exhibit dilatant behavior with a distinct peak shear stress and post-peak loss in strength. Exceptions from the generalized stress-displacement behavior include P2-S3 (Group 2) and P2-S4 and P3-S2 (Group 3), which showed contractive behavior and an ultimate shear stress (Fig. 12). These sands also are the outlier points in Fig. 8b (ϕ' vs. RHD).

Group 1 includes three weathered sandstone deposits and one fluvial outwash deposit that have friction angles between 32° and 33° . Each of these sands consists predominantly of well-rounded medium to fine grained quartz particles (Table 2) from the Cambrian and St. Peter

sandstones. The rounded grain shape and the uniformity in grain size (Fig. 3) limit interlocking between neighboring particles, resulting in very little dilation (Fig. 8 and 11) and an ultimate shearing strength that is attained primarily from particle frictional resistance and rearrangement. Holtz and Kovacs (1981) report ϕ' for sand from the St. Peter sandstone ranging from 31° for loose specimens ($e = 0.69$) to 37° for dense specimens ($e = 0.47$). The compacted void ratio for the DS tests for sands in Group 1 ranges between 0.50 – 0.54; and thus, friction angles between 32° to 33° obtained in this study for sand from the St. Peter Sandstone compare well to those reported by Holtz and Kovacs (1981).

Group 2 includes eight sands that have friction angles ranging from 34° to 36° . Five of the sands are from fluvial outwash deposits. Two glaciolacustrine sands and a weathered sandstone comprise the rest of Group 2. The sands in Group 2 have larger particle size or lower roundness compared to the sands in Group 1, resulting in higher friction angles. The larger particle size and lower roundness of the fluvial outwash materials (Fig. 3) are attributed to the influx of sediments from recent glaciations. The fluvial deposits in Group 2 were obtained from gravel pits of major river systems in Wisconsin, which accommodated glacial meltwater as recently as the Wisconsin Glaciation. The influx of glacial sediments provides particles to the fluvial systems that are less rounded and coarser, compared to particles eroded from the underlying sandstones. The glaciolacustrine sands have low roundness due to glacial sediments that are deposited in a lake setting where there is no further particle shape modification. The weathered sandstone in Group 2 has a lower roundness and larger D_{50} compared to weathered sandstones of Group 1. These differences in physical properties are likely due to differences of the sediments contained in the parent sandstone.

Sand P2-S3, the only sand in Group 2 not exhibiting dilatant shearing behavior (Fig. 6b), is angular predominantly fine sand from a glaciolacustrine sand deposit, and contains more that

12% fines. The larger percentage of fine material in P2-S3 compared to other sands in Group 2 may be the source of the contractive behavior during shear.

Group 3 includes ten sands that have friction angles ranging from 37° to 39°. Six of the sands in Group 3 consist of glacial outwash sediments deposited in the medial and proximal zones. Group 3 also includes two sands from ICS deposits, one sand from an esker deposit, and one glaciolacustrine sand deposit. The glacial outwash sands are more broadly graded (P4-S1 is an exception), contain a larger fraction of coarse particles, and consist of more angular particles compared to those in Groups 1 and 2, which combine to produce a denser packing, more dilation, and higher ϕ' (Kolbuszewski and Frederick 1963, Youd 1973, Edil et. al. 1975). Each of the physical characteristics of the glacial outwash sands (particle size, gradation, and shape) is directly influenced by glacial processes. The glacial outwash sands are more broadly graded (Fig. 3b) due to varying sized particles contained in the glacial meltwater that are often deposited rapidly near the glacier margin. The glacial outwash sands are also deposited at a shorter distance to the glacier margin compared to fluvial outwash deposits, which results in coarser (Fig. 3a) and more angular (Fig. 3c) particles.

The higher ϕ' associated with the non-glacial outwash materials is also due to more angular particles, larger particle size, and/or broader particle gradation compared to sands in Groups 1 and 2. The low roundness of the ICS deposits and the esker deposit is due to the short transport distance of the particles. The low roundness of the glaciolacustrine sand is due to similar processes as for the glaciolacustrine sands in Group 2. The particle size and gradation of the non-glacial outwash sands depends on the sediment contained in the glacial meltwater, and can be highly variable. All of the sands in Group 3 also contain a greater fraction of non-quartz material (potassium-feldspar, plagioclase, calcite and/or dolomite,) compared to the sands in Groups 1 and 2 (Table 3), which may also contribute to the higher ϕ' of the sands in Group 3 compared to the sands in Groups 1 and 2. As depicted in Fig. 7, glacial

outwash and ICS deposits have a greater contribution of non-quartz material, primarily from the formation of these types of deposits in regions of non-sandstone bedrock.

As mentioned previously, samples P2-S4 and P3-S2 do not exhibit the dilative strength-deformation behavior characteristic of the other sands in Group 3. The reason for this difference is not apparent, but may be related to the characteristics of the fines in these sands, which was not a focal point of this study.

The eight sands in Group 4 have friction angles ranging between 40° and 42°. They are glacial outwash and ICS deposits (the exception is Sand P3-S4, which is fluvial outwash). The sands in Group 4 are not necessarily as well-graded as the sands in Group 3, but they are more angular and/or coarser grained, which combine to produce a higher ϕ' . Sands in Group 4 also have the highest fraction of non-quartz material (Table 3). The lower roundness, larger particle size, and/or broader gradation, combined with minerals exhibiting higher friction, result in the largest ϕ' of the sands that were studied. Glacial processes impact the physical characteristics of the glacial outwash and ICS sands in a similar manner as described for Group 3. The fluvial outwash sand in Group 4 contains particles with a higher roundness compared to other sands in Group 4 (Table 2); however, this sand contains coarser particles relative to other fluvial outwash deposits, which contributes to higher ϕ' .

Two silty sands were sampled for this study; one from Group 2, with ϕ' of 35 (P2-S3), and the other from Group 4, with ϕ' of 40 (P2-S7). The friction angles for these silty sands compare well with friction angles reported for dense specimens of similar materials (37° - 40°) in Holtz and Kovacs (1981). Holtz and Kovacs (1981) also report ϕ' of 43° for dense screened glacial sand. Similar materials of glacial origin were obtained for this study and comprise Groups 3 and 4. Considering variation in physical properties and compacted densities between the materials in this study and to the material reported in Holtz and Kovacs (1981), similar friction angles were obtained for screened glacial sands.

Friction angles superimposed on sample locations are shown in Fig. 13. Group 1 sands, which comprise the lowest strength sands, are confined to a narrow region in the western portion of the state of Wisconsin. Group 2 sands are primarily in the immediate vicinity of the Group 1 sands, indicating that the lowest strength sands will be found in regions absent from glacial deposition and also in regions furthest from the glacial boundaries. The strongest sands, Groups 3 and 4, are dispersed through the remainder of the state of Wisconsin and are primarily found in regions of recent glacial advance.

6.2. ESTIMATING SHEAR STRENGTH BASED ON PHYSICAL PROPERTIES

A multiple regression analysis was used to develop a model to predict ϕ' based on relevant physical characteristics. Forward and backward stepwise regressions were performed with ϕ' as the dependent variable and the following as independent variables: D_{60} , D_{50} , D_{10} , C_u , C_c , % fines, G_s , e_{max} , e_{min} , γ_{d-max} , and roundness. A forward stepwise regression begins with no independent variables and sequentially adds variables to a model in order of their significance in predicting the dependent variable. A backward stepwise regression begins with all independent variables and sequentially removes variables from a model that are least significant in predicting the dependent variable. Independent variables are added (forward regression) or removed (backward regression) until only those variables that are statistically significant (as measured by a F-test) are included in the model. A significance level (α) of 0.05 was used to evaluate statistical significance of each independent variable.

Forward and backward stepwise regression results were analyzed to obtain the best overall model (i.e., highest coefficient of determination, R^2). Variables included in the model

were required to have statistical and physical significance and to be readily measured in conventional laboratories. The following model was obtained:

$$\phi' = 1.89 + 20.56 \times D_{10} + 2.35 \times \gamma_{dmax} - 24.10 \times R_s \quad (2)$$

where D_{10} is in mm, γ_{dmax} is in kN/m^3 , and R_s is the weighted average Krumbein roundness for the whole sample. The model has an adjusted coefficient of determination of 0.83 and all three independent variables had p-values < 0.0001 (i.e., $<< 0.05$). The coefficients also have physical significance. The positive coefficient on D_{10} infers that ϕ' increases with increasing particle size (i.e., as reported by Hennes 1951 and as shown in Fig. 9) and the negative coefficient on R_s infers that ϕ' decreases with increasing roundness (i.e., as reported by Koerner 1970, Zelasko et al. 1975, and Cho et. al. 2006 and shown in Fig. 9). The variable γ_{dmax} reflects the packing characteristics of a sand for a specific packing energy, and is influenced by the size, gradation, and shape of the particles (Youd 1973, Edil et. al. 1975). Materials that pack more efficiently have higher ϕ' , when all other factors are equal (Kolbuszewski and Frederick 1963, Zelasko et al. 1975). Thus, the coefficient for γ_{dmax} should be positive. A positive relationship between ϕ' and γ_{dmax} is also reported in NAVFAC D 7.01 (1986). The relationship between friction angle and density as reported in NAVFAC D 7.01 is shown in Fig. 13, with friction angle vs. compacted density (i.e. 95% of maximum dry density) data from this study superimposed. The friction angle vs. compacted density relationships are segregated with respect to USCS classification.

A graph of ϕ' predicted using Eq. 2 versus the measured ϕ' is shown in Fig. 13a. The regression model predicts ϕ' within $\pm 2^\circ$ of the measured ϕ' for nearly all sands. An additional comparison was made between the average friction angle in each strength group and friction

angles computed using Eq. 2 and the average D_{10} , γ_{dmax} , and roundness for each group (Table 5). This comparison is shown as the solid symbols in Fig. 13a. The difference between the average measured ϕ' in each group and ϕ' computed using the average properties in each group is less than 1° for each group.

Of the three independent variables in Eq. 2, roundness is measured least frequently in practice. Thus, an analysis was conducted to evaluate the efficacy of Eq. 2 for cases where roundness was determined by a simple visual inspection. The Krumbein roundness scale (0.1 to 0.9) was partitioned into five roundness categories (angular, subangular, subrounded, rounded, and well-rounded), with each category assigned a range and average roundness as tabulated in Table 6. Each sand was categorized as well-rounded ($R_s = 0.82$) rounded ($R_s = 0.66$), subrounded ($R_s = 0.50$), subangular ($R_s = 0.34$), or angular ($R_s = 0.18$). For this analysis, the average roundness in each roundness category was assigned to each of the 30 sands based on the determined weighted roundness for each sand (Table 2) falling within the range of roundness measurements for the five roundness categories (Table 6). The actual D_{10} and γ_{dmax} for each sand along with the average roundness were used to calculate ϕ' based on Eq. 2. Predictions of ϕ' from Eq. 2 using the average roundness as input are compared to the measured ϕ' in Fig. 13b. Even with roundness defined using the five general categories, the multiple regression model predicts ϕ' within $\pm 2^\circ$ for nearly all of the sands.

Eq. 2 can be used to estimate ϕ' for preliminary geotechnical design or to provide a reasonable check for ϕ' measured in direct shear. However, Eq. 2 was developed using data from sands from Wisconsin compacted at 95% of maximum dry unit weight, most of which were poorly graded. The applicability of the model to other sands, sands with greater fines, or sands prepared at other densities is not known and needs greater evaluation. Eq. 2 also corresponds to friction angles determined for normal stresses ranging from 26 to 184 kPa. The applicability outside this range is not known.

SECTION 7

7. SUMMARY AND CONCLUSIONS

This paper presents the findings of a study conducted to determine how geologic processes and physical properties affect the shear strength of compacted natural sands from Wisconsin used as granular backfill material. Thirty naturally occurring sands were sampled representing the regional variation throughout Wisconsin. Shear strength of each sand was measured in direct shear for a range of normal stresses characteristic of MSE wall and RS slope backfills. Friction angles (ϕ') obtained from the direct shear tests were related to the geologic origins and physical characteristics of the sands.

The thirty sands were differentiated into four strength groups based on shear strength and deformation behavior. Sands comprising each strength group share similar geologic origin and/or physical characteristics that contribute to similarity in the shear strength and deformation behavior. The lowest strength sands are comprised of quartz particles that have undergone extensive transport and physical weathering. These particles are mechanically weathered from the underlying Cambrian and St. Peter Sandstones and are well-rounded, medium to fine in size, and uniformly graded. The highest strength sands, derived primarily from outwash of the Wisconsin Glaciation, have undergone less transport and physical weathering, have lower quartz content, are more angular, are larger in size, and have broader gradation compared to the other sands. Sands with higher ϕ' also have higher dilatancy factor, confirming that the shear strength of compacted sands is directly related to the propensity for dilation.

A multiple regression model was developed that predicts ϕ' of compacted sands in Wisconsin. The model predicts ϕ' within $\pm 2^\circ$ based on D_{10} , γ_{dmax} , and particle roundness ($\phi' = 1.89 + 20.56D_{10} + 2.35\gamma_{dmax} - 24.10R_s$). Variables included in the regression model were required to be statistically significant (p-value < 0.05), to have physical significance regarding effect on ϕ' , and to be readily measured in the laboratory. The multiple regression model can be

used to estimate ϕ' for preliminary geotechnical design or to provide a reasonableness check on ϕ' for granular backfill materials measured in direct shear.

8. REFERENCES

- Arcement, B. J., and Wright, S. G. (2001). Evaluation of laboratory compaction procedures for specification of densities for compacting fine sands, Report, Center for Transportation Research, The University of Texas at Austin, Austin, TX.
- Bareither, C. A., Benson, C. H., and Edil, T. B. (2006a). "Comparison of shear strength of granular backfill measured in small-scale and large-scale direct shear tests." In Review: *Canadian Geotechnical Journal*.
- Bareither, C. A., Benson, C. H., and Edil, T. B. (2006b). "Reproducibility of direct shear tests conducted on granular backfill materials." In Review: *Geotechnical Testing Journal*.
- Benn, D. I. and Evans, D. J. A. (1998). *Glaciers & Glaciation*, Oxford University Press Inc., New York, NY.
- Bennett, M. R. and Glasser, N. F. (1996). *Glacial geology: Ice sheets and landforms*, John Wiley & Sons, Chichester, England.
- Clayton, L., Attig, J. W., Mickelson, D. M., and Johnson, M. D. (1991). Glaciation of Wisconsin, University of Wisconsin-Extension, Geologic and Natural History Survey, Madison, Wisconsin.
- Cho, G. C., Dodds, J., and Santamarina, J. C. (2006). "Particle shape effects on packing density, stiffness, and strength: natural and crushed sands." *Journal of Geotechnical and Geoenvironmental Engineering*, 132(5), 591-602.
- Church, M. and Gilbert, R. (1975). "Proglacial fluvial and lacustrine environments." *Glaciofluvial and Glaciolacustrine Sedimentation, Society of Economic Paleontologists and Mineralogists, Special Publication No. 23*, Jopling, A. V. and McDonald, B. C., Eds., Tulsa, Oklahoma, 22-100.
- Cubrinovski, M. and Ishihara, K. (2002). "Maximum and minimum void ratio characteristics of sands." *Soils and Foundations*, 42(6), 65-78.
- Dott, R. H., Jr. and Attig, J. W. (2004). *Roadside geology of Wisconsin*, Mountain Press Publishing Company, Missoula, Montana.
- Drewry, D. J. (1986) *Glacial Geologic Processes*, Edward Arnold, London.
- Edil, T. B., Krizek, R. J., and Zelasko, J. S. (1975). "Effect of grain characteristics on packing of sands." *Proc. Istanbul Conference on Soil Mechanics and Foundation Engineering*, Turkish National Committee of Soil Mechanics and Geotechnical Engineering, Istanbul, Turkey, 46-54.
- Elias, V., Christopher, B. R., and Berg, R. R. (2001). Mechanically Stabilized Earth Walls and Reinforced Soil Slopes Design and Construction Guidelines, U.S. Department of Transportation Federal Highway Administration, Publication No. FHWA-NHI-00-043., Turner-Fairbank Highway Research Center, McLean, Virginia.

- Hennes, R. G. (1952). "The strength of gravel in direct shear." *Symposium on Direct Shear Testing of Soils, ASTM STP 131*, American Society for Testing and Materials, 51-62.
- Holtz, R. D. and Kovacs, W. D. (1981) *An Introduction to Geotechnical Engineering*, Prentice Hall, Upper Saddle River, New Jersey.
- Horn, H. M. and Deere, D. U. (1962). "Frictional characteristics of minerals." *Geotechnique*, 12, 319-335.
- Janoo, V. C. (1998). Quantification of Shape, Angularity, and Surface Texture of Base Course Materials." Special Report 98-1, Cold Regions Research and Engineering Laboratory, US Army Corps of Engineers, Lebanon, NH.
- Jensen, R. P., Edil, T. B., Bosscher, P. J., and Plesha, M. E. (2001). "Effect of particle shape on interface behavior of DEM-simulated granular materials." *International Journal of Geomechanics*, 1(1), 1-19.
- Koerner, R. M. (1970). "Effect of particle characteristics on soil strength." *Journal of the Soil Mechanics and Foundations Division*, American Society of Civil Engineers, 96(4), 1221-1233.
- Kolbuszewski, J. and Frederick, M. R. (1963). "The significance of particle shape and size on the mechanical behavior of granular materials." *Proc. 2nd International Conference on Soil Mechanics and Foundation Engineering*, 4, 253-263.
- Krumbein, W. C. (1941). "Measurement and geological significance of shape and roundness of sedimentary particles." *Journal of Sedimentary Petrology*, 11(2), 64-72.
- Lee, H. A. (1965) Investigation of eskers for mineral exploration, Paper 65-14, Geological Survey of Canada, Ottawa, 1-17.
- Maizels, J. (2002). Sediments and landforms of modern proglacial terrestrial environments, In Menzies, J. (ed), *Modern and past glacial environments*, Butterworth-Heinemann, Oxford, 279-316.
- Naval Facilities Engineering Command (1986). *Soil Mechanics, Design Manual 7.01*.
- Ohnaka, M. (1975). "Frictional characteristics of typical rocks." *Journal of Physics of the Earth*, 23, 87-112.
- Pettijohn, F. J., Potter, P. E., and Siever, R. (1965). *Geology of Sand and Sandstone*, Indiana University, Bloomington, IN.
- Price, R. J. (1973). *Glacial and fluvio-glacial landforms: Geomorphology Text 5*, Clayton, K. M., Ed., Hafner Publishing Company, New York.
- Prothero, D. R. and Schwab, F. (2004). *Sedimentary geology: An introduction to rocks and stratigraphy*, W. H. Freeman and Company, New York.

- Werritty, A. (1992). "Downstream fining in a gravel-bed river in southern Poland; lithological controls and the role of abrasion." In Billi, P., Hey, R. D., Thorne, C. R., and Tacconi, P. (eds.), *Dynamics of Gravel-Bed Rivers*, Wiley, London, 333-350.
- Youd, T. L. (1973). "Factors controlling maximum and minimum densities of sands." *Evaluation of Relative Density and Its Role in Geotechnical Projects Involving Cohesionless Soils*, ASTM STP 523, American Society for Testing and Materials, 98-112.
- Zelasko, J. S. (1966). "An investigation of the influences of particle size, size gradation and particle shape of the shear strength and packing behavior of quartziferous sands." PhD thesis, Northwestern University, Evanston, Illinois.
- Zelasko, J. S., Krizek, R. J. and Edil T. B. (1975). "Shear Behavior of Sands as a Function of Grain Characteristics." *Proc. Istanbul Conference on Soil Mechanics and Foundation Engineering*, Turkish National Committee of Soil Mechanics and Geotechnical Engineering, Istanbul, Turkey, 55-64.

9. TABLES AND FIGURES

Table 1. Index properties of the sands.

Sample	D ₅₀ ¹ (mm)	D ₁₀ ¹ (mm)	C _u ²	C _c ²	% Fines	% Gravel	G _s ³	USCS ²	AASHTO Classification ⁴
P1-S2	0.38	0.20	2.18	1.03	0.4	2.0	2.63	SP	A-3(0)
P1-S4	0.30	0.15	2.67	0.95	1.0	5.7	2.65	SP	A-3(0)
P1-S5	0.44	0.19	2.63	1.01	0.2	1.8	2.65	SP	A-1-b(0)
P1-S6	0.34	0.17	2.35	1.15	0.8	1.8	2.63	SP	A-3(0)
P1-S1	0.31	0.18	1.86	1.12	0.8	0.0	2.64	SP	A-3(0)
P1-S3	0.31	0.15	2.33	0.92	0.8	0.0	2.66	SP	A-3(0)
P1-S7	0.29	0.15	2.03	0.96	0.7	0.0	2.66	SP	A-3(0)
P2-S3	0.16	0.08	2.27	0.86	12.6	10.2	2.68	SM	A-2-4(0)
P3-S3	0.54	0.25	2.48	0.92	0.6	0.3	2.66	SP	A-1-b(0)
P3-S5	0.48	0.19	3.00	0.89	0.8	4.9	2.65	SP	A-1-b(0)
P3-S6	0.29	0.15	2.07	1.04	0.8	0.0	2.65	SP	A-3(0)
P3-S7	0.22	0.15	1.79	0.96	0.6	0.0	2.66	SP	A-3(0)
P2-S1	0.30	0.17	1.88	0.97	1.1	1.0	2.68	SP	A-3(0)
P2-S2	0.20	0.10	2.10	1.20	0.9	0.0	2.67	SP	A-3(0)
P2-S4	0.32	0.08	5.30	1.92	9.8	17.8	2.68	SP-SC	A-3(0)
P2-S9	0.50	0.19	4.16	0.68	0.5	22.1	2.67	SP	A-1-b(0)
P2-S10	0.20	0.09	2.33	1.35	5.0	0.7	2.7	SP	A-3(0)
P2-S11	3.50	0.27	34.07	0.14	0.8	47.8	2.71	SW	A-1-a(0)
P3-S1	0.63	0.25	3.20	0.82	1.1	10.0	2.72	SP	A-1-b(0)
P3-S2	0.48	0.13	4.77	1.04	5.7	12.1	2.72	SP-SM	A-1-b(0)
P4-S1	0.58	0.31	2.00	1.10	0.1	3.3	2.69	SP	A-1-b(0)
P5-S1	0.69	0.18	5.28	0.76	5.2	16.6	2.67	SP-SM	A-1-b(0)
P2-S5	0.64	0.28	2.82	0.84	0.5	8.3	2.76	SP	A-1-b(0)
P2-S6	0.27	0.11	2.82	1.06	3.5	0.4	2.75	SP	A-3(0)
P2-S7	0.15	0.054	3.15	1.32	14.4	0.0	2.75	SM	A-2-4(0)
P2-S8	0.50	0.21	3.05	0.81	1.2	6.7	2.71	SP	A-1-b(0)
P2-S12	0.42	0.18	3.06	0.85	1.6	2.2	2.7	SP	A-3(0)
P3-S4	0.70	0.29	2.86	1.00	0.4	4.3	2.69	SP	A-1-b(0)
P4-S2	0.48	0.21	2.86	0.81	2.3	3.3	2.71	SP	A-1-b(0)
P4-S3	0.77	0.20	6.50	0.59	1.7	13.2	2.74	SP	A-1-b(0)

¹Particle size determined by ASTM D 422, D₅₀=particle diameter at 50% finer, D₁₀=particle diameter at 10% finer

²USCS=Unified Soil Classification System (ASTM D 2487), C_u=coefficient of uniformity, C_c=coefficient of curvature

³Specific gravity (G_s) determined by ASTM C 127 and ASTM D 854

⁴AASHTO=American Association of Highway and Transportation Officials (M 145-91)

Table 2. Physical properties and geological origins of the sands.

Sample	Roundness	e_{\max}^1	e_{\min}^1	$\gamma_{d-\max}^2$ (kN/m ³)	$e_{\gamma d}^2$	ϕ'	Deposit Type	Strength Group
P1-S2	0.61	0.67	0.42	17.92	0.44	32.9	Fluvial Outwash	1
P1-S4	0.59	0.70	0.40	18.30	0.39	33.4	Weathered Sandstone	1
P1-S5	0.62	0.76	0.43	18.15	0.43	32.3	Weathered Sandstone	1
P1-S6	0.62	0.69	0.43	17.59	0.48	32.5	Weathered Sandstone	1
P1-S1	0.50	0.76	0.48	17.36	0.49	35.8	Fluvial Outwash	2
P1-S3	0.40	0.83	0.50	17.08	0.53	34.3	Fluvial Outwash	2
P1-S7	0.42	0.81	0.52	16.88	0.55	34.8	Fluvial Outwash	2
P2-S3	0.24	0.96	0.58	16.02	0.55	35.1	Glaciolacustrine Sand	2
P3-S3	0.59	0.64	0.37	18.39	0.41	35.4	Fluvial Outwash	2
P3-S5	0.56	0.62	0.38	18.54	0.38	36.4	Weathered Sandstone	2
P3-S6	0.36	0.77	0.50	17.12	0.52	34.5	Fluvial Outwash	2
P3-S7	0.46	0.80	0.51	16.98	0.54	35.4	Glaciolacustrine Sand	2
P2-S1	0.31	0.80	0.51	16.98	0.54	36.6	Ice Contact Stratified	3
P2-S2	0.29	0.83	0.56	16.51	0.59	37.8	Glaciolacustrine Sand	3
P2-S4	0.40	0.68	0.39	18.46	0.37	36.5	Glacial Outwash	3
P2-S9	0.43	0.56	0.33	18.11	0.34	38.5	Glacial Outwash	3
P2-S10	0.31	0.75	0.46	17.51	0.50	36.4	Esker	3
P2-S11	0.52	0.43	0.26	18.58	0.23	38.7	Glacial Outwash	3
P3-S1	0.50	0.58	0.35	18.68	0.36	39.2	Glacial Outwash	3
P3-S2	0.48	0.70	0.39	19.08	0.31	36.9	Glacial Outwash	3
P4-S1	0.42	0.84	0.56	16.67	0.58	36.7	Glacial Outwash	3
P5-S1	0.38	0.55	0.31	18.84	0.33	39.1	Ice Contact Stratified	3
P2-S5	0.33	0.69	0.44	18.02	0.44	40.9	Glacial Outwash	4
P2-S6	0.25	0.76	0.46	17.86	0.47	40.5	Drumlin	4
P2-S7	0.22	0.86	0.52	17.69	0.48	39.6	Ice Contact Stratified	4
P2-S8	0.37	0.64	0.40	18.30	0.42	41.5	Glacial Outwash	4

Table 2. Physical properties and geological origins of the sands (Continued).

Sample	Roundness	e_{\max}^1	e_{\min}^1	$\gamma_{d-\max}^2$ (kN/m ³)	$e_{\gamma d}^2$	ϕ'	Deposit Type	Strength Group
P2-S12	0.42	0.64	0.39	18.64	0.42	42.5	Glacial Outwash	4
P3-S4	0.52	0.60	0.37	18.77	0.38	40.3	Fluvial Outwash	4
P4-S2	0.31	0.72	0.44	17.52	0.49	40.7	Ice Contact Stratified	4
P4-S3	0.35	0.62	0.33	18.97	0.37	42.4	Glacial Outwash	4

¹ e_{\max} =maximum void ratio, e_{\min} =minimum void ratio.

² $\gamma_{d-\max}$ =maximum dry unit weight of P4 material, $e_{\gamma d}$ =void ratio at $\gamma_{d-\max}$.

Table 3. Mineralogical percentages of select sands from X-Ray diffraction.

Sample	Quartz	Potassium-Feldspar	Plagioclase	Calcite	Hematite	Dolomite	Pyrite	Total Phyllosilicates*
P1-S1	91.0	3.0	5.6	0.4	0.4	0.0	0.0	0.0
P1-S2	97.0	1.3	0.2	0.1	0.0	0.4	0.4	1.0
P1-S3	69.0	5.3	21.0	0.0	1.2	1.8	0.0	2.3
P1-S6	99.0	0.6	0.1	0.0	0.0	0.0	0.0	0.7
P2-S1	73.0	6.0	2.8	2.5	0.0	15.0	0.0	0.2
P2-S5	25.0	2.6	7.9	0.3	0.0	62.0	0.0	2.0
P2-S12	58.0	2.2	5.5	0.0	2.6	31.0	0.0	1.1
P3-S1	72.0	3.8	2.3	0.3	0.0	21.0	0.0	1.0
P3-S2	70.0	0.5	6.7	1.8	0.0	20.0	0.0	1.1
P3-S3	93.0	2.7	1.6	0.9	0.0	0.0	0.0	1.3
P3-S4	83.0	4.7	8.9	0.0	0.0	0.0	1.9	1.8
P3-S5	95.0	3.0	1.3	0.0	0.0	0.0	0.0	0.8
P4-S1	88.0	1.1	8.7	0.3	1.2	0.0	0.0	1.2
P4-S2	60.0	5.6	25.0	0.4	2.5	0.0	0.0	6.4
P5-S1	74.0	9.3	12.0	0.7	1.0	0.0	0.0	2.6

*Includes Illite, Mica, Kaolinite and Chlorite

Table 4. Friction angle groups with respective range of friction angles and geologic origin

Group 1 ϕ' (32°-34°)	Group 2 ϕ' (34°-36°)	Group 3 ϕ' (36°-39°)	Group 4 ϕ' (39°-43°)
WS	WS	GO	FO
WS	FO	GO	GO
WS	FO	GO	GO
FO	FO	GO	GO
	FO	GO	GO
	FO	GO	ICS
	GL	ICS	ICS
	GL	ICS	Drumlin
		Esker	
		GL	

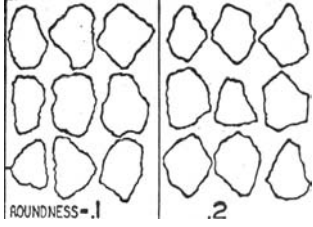
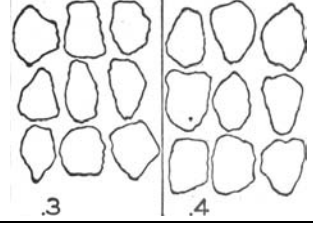
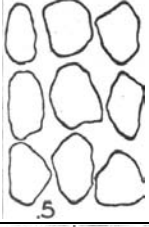
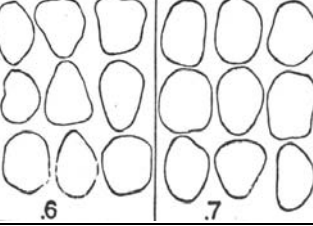
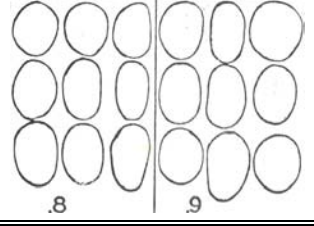
WS: Weathered Sandstone; FO: Fluvial Outwash; GO: Glacial Outwash
GL: Glacial Lacustrine; ICS: Ice Contact Stratified

Table 5. Average and standard deviation of independent variables in Eq. 2 for strength groups, ϕ' predicted with Eq. 2 using average independent variables, and range of ϕ' predicted with Eq. 2 using independent variables unique to each sand.

Group	D_{10} (mm)	γ_{d-max} (kN/m ³)	Roundness	Measured ϕ'	Predicted Average ϕ'	Predicted Range ϕ'
1	$0.192 \pm 0.079^*$	18.22 ± 0.53	0.35 ± 0.10	41.0 ± 1.0	40.3	42.2 - 39.3
2	0.177 ± 0.08	17.94 ± 0.95	0.40 ± 0.08	37.6 ± 1.2	38.1	40.7 - 35.8
3	0.161 ± 0.049	17.30 ± 0.82	0.44 ± 0.11	35.2 ± 0.7	35.3	36.6 - 33.7
4	0.178 ± 0.022	17.99 ± 0.31	0.61 ± 0.01	32.8 ± 0.5	33.2	33.8 - 31.8

* Standard deviation

Table 6. Roundness categories including Krumbein images, range of roundness, and average roundness.

Roundness	Krumbein Image*	Range	Average
Angular		0.10 - 0.26	0.18
Subangular		0.26 - 0.42	0.34
Subrounded		0.42 - 0.58	0.50
Rounded		0.58 - 0.74	0.66
Well-Rounded		0.74 - 0.90	0.82

*adapted from Krumbein (1941).

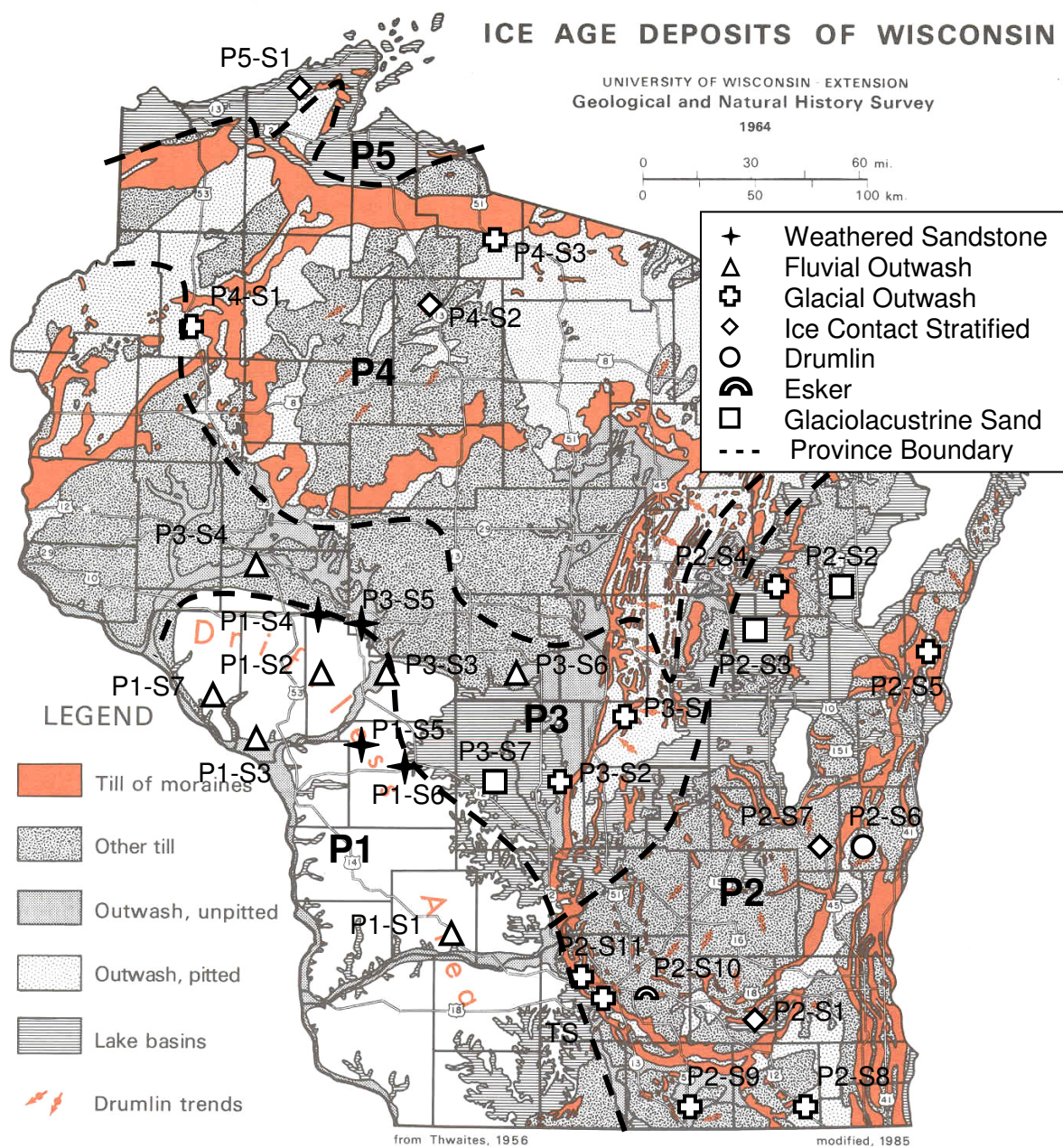


Fig. 1. Sample location and geologic origin of the sands.

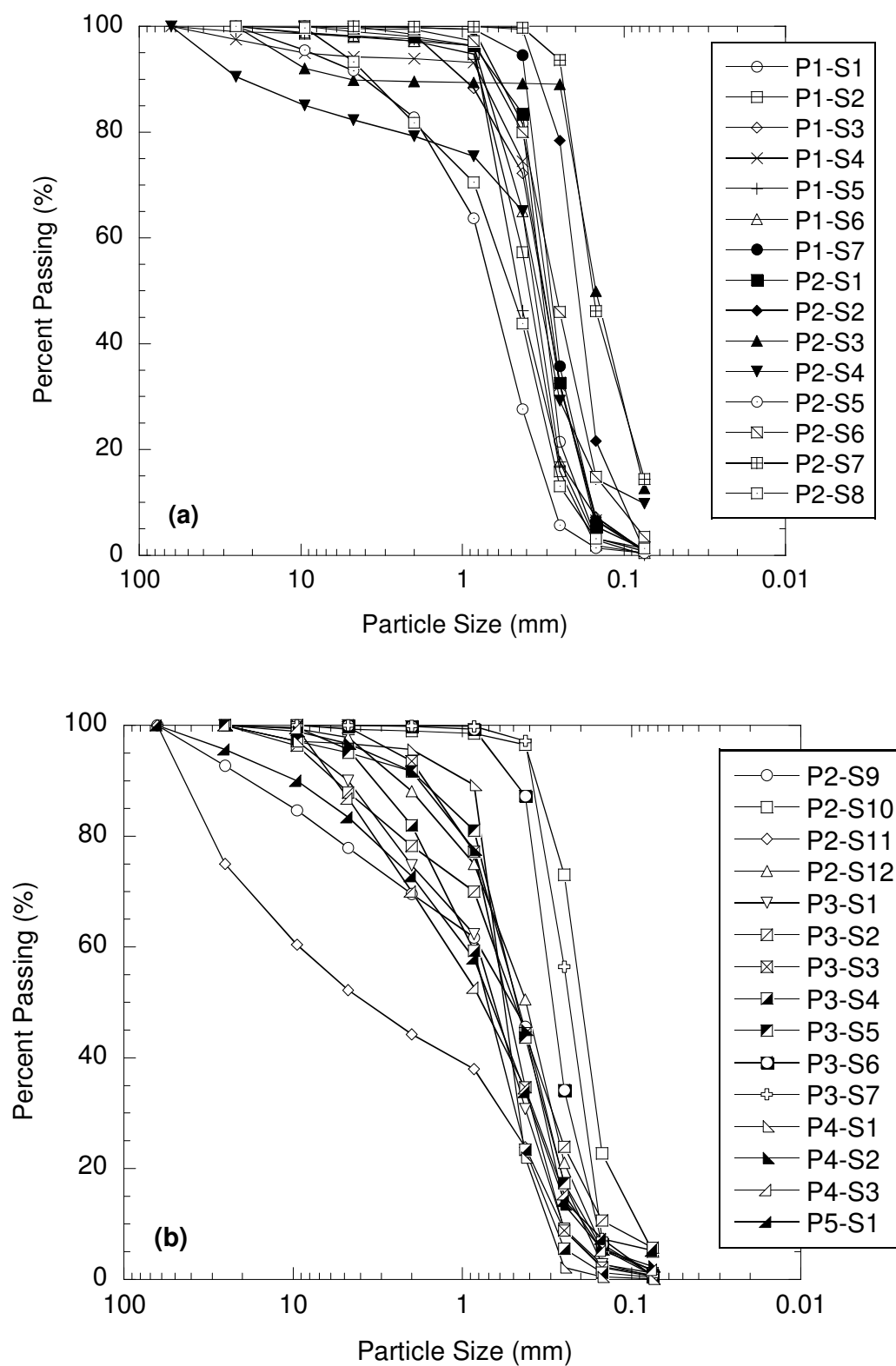


Fig. 2 Particle-size distribution curves: (a) P1-S1 through P2-S8, (b) P2-S9 through P5-S1.

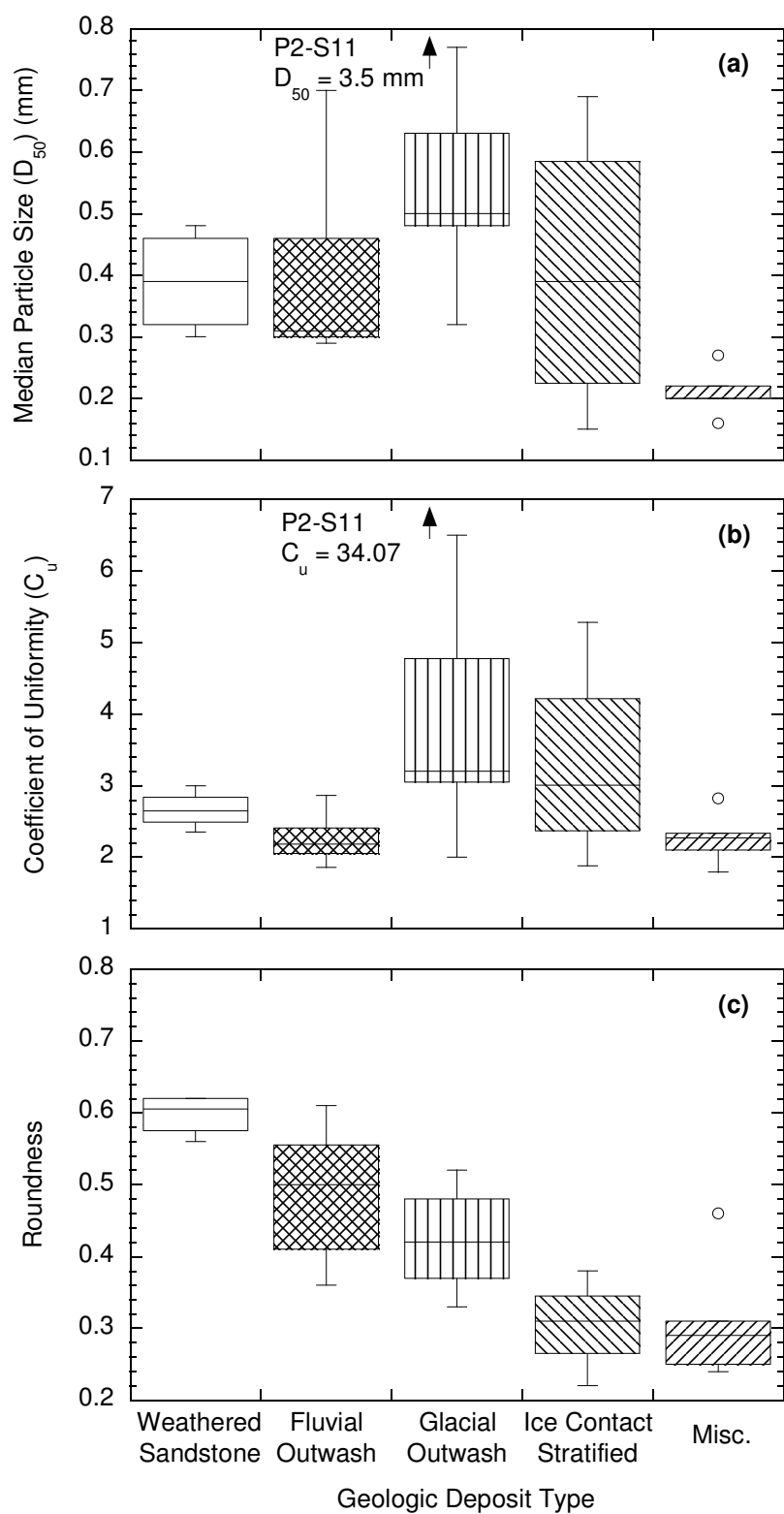


Fig. 3. Influence of geologic deposit type on physical characteristics of sands: (a) median particle size, (b) coefficient of uniformity, (c) particle roundness.

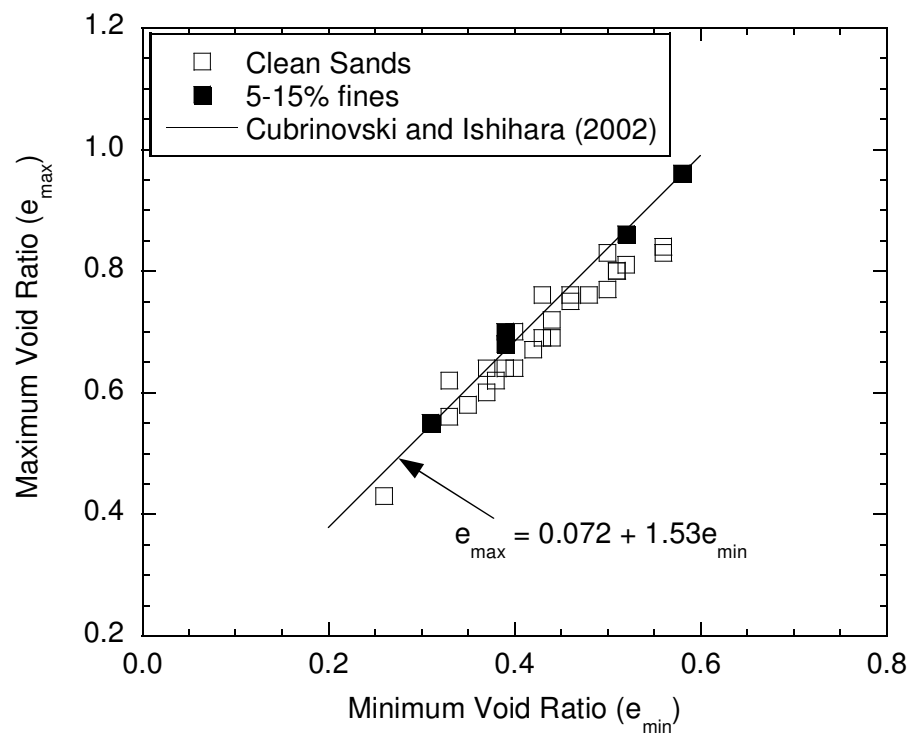


Fig. 4. Relationship between maximum void ratio and minimum void ratio and comparison to trend line for clean sands (< 5% fines) reported by Cubrinovski and Ishihara (2002).

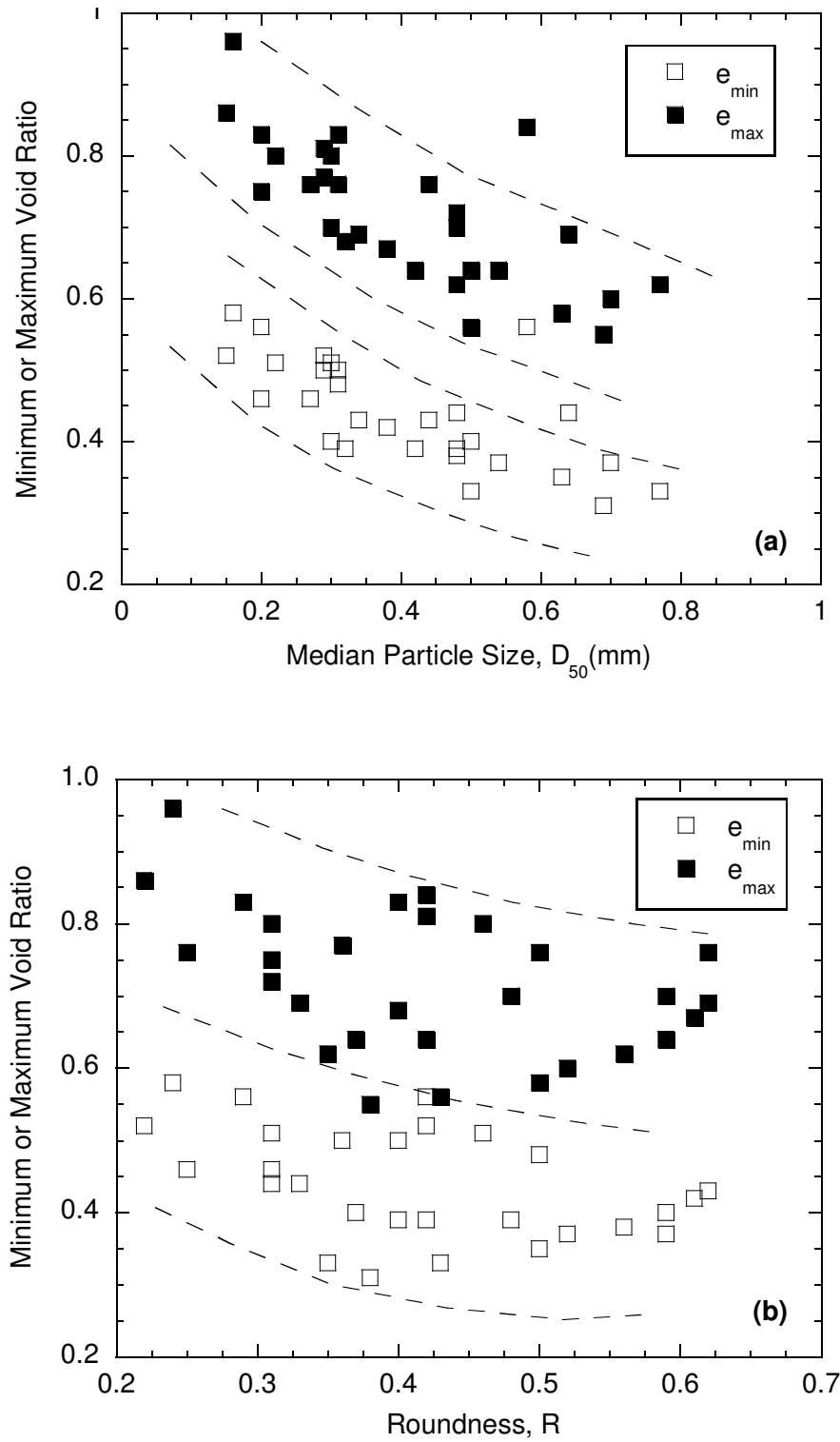


Fig. 5. Relationships between minimum and maximum void ratio and (a) median grain size (D_{50}) and (b) roundness.

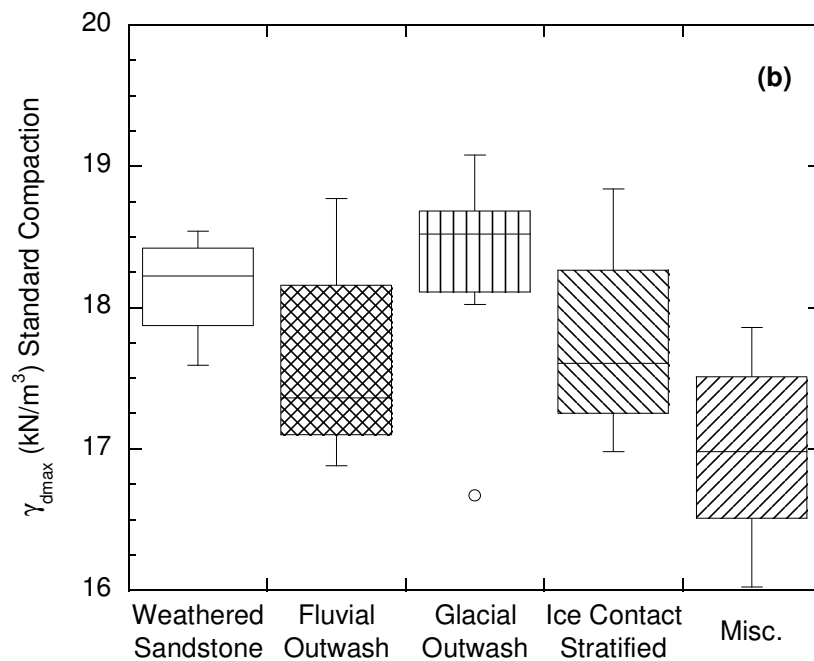
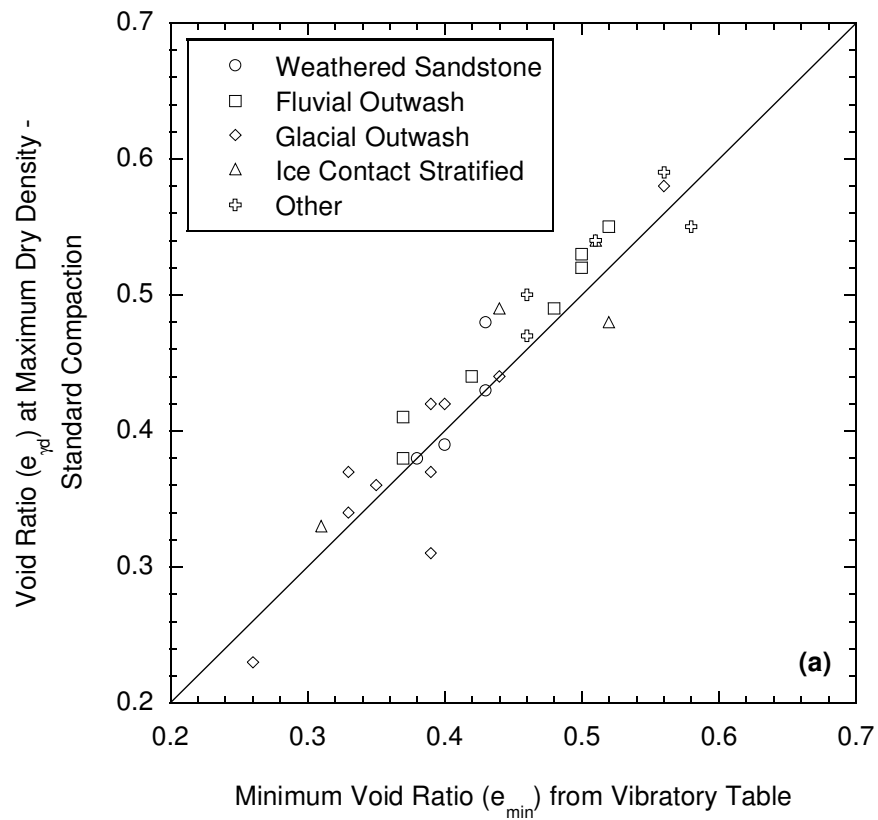


Fig. 6. Minimum void ratio at maximum dry density from standard compaction vs. minimum void ratio from vibratory table (a) and influence of geologic origin on maximum dry unit weight (b).

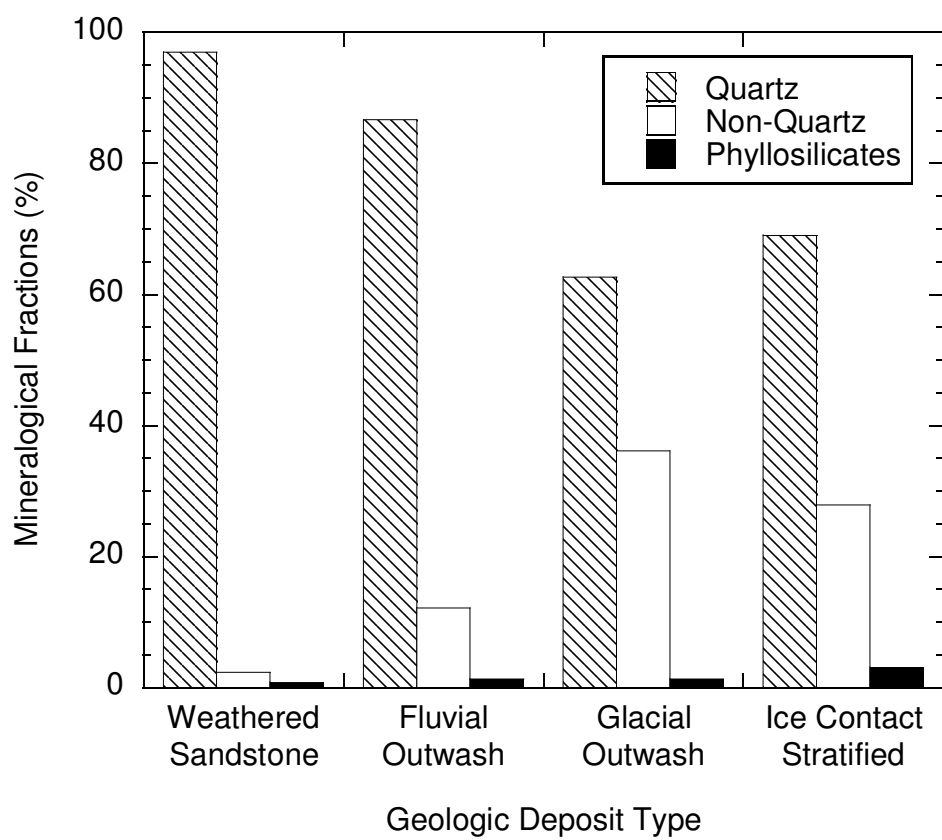


Fig. 7. Percentages of mineralogical components in sands for different geologic deposits.

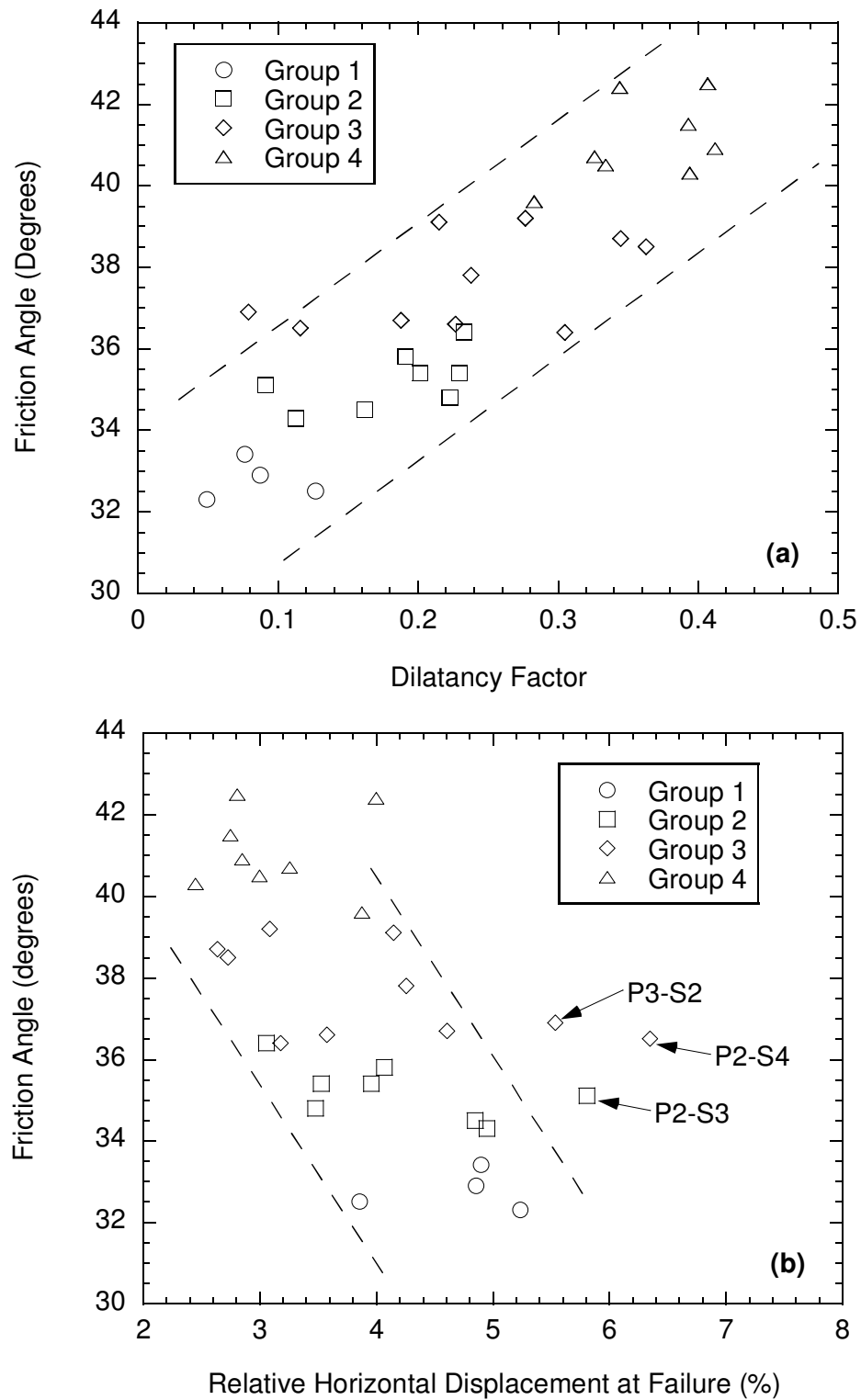


Fig. 8. Comparison of ϕ' and dilatancy factor (a) and comparison of ϕ' and relative horizontal displacement at failure (%) (b).

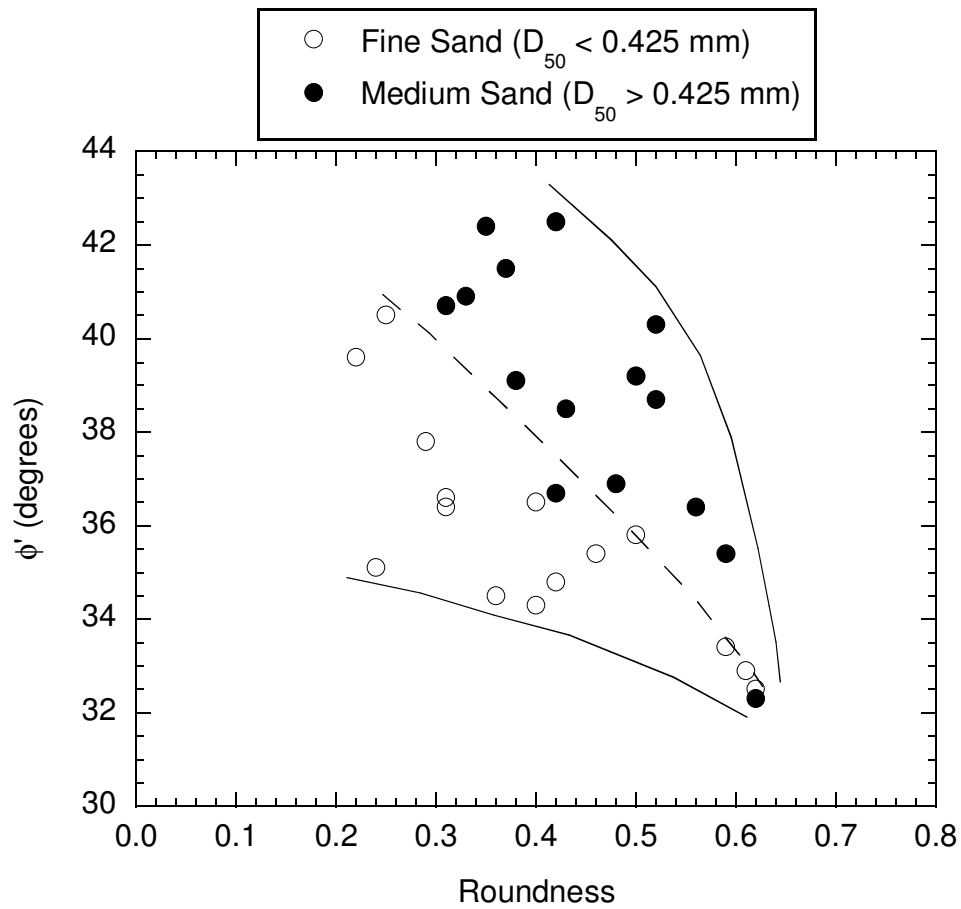


Fig. 9. Relationship between friction angle and roundness for fine sand ($D_{50} < 0.425$ mm) and medium sand ($D_{50} > 0.425$ mm).

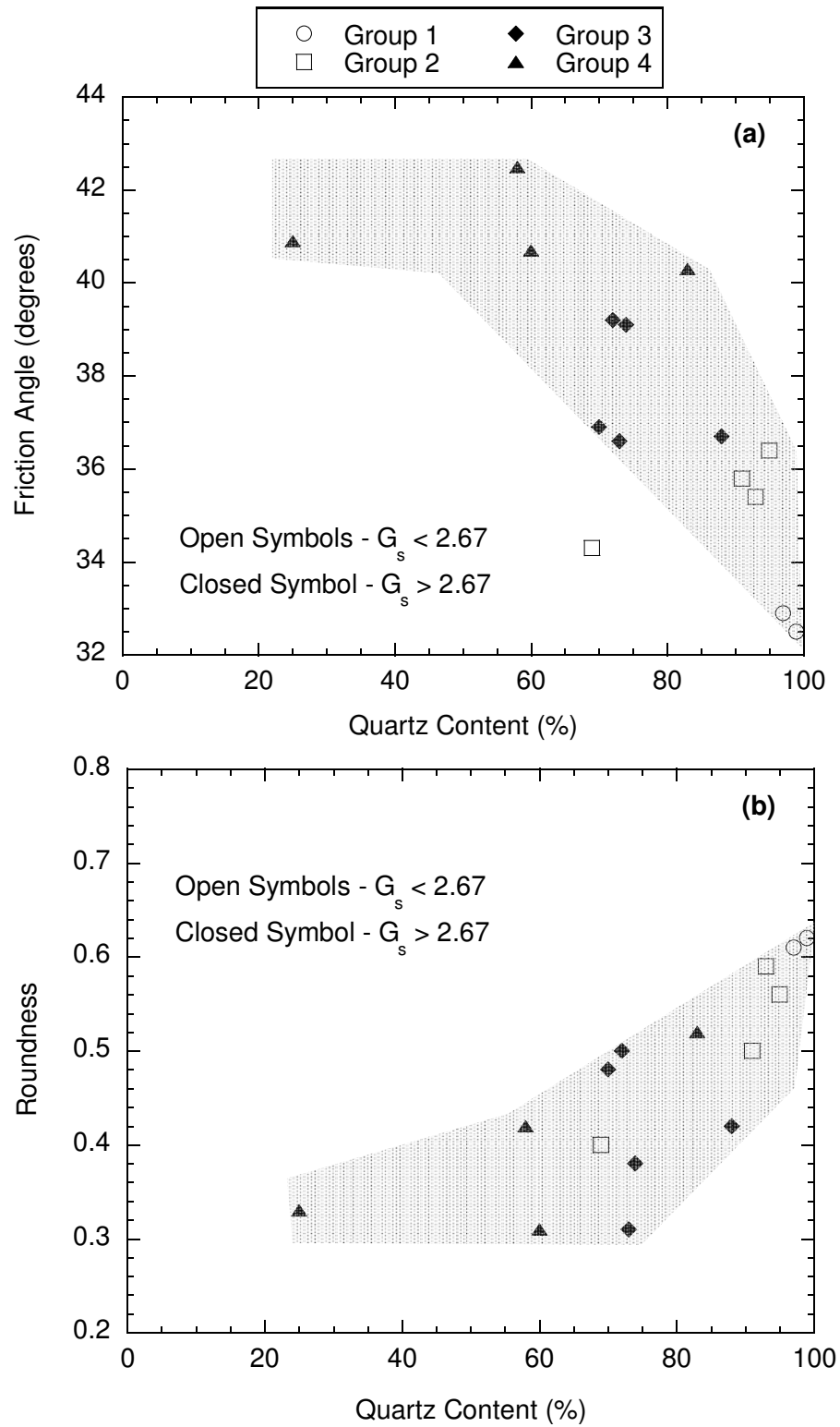


Fig. 10. Influence of quartz content (%) on ϕ' (a) and roundness (b).

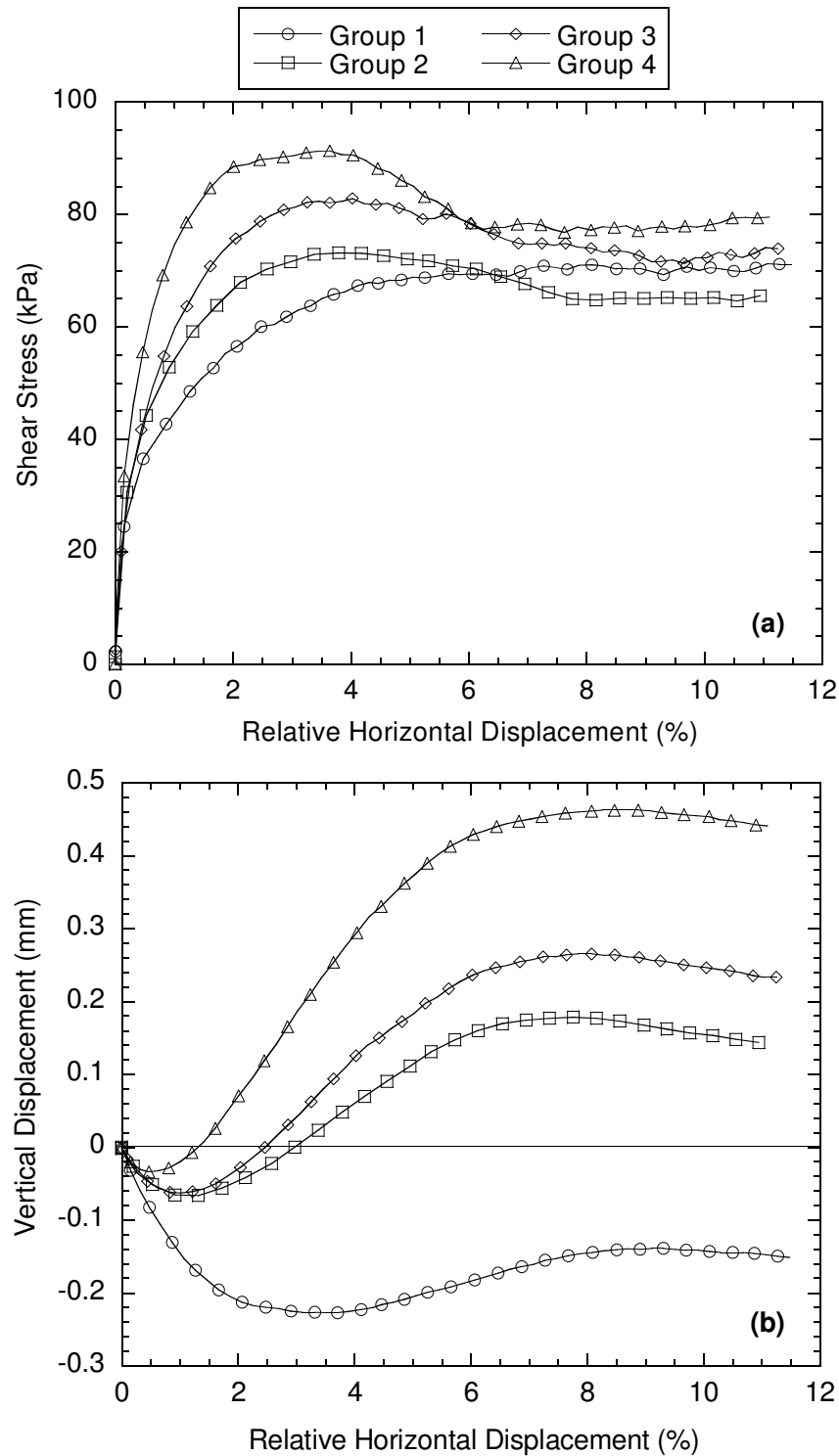


Fig. 11. Representative behavior of sands: (a) shear stress vs. relative horizontal displacement (RHD) and (b) vertical displacement vs. RHD in each strength group at normal stress of 99 kPa. Group 1 (P1-S4), Group 2 (P3-S7), Group 3 (P5-S1) and Group 4 (P2-S5).

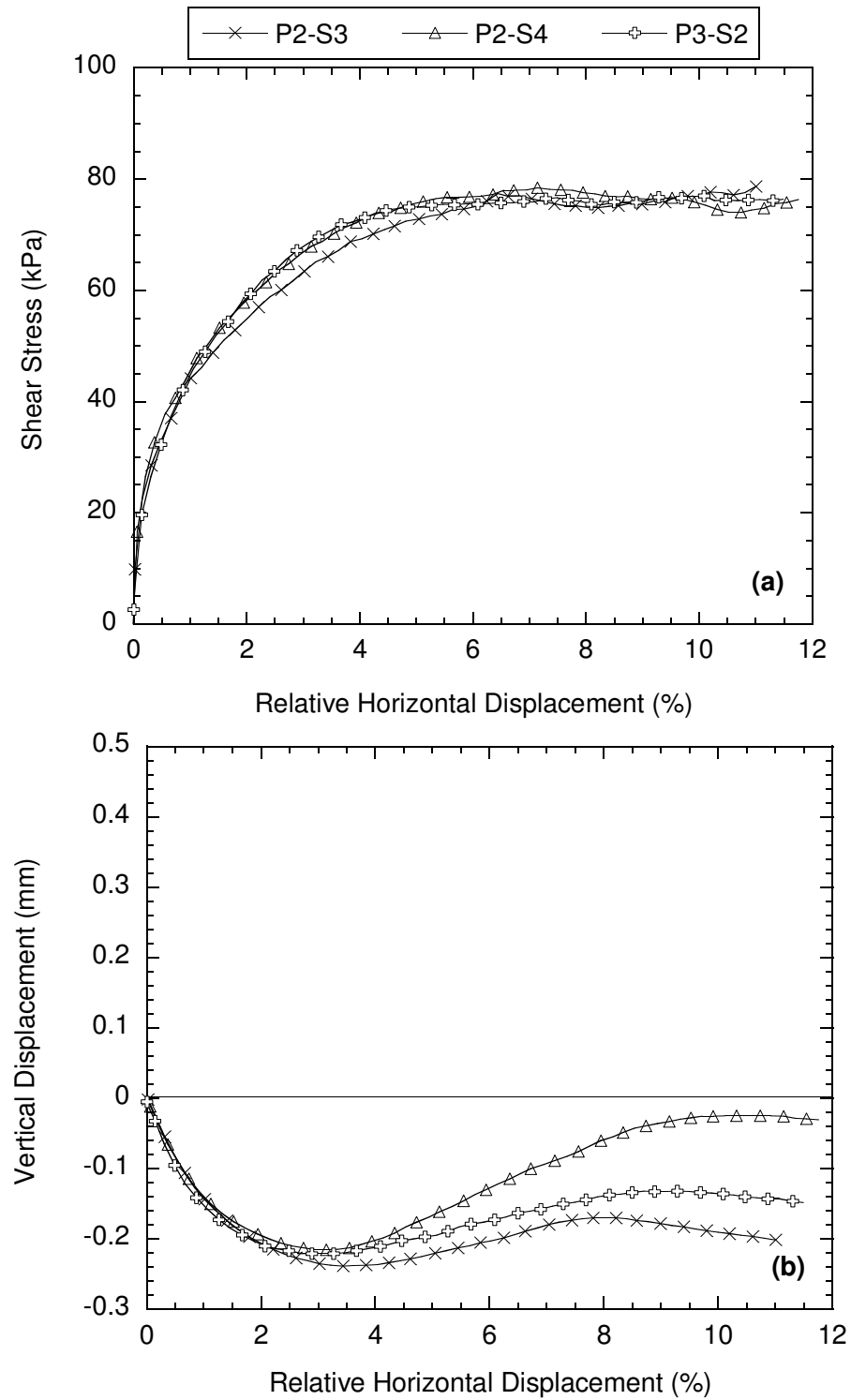


Fig. 12. Relationships between shear stress and relative horizontal displacement (RHD) (a) and vertical displacement and RHD (b) at normal stress of 99 kPa for sands P2-S3, P2-S4, and P3-S2.

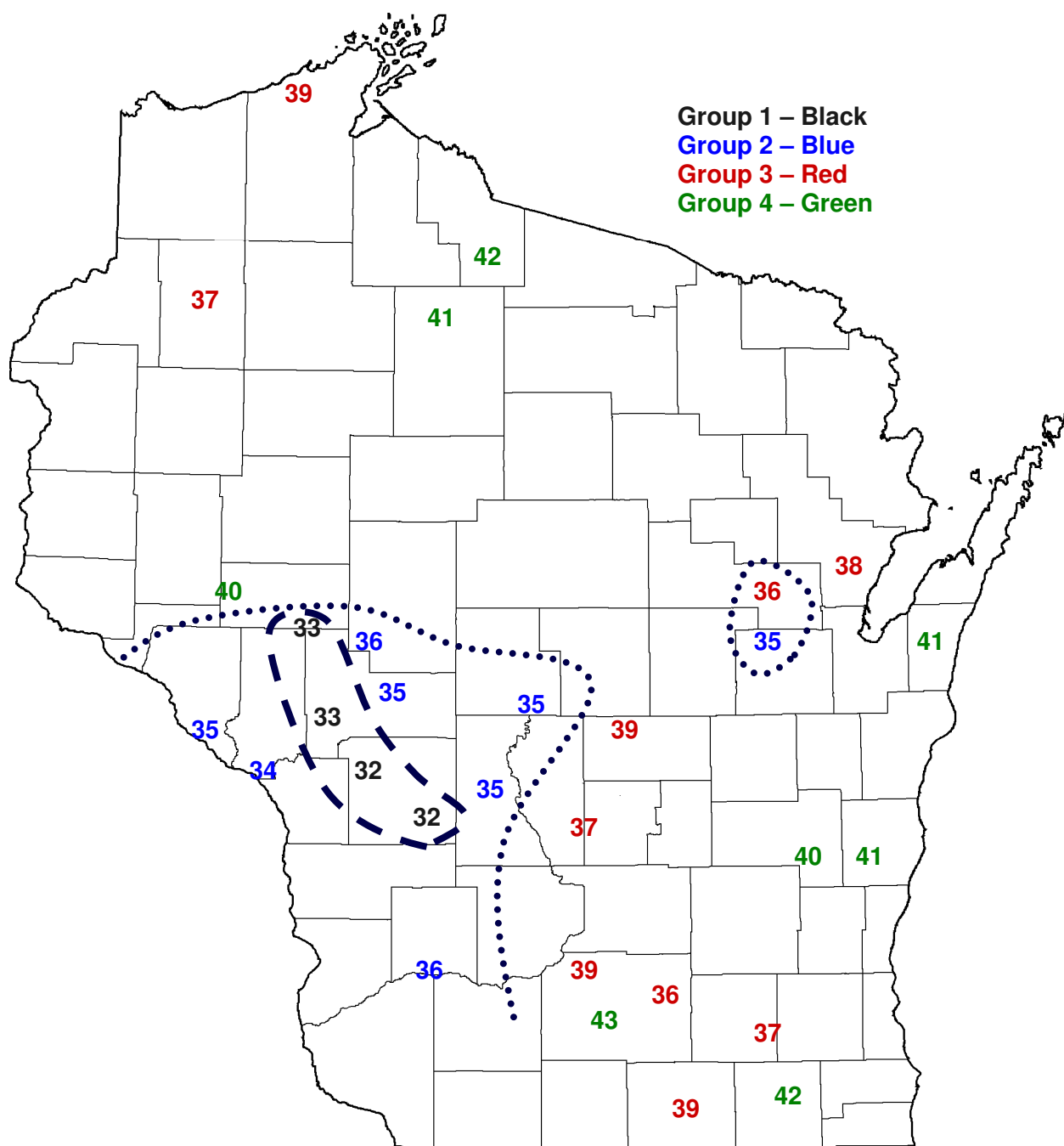


Fig. 13. Wisconsin state map with friction angles superimposed on sample locations.

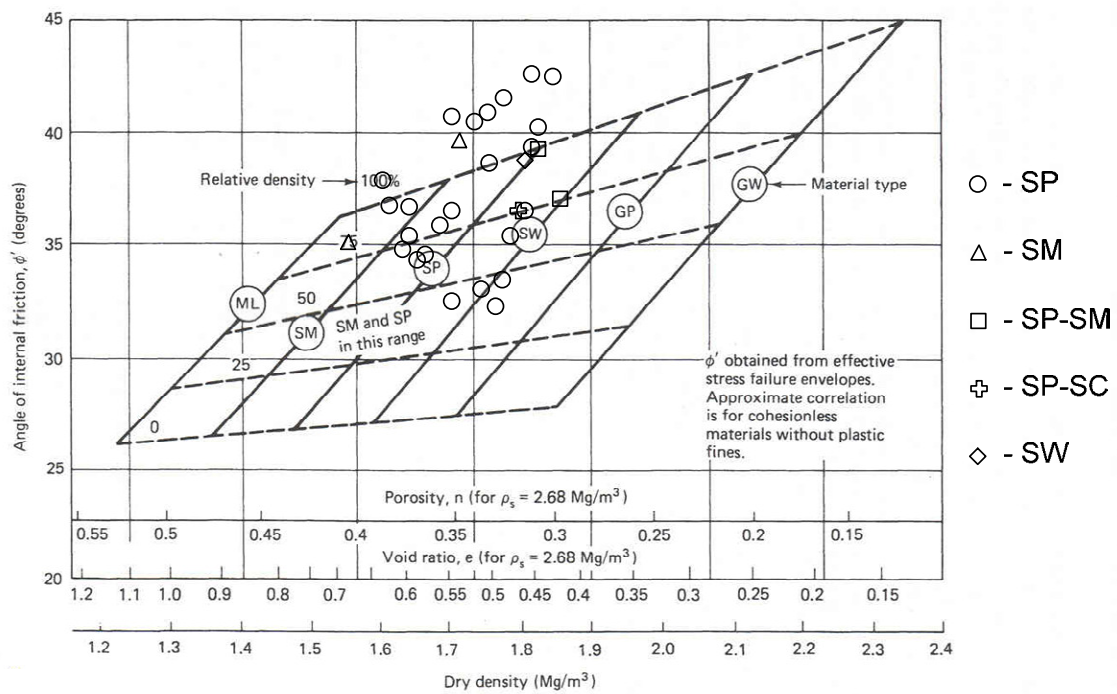


Fig. 14. Relationships of friction angle and density as reported in NAVFAC D 7.01 (1986) with friction angle vs. compacted density for the present study superimposed.

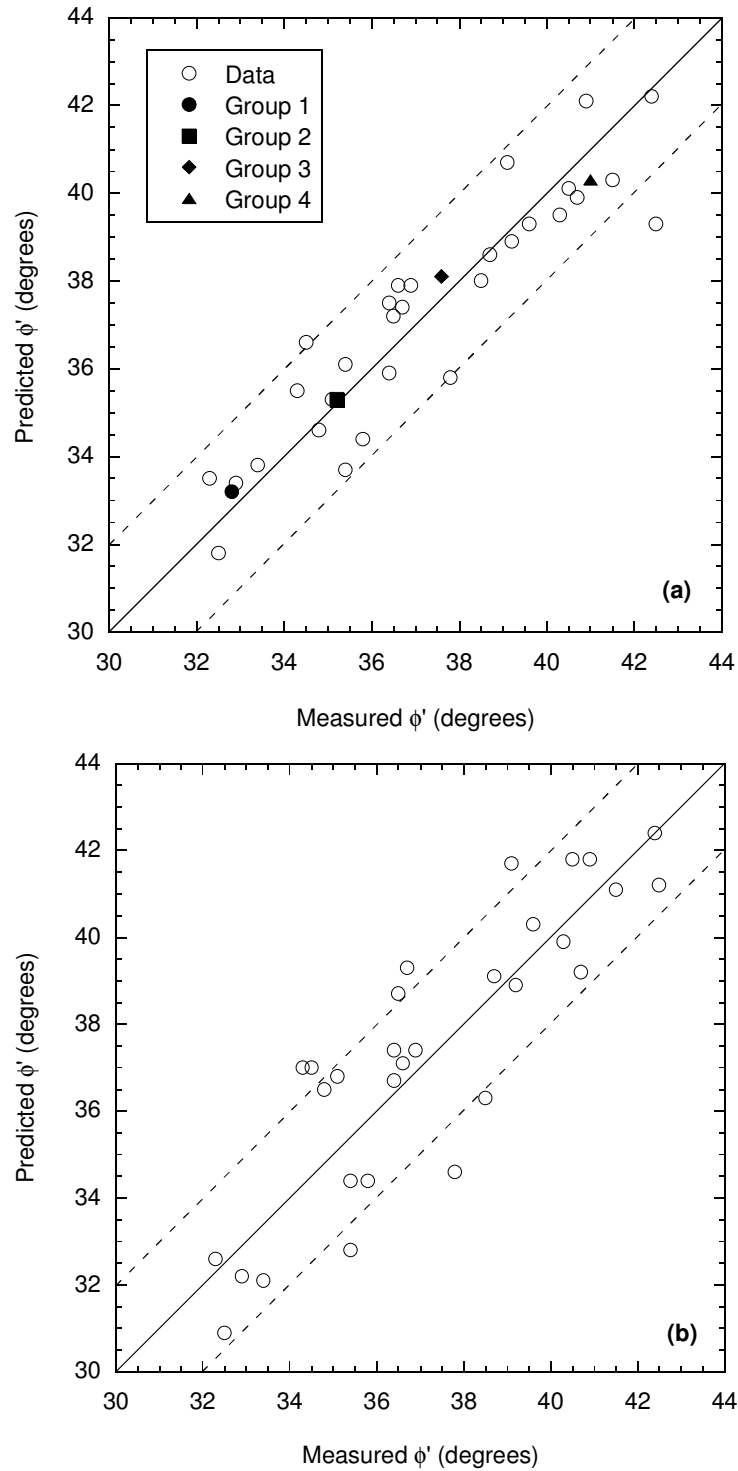


Fig. 15. Comparison between ϕ' predicted using regression model and ϕ' measured in direct shear (a) and ϕ' predicted using regression model with average roundness and ϕ' measured in direct shear (b).

APPENDICIES

APPENDIX A

COMPARISON OF SHEAR STRENGTH OF GRANULAR BACKFILL MEASURED IN SMALL-SCALE AND LARGE-SCALE DIRECT SHEAR TESTS

ABSTRACT: Direct shear tests were conducted on 30 granular backfill materials having gravel contents ranging from 0 to 30% in a 64-mm square small-scale direct shear (SS-DS) box and a 305-mm square large-scale direct shear (LS-DS) box. The objective was to compare the shear behavior and shear strength of clean granular backfills in SS-DS and LS-DS. Triaxial compression (TC) tests were also conducted on four of the backfill materials for comparison with the SS-DS and LS-DS tests. Specimens tested in SS-DS and TC included only material passing the No. 4 sieve (P4). Test specimens in LS-DS included the P4 material as well as material retained on No. 4 sieve (R4). Friction angles corresponding to peak strength (ϕ') measured in SS-DS and LS-DS differed by no more than 4° for a given granular backfill, and in most cases were within 2° . The friction angles also were unaffected by removal of the R4 material. Repeatability tests showed that statistically similar failure envelopes (p -value = 0.98) are obtained in SS-DS and LS-DS, and that highly repeatable friction angles (ϕ') are obtained using the SS-DS ($\phi' \pm 0.25^\circ$) and the LS-DS ($\phi' \pm 0.45^\circ$) methods. No statistically significant difference was found between the failure envelopes measured in SS-DS, LS-DS, and TC, suggesting that ϕ' for clean granular backfill can be measured with similar accuracy using any of the three test methods.

A-1.INTRODUCTION

The direct shear (DS) test is commonly used in commercial geotechnical laboratories in North America for testing granular materials used as backfill for mechanically stabilized earth (MSE) walls and reinforced soil (RS) slopes. Most tests are conducted following the procedures described in AASHTO T 236 (*Standard Method of Test for Direct Shear Test of Soil Under Consolidated Drained Conditions*) or ASTM D 3080 (*Standard Test Method for Direct Shear Test of Soils Under Consolidated Drained Conditions*) in a small-scale direct shear (SS-DS) box that is square or circular. Both test methods require that the width (or diameter) of the shear box must be at least 50 mm, the specimen thickness must be at least 13 mm, and the specimen width-to-thickness ratio be at least 2:1. The test methods also require that the width (or diameter) of the shear box be at least 10 times the maximum particle diameter and that the initial specimen thickness be at least 6 times the maximum particle diameter. Thus, for typical SS-DS boxes, which have a width of diameter of 64 - 73 mm (Bareither 2006), the maximum particle size is approximately 5 mm. Therefore, when granular backfill materials contain gravel (i.e., particles > 4.75 mm), the gravel-size particles are removed ('scalped') if tests are conducted in SS-DS. Alternatively, a large-scale direct shear (LS-DS) box that accommodates larger particles is used.

Previous studies have shown that similar shear strength and shear behavior can be obtained in direct shear using shear boxes of different size (Taylor and Leps 1938, Bishop 1948, Palmeira and Milligan 1989). However, the previous studies have been limited to uniformly graded sands, and each study focused on a single sand. The influence of gravel content on the shear strength and shear behavior of sands has also been studied (Fragaszy et al. 1992, Simoni and Houlsby 2006), but these studies have focused on a single sand matrix blended with one or two gravels. To the authors' knowledge, no studies have been conducted to evaluate the

significance of test size or gravel content for a broad variety of naturally occurring granular backfill materials.

This study had two objectives. One objective was to compare the shearing behavior of a broad range of natural granular backfill materials tested in SS-DS and LS-DS. Another objective was to determine if the same friction angle (ϕ') is obtained in SS-DS and LS-DS when the natural backfill material contains or excludes gravel. Tests were conducted on 30 naturally occurring granular backfill materials from Wisconsin under identical conditions in a LS-DS box (305 mm square) that accommodates a maximum particle diameter of 25.4 mm (based on the criterion in AASHTO T 236) and a SS-DS box (64 mm square) that accommodates a maximum particle diameter of 4.75 mm. The backfill materials contained gravel contents ranging from 0 to 30%, of which 12 backfill materials required different amounts of scalping to meet the maximum particle size criteria in SS-DS. Consolidated-drained triaxial compression (TC) tests were also conducted on four of the backfill materials for comparison with the SS-DS and LS-DS tests.

A-2. BACKGROUND

Taylor and Leps (1938) performed comparative tests on oven-dried Ottawa sand in small (76 mm) and large (305 mm) square direct shear boxes to assess the influence of specimen size on ϕ' . They report that ϕ' measured in the large shear box was 0.5° smaller, on average, than ϕ' measured in the small box.

Bishop (1948) also conducted direct shear tests on a dry sand in small (60 mm) and large (305 mm) shear boxes. For porosities ranging from 0.36 to 0.46, ϕ' from the small shear box was within $\pm 2^\circ$ of ϕ' measured with the large shear box. Bishop also tested various well-graded gravels with a maximum particle diameter of 38 mm in the large shear box to investigate

the influence of gradation on shear behavior. Bishop concluded that the larger particles did not control the shear behavior of well-graded gravels.

Palmeira and Milligan (1989) performed direct shear tests on dry Leighton Buzzard sand in a 1 m cubic box, a 252 mm by 152 mm box (thickness = 152 mm), and a traditional 60 mm square box (thickness = 32 mm) to analyze scale effects. The sand had particles ranging in size from 0.6 to 1.2 mm. They report ϕ' between 49° and 50° for tests conducted in all three boxes.

Fragaszy et al. (1992) conducted consolidated-drained and consolidated-undrained triaxial tests on mixtures of “oversize” particles (12.7 mm to 25.4 mm) and sandy gravel (particles < 12.7 mm) to evaluate how the oversize particles affected shear strength. Tests were conducted on the sandy gravel matrix alone, the oversize particles alone, and on mixtures of the sandy gravel blended with oversize particles (10% to 90%, by weight). They conclude that the peak strength and deformation behavior of soils containing < 40% sub-rounded to rounded oversize particles in a finer-grained matrix can be determined by testing the matrix material alone provided that the density of the matrix material is the same.

Simoni and Houlsby (2006) performed shear box tests in a large apparatus (254 mm x 152 mm, specimen thickness = 150 mm) on poorly graded silica sand blended with 10 to 60% gravel, defined as particles larger than 2 mm and smaller than 20 mm. They report similar peak friction angles for pure sand and sand and gravel mixtures with up to 20% gravel tested at similar sand matrix densities. For sand and gravel mixtures with gravel $\geq 30\%$, they report an increase in peak-strength friction angle for specimens tested at similar sand matrix densities.

A-3. MATERIALS AND METHODS

A-3.1. SANDS

Shear tests were conducted on thirty naturally occurring sands from Wisconsin having different geologic origins. The sands were obtained from borrow pits used for granular backfill by the Wisconsin Department of Transportation (WisDOT) and are grouped into five geographical-geological provinces. Particle size distribution curves for the 30 sands are shown in Fig. A-1. Physical characteristics of the sands are summarized in Table A-1. The maximum dry unit weight (γ_{d-max}) in Table A-1 was determined using a standard Proctor compaction test. Compaction testing was conducted in addition to testing for e_{max} and e_{min} because γ_{d-max} is commonly used in practice for controlling the unit weight of granular backfill.

Twenty-four sands classify as poorly graded sand (SP), three as poorly graded sands with fines and/or gravel (SP-SM or SP-SC), two as silty sands (SM), and one as well graded sand with gravel (SW). Although the majority of the sands share a common classification (SP), the gradations vary considerably (Fig. A-1) with Coefficient of Uniformity (C_u) ranging from 1.79 to 6.50. The other physical properties also exhibit considerable variation: $G_s = 2.63$ to 2.76 , $e_{max} = 0.43$ to 0.96 , $e_{min} = 0.26$ to 0.58 , $\gamma_{d-max} = 16.02$ to 19.08 kN/m^3 , and roundness = 0.22 to 0.62 .

A-3.2. SMALL-SCALE DIRECT SHEAR TESTS

Small-scale direct shear (SS-DS) tests were conducted following the procedure in AASHTO T 236-92 using a square shear box 64-mm wide containing a specimen 31 mm thick. Tests were conducted for normal stresses between 26 and 184 kPa. The maximum stress is comparable to the stress expected at the bottom of a 10-m high MSE wall backfilled with dense granular fill having a unit weight of approximately 18 kN/m^3 .

Sands tested in SS-DS were air dried and sieved past a No. 4 sieve (4.75 mm). Material passing the No. 4 sieve (P4) was used to ensure that the ratio of box length to maximum particle diameter was at least 10 and that the ratio of box thickness to maximum particle diameter was at least 6, as stipulated in AASHTO T 236-92. The sand was compacted in the shear box in three lifts of equal thickness by tamping the top of each lift with a wood tamper. The number of tamps per layer was adjusted to achieve the target density for each specimen (95% of maximum dry density determined by standard Proctor compaction, which is the backfill compaction criterion recommended by the US Federal Highway Administration, Elias et al. 2001).

Inundation of the specimen followed immediately after the normal stress was applied. Drainage was permitted through 9-mm-thick perforated PVC plates placed on the top and bottom of the specimen. Separation was provided by a thin non-woven heat-bonded calendered geotextile placed between the sand and the plates. Compression of the PVC and geotextile was measured at each normal stress. Volume change measurements on initial normal loading were corrected for compression of the PVC plate and geotextile.

All tests were conducted at a constant rate of horizontal displacement of 0.24 mm/min to a maximum horizontal displacement of 7 mm. Measurements of horizontal displacement, vertical displacement, and shear force were recorded using a personal computer equipped with a Validyne data acquisition card (UPC601-U) and LABView software. Two linear variable displacement transducers (LVDTs) (Schlumberger Industries Model AG/5, 5 ± 0.003 mm) were used to measure horizontal and vertical displacements and a load cell (Revere Transducer Model 363-D3-500-20P1, 2.2 ± 0.00015 kN) was used to measure shear force. Sixty data points were recorded during each test. Normal and shear stresses were computed from the loads using a displacement-corrected area of the shear plane.

A-3.3. LARGE-SCALE DIRECT SHEAR TESTS

The large-scale direct shear (LS-DS) tests were also performed following the procedures in AASHTO T 236-92. A schematic of the LS-DS box is in Fig. A-2. The LS-DS box is 305 mm square, contains a 152-mm-thick specimen, and is constructed from stainless steel plate (13 mm for the sides, 19 mm for the front and back). A rear platform (19 mm thick aluminum plate) (Fig. A-2) was included to allow displacement of the upper and lower boxes without loss of soil. Teflon[®] sheet was affixed to the inner walls of the box to reduce side wall friction. The Teflon lining was inspected prior to each test and replaced periodically as needed. The shear box is contained within an external box that acts as a reservoir for inundation of the specimen.

Shear displacement is controlled by a stepper motor that drives the external box on a slide track (the lower half of the shear box is bolted to the external box). Movement of the upper portion of the shear box is prevented by a horizontal arm affixed to the frame of the machine. A load cell mounted between the arm and the frame is used to measure the shear force. Normal force is applied through a rubber bladder filled with compressed air that is overlain by two steel plates. A vertical arm mounted to the frame acts on the steel plates to provide the reaction for the rubber bladder. A load cell mounted on the arm monitors the normal force. Normal forces are maintained by a feedback-controlled pressure regulator attached to the rubber bladder and the load cell attached to the vertical arm.

Measurements of horizontal displacement, vertical displacement, normal force, and shear force were recorded using a personal computer equipped with a Validyne data acquisition card (UPC601-U) and LABView software. Two LVDTs were used for measuring vertical displacements (Solartron model M9200000721-02, 30 ± 0.02 and HR Series 1000 HR, 50 ± 0.025 mm) and one LVDT was used to measure horizontal displacement (Solartron model M920002A721-01, 100 ± 0.01 mm). One load cell (Sensotec 89 ± 0.15 kN load cell model

41/0573-05) was used to measure shear force and one load cell (Sensotec 133 \pm 0.22 kN load cell model 41/0573-05) were used to measure normal force.

Sand used in the LS-DS tests was sieved past a 25.4 mm sieve to meet criterion of maximum particle diameter to box dimensions as stipulated in AASHTO T 236. To ensure that shear strengths measured in SS-DS and LS-DS could be compared directly, the density of P4 material (i.e., the fraction used in the SS-DS tests) was maintained the same in the SS-DS and LS-DS tests. Particles larger than the No. 4 sieve and smaller than 25.4 mm were assumed to behave as independent clasts within the P4 matrix (The method used to compute the density of the material tested in LS-DS is in Appendix C). Specimens for LS-DS testing were prepared using the same procedure used for the SS-DS tests and were placed between perforated PVC plates (13 mm thick) using non-woven heat-bonded calendered geotextiles for separation. Each sand was tested in LS-DS at five normal stresses (26, 69, 105, 148, and 184 kPa), with inundation immediately following application of the normal stress. Compression of the specimen was monitored during normal stress application and inundation. All specimens were sheared at a rate of 0.24 mm/min to a maximum horizontal displacement of 38 mm. Approximately 300 data points were recorded during each test.

Due to the weight and size of the LS-DS shear box, a gap between the upper and lower boxes could not be maintained during shearing. Therefore, LS-DS data were corrected to account for box friction at the shear box interface. Similar corrections were not applied to the SS-DS data because testing showed that box friction in SS-DS was negligible (See Appendix A1). Shear resistance due to box friction (τ_B) was determined by the following equation:

$$\tau_B = \left[\frac{F_N(1 - \alpha) + W'_B}{A_{CB}} \right] \times \mu_B \quad (3)$$

where F_N is the applied normal force, α is the fraction of the applied normal force transmitted to the shear plane and accounts for load transfer into the box walls, W'_B is the effective weight of the upper box, A_{CB} is the contact area of the shear box interface, and μ_B is the coefficient of friction of the shear box interface. Details of the LS-DS box friction correction are included in Appendix A2. Tests were conducted on sands to determine α (see Appendix A1). These tests showed that α ranged between 0.907 and 0.936. An $\alpha = 0.9203$ was used to compute the applied normal stress and the box friction in each test.

A-3.4. REPEATABILITY OF DIRECT SHEAR METHODS

Repeatability of the testing method was evaluated by conducting five replicate tests in SS-DS and LS-DS on Sand TS. The failure envelopes are shown in Fig. A-3. All tests exhibited strain softening behavior with failure was defined at peak strength. Shear behavior in SS-DS and LS-DS is described subsequently. The failure envelopes in SS-DS (Fig. A-3a) are nearly identical with shear strength at a given normal stress varying within ± 4.0 kPa. The failure envelopes in LS-DS (Fig. A-3b) show slightly greater variation with shear strength at a given normal stress varying within ± 8.0 kPa. The shear strength parameters and coefficients of determinations (R^2) for the SS-DS and LS-DS envelopes are tabulated in Table A-2. The range in ϕ' for SS-DS is from 42.5° to 42.8° with an average of 42.6° and standard deviation of 0.25° . For LS-DS ϕ' ranges from 40.1° to 41.1° with an average of 40.5° and standard deviation of 0.45° .

To confirm that the replicate failure envelopes obtained in each test were the same, analysis of covariance (ANCOVA) was conducted at a significance level of 0.05 on both sets of failure envelopes by testing for homogeneity of slopes. The analysis evaluates the similarity of slopes of regression lines (in this case $\tan \phi'$) under the null hypothesis that the slopes are identical, and returns a p-value corresponding to the probability of falsely rejecting the null

hypothesis (Lowry 2006). One test compared the five failure envelopes obtained in SS-DS to each other, another compared the five failure envelopes in LS-DS to each other, and a third test compared the five failure envelopes from SS-DS to the five failure envelopes from LS-DS. The ANCOVA yielded a p-value of 0.99 for the SS-DS envelopes, a p-value of 0.80 for the LS-DS envelopes, and p-value of 0.98 when comparing the SS-DS and LS-DS envelopes. Thus, for all three analyses, no statistically significant difference was observed between the failure envelopes (i.e., $p \gg 0.05$ in each case).

A-3.5. TRIAXIAL COMPRESSION TESTS

Triaxial compression (TC) tests were conducted on sands P1-S1, P1-S6, P2-S9, and TS for comparison with shear strengths obtained in direct shear. These sands were selected to provide a range of ϕ' and shear behavior, as illustrated subsequently. These sands also have negligible fines, thereby precluding issues regarding drainage. No standard method exists for performing consolidated drained TC tests on granular soils. Thus, the triaxial testing procedure simulated, as closely as possible, conditions imposed in the direct shear tests.

Specimens for the TC tests were prepared in a split mold (74 mm diameter, 147 mm tall) lined with a latex membrane in a similar manner as those used for SS-DS testing. Air-dried sand sieved past the No. 4 sieve was used for all specimens. Compaction was performed in three layers of equal thickness by tamping the top of each layer with a tamper, with the number of tamps per layer adjusted to achieve the target density for each specimen. The specimens were prepared to the same density as used in the SS-DS tests.

A cell pressure of 34 kPa was initially applied and water was circulated through the specimen from the bottom up using a small head difference (< 0.6 m). Backpressure was not used and B-checks were not performed so as to simulate the inundation condition used for the SS-DS tests. Each sand was tested at effective confining pressures of 21, 41, 62, and 83 kPa.

The effective confining pressures were chosen so that the normal and shear stresses at failure fell within a range similar to the stresses in the SS-DS tests.

An axial strain rate of 0.11 mm/min was used to provide a similar displacement rate along the failure plane as was applied in the direct shear tests. Measurements of axial displacement, axial force, and volume change were recorded using a personal computer equipped with a National Instruments data acquisition card (Model SC-2345) and LABView software. A linear variable displacement transducer (RDP LLECTRONICS Model ACTL000A, 50 ± 0.09 mm) was used to measure vertical displacement, a load cell (Revere Transducer Model 363-D3-500-20P1, 2.2 ± 0.00015 kN) was used for axial force measurements, and a pressure transducer (Validyne Model DP15-26 connected to a Valdyne Model CD379 digital transducer indicator) was used to monitor volume change. A burette was used to record the volume of water expelled or imbibed by the specimen, with the level in the burette measured with the pressure transducer.

A-4. SHEAR BEHAVIOR IN DIRECT SHEAR TESTING

Typical curves relating shear stress and relative horizontal displacement (RHD) for the SS-DS tests are shown in Fig. A-4. Two shear stress versus RHD relationships were observed: (1) shear stress increasing to a peak stress and then decreasing to a large-displacement stress (Fig. A-4a) and (2) shear stress increasing to an ultimate stress and remaining essentially constant thereafter (Fig. A-4b). Failure was defined as the peak shear stress for all sands exhibiting peak stress behavior. For sands exhibiting only an ultimate stress, the failure stress was defined by the initial horizontal tangent to the shear stress-RHD curve. Periodically, a small increase in shear stress was observed after the initial horizontal tangent. This increase in shear stress was always less than 5 kPa and is believed to be a test artifact (see subsequent

discussion of plowing in LS-DS tests). For consistency, these small increases in shear stress were disregarded.

Three shapes were observed for the shear stress-RHD curves for the LS-DS tests: (1) a peak stress similar to that observed in SS-DS, (2) shear stress increasing to an ultimate stress similar to that observed in SS-DS, but followed by a gradual increase in shear stress at a constant rate at larger horizontal displacement (Fig. A-5a), and (3) shear stress increasing until the slope of the shear stress-RHD curve reached a minimum, after which the shear stress increased at the same rate with additional horizontal displacement (Fig. A-5b). The gradual increase in shear stress (Fig. A-5a) and the constant rate of increasing shear stress (Fig. A-5b) observed at large displacements are due to plowing, as described subsequently.

Failure was defined as the peak shear stress for the tests exhibiting a distinct peak and as the shear stress at the initial horizontal tangent when a horizontal tangent was evident (Fig. A-5a). For the tests where the shear stress increased monotonically with horizontal displacement (Fig. A-5b), the failure stress was defined as the shear stress at the same RHD as failure was defined in SS-DS. This definition was selected because failure occurred at essentially the same RHD in SS-DS and LS-DS when a distinct peak shear stress was observed in both tests (Fig. A-6). A two-sided paired t-test was conducted at the 5% significance level on the 28 observations in Fig. A-6 to confirm that the RHD at failure for the SS-DS and LS-DS tests was essentially the same. The test yield a two-sided p-value of 0.35 (> 0.05), indicating that there is no statistically significant difference in the relative horizontal displacements at failure for these SS-DS and LS-DS tests.

The increases in shear stress at larger displacements that were observed in the LS-DS tests (Fig. A-5), and occasionally in the SS-DS tests, are believed to be due to particle “plowing” within the shear box. This effect was evident when vertical displacements at the front and back of the LS-DS box (see box schematic in Fig. A-2) were compared for those tests without a

distinct peak shear stress, as illustrated in Fig. A-7 for Sand P2-S4. Vertical displacements at a normal stress of 26 kPa were omitted from Fig. A-7 because “plowing” was not observed at this normal stress for any of the tests. In Fig. A-7, dilation is occurring at the front of the box and contraction at the back of the box. Particle movements within the LS-DS box corresponding to these volume changes are shown schematically in Fig. A-8. Simulations of direct shear tests on sand by Liu (2006) with a discrete element model have shown particle movements similar to those illustrated in Fig. A-8. Downward particle movement at the back of the box plows particles against the edge of the lower shear box and supporting platform (Fig. A-8), resulting in a continuous increase in shear resistance.

The “plowing effect” was far less significant in the SS-DS test than in the LS-DS test. The exaggerated “plowing effect” in LS-DS probably is due to a greater number of particles moving within the shear band in the larger scale test and due to rotation of the material within the shear box in response to a couple imposed by shear forces acting on the end walls of the box. Both of these effects, which have been observed in direct shear tests, will cause a greater force on the lower shear box and supporting platform. For example, Palmeira and Milligan (1989) measured the shear band thickness in three different size direct shear box tests and report an increase in shear band thickness with increase in specimen thickness. Also, Jewell (1989) has shown that rotation occurs in direct shear tests with free top platens (as used in the SS-DS and LS-DS), and that rotation is more significant when the normal stress is applied by a pressure bag (as in the LS-DS) than with a rigid top platen (as in the SS-DS).

A-5. SMALL-SCALE VERSUS LARGE-SCALE SHEAR STRENGTH

SS-DS and LS-DS tests were performed on the 30 sands described in Table A-1. A Mohr-Coulomb failure envelope for each test was defined by linear least-squares regression

with a non-negative intercept. Strength parameters for the envelopes are summarized in Table A-3. The envelopes were linear for all practical purposes, with R^2 ranging from 0.997 to 1.000 for SS-DS and 0.991 to 1.000 for LS-DS. The cohesion intercepts represent friction in the shear box not accounted for by the box friction correction and possibly non-linearity of the failure envelopes near the origin. However, in all cases, the apparent cohesion was small, typically 3.0 to 4.0 kPa in SS-DS and 6.0 to 7.0 kPa in LS-DS.

A comparison of friction angles obtained from the LS-DS tests ($\phi'_{\text{LS-DS}}$) and those obtained from the SS-DS tests ($\phi'_{\text{SS-DS}}$) is shown in Fig. A-9. The data are segregated into two sets corresponding to sands with less than 5% R4 material and more than 5% R4 material. For both data sets, $\phi'_{\text{LS-DS}} \approx \phi'_{\text{SS-DS}}$, although considerable scatter exists in the data. The largest difference between $\phi'_{\text{LS-DS}}$ and $\phi'_{\text{SS-DS}}$ is 4.0° , corresponding to Sand P2-S11, which contains 30% R4 material (the largest R4 for the sands that were tested). For the other 29 sands, $\phi'_{\text{LS-DS}}$ and $\phi'_{\text{SS-DS}}$ differ by less than 4.0° , with most of the friction angles differing by less than 2° .

Two-sided paired t-tests were performed at the 5% significance level on the $< 5\%$ R4 data and $> 5\%$ R4 data to determine if the friction angles obtained from LS-DS and SS-DS were statistically similar. The t-test on sands with $< 5\%$ R4 (18 sands) yielded a p-value of 0.65, whereas the p-value was 0.70 for the sands with $> 5\%$ R4. Thus, for both data sets, there is no statistically significant difference in ϕ' obtained with LS-DS and SS-DS (i.e., $p \gg 0.05$). These findings suggest that the conclusions reported by Taylor and Leps (1938), Bishop (1948), and Palmeira and Milligan (1989) in comparisons of LS-DS and SS-DS, and those reported by Fragaszy et al. (1992) and Simoni and Houlsby (2006) for laboratory-prepared mixtures of sand and gravel also apply to a broad range of natural granular backfills having $R4 < 30\%$. In particular, for natural granular backfills with $R4 < 30\%$, the shear strength can be determined by performing shear tests on the P4 (i.e. matrix) material alone provided the P4 material is tested at the same density as the P4 matrix in backfill containing R4 material. A threshold gravel

content may exist beyond which the R4 material does affect ϕ' . Fragaszy et al. (1992) suggest that this threshold corresponds to 40-50% gravel, whereas Simoni and Houlsby (2006) indicate that the threshold is between 20-40% gravel. Conclusively identifying this threshold was not a focal point of this study, and is a topic in need of further research. However, the data from this study suggest that the threshold on gravel content for natural granular backfills is near 30%.

A-6. COMPARISON OF TRIAXIAL COMPRESSION, SMALL-SCALE DIRECT SHEAR AND LARGE-SCALE DIRECT SHEAR

Friction angles obtained from the TC compression tests are tabulated in Table A-4 along with the friction angles from the SS-DS and LS-DS tests on the same sands. Failure envelopes for the TC, SS-DS, and LS-DS tests are presented in Fig. A-10. For the TC tests, the normal stress and shear stress on the failure plane (assumed to be at $45+\phi'/2$) were determined from Mohr's circle so that the envelopes from direct shear and triaxial compression could be compared directly.

For each of the four sands, good agreement exists between the failure envelopes obtained for all three tests, and the ϕ' differ by at most 3.3° (Sand P1-S1, Table A-4). To confirm that the failure envelopes from each test were statistically similar, an analysis of covariance (ANCOVA) was conducted at the 5% significance level on each set of envelopes. A summary of the p-values from the ANCOVA is in Table 4. In all cases, $p > 0.05$, indicating that there is no statistically significant difference between the envelopes.

The friction angles obtained from the TC tests were also compared to those from the SS-DS and LS-DS tests to determine if statistically significant differences existed between the friction angles measured in triaxial compression and direct shear. The differences $\phi'_{SS-DS} - \phi'_{TC}$ and $\phi'_{LS-DS} - \phi'_{TC}$ were evaluated using t-tests at a significance level of 0.05. The tests yielded 2-sided p-values of 0.61 (SS-DS vs. TC) and 0.55 (LS-DS vs. TC), indicating that there is no

statistically significant difference between the friction angles measured in DS and TC ($p > 0.05$). This finding suggests that the conclusions in Taylor (1939), Nash (1953), Rowe (1969), and Pells et al. (1973), which indicate that ϕ' measured in triaxial compression and direct shear differs less than $\pm 3^\circ$ for medium-dense sands (i.e. relative density ranging between 60% and 75%), also apply to natural compacted granular backfills.

A-7.CONCLUSIONS

The shear strength of 30 compacted granular backfill materials having a gravel content (particles greater than 4.75 mm) ranging from 0-30% was measured in small-scale (SS) and large-scale (LS) direct shear (DS) tests. The SS-DS tests were conducted in a 64-mm square box accommodating a maximum particle diameter of 4.75 mm, whereas the LS-DS tests were conducted in a 305-mm square box accommodating a maximum particle diameter of 25.4 mm. Tests conducted in SS-DS required removal of the gravel. Triaxial compression (TC) tests were also conducted on four of the backfill materials tested in SS-DS and LS-DS tests. The results of these tests were compared, from which the following conclusions are drawn:

1. For sands exhibiting peak stress behavior in both SS-DS and LS-DS, relative horizontal displacements corresponding to peak stress were similar, differing by $\pm 0.88\%$.
2. A gradual increase in shear stress occurred at larger horizontal displacements in some of the LS-DS tests. This increase in shear stress, referred to as the “plowing effect,” is attributed to downward particle movement at the back of the shear box, which increases stresses on the lower box and supporting platform, thereby increasing the measured shear resistance. A similar effect was observed to a minor extent in a few of the SS-DS tests. This is an artifact of direct shear testing, and does not reflect the shearing behavior of compacted granular backfills.

3. Replicate testing showed that the peak friction angle (ϕ') obtained with the SS-DS and LS-DS procedures was highly repeatable, within $\phi' \pm 0.25^\circ$ in SS-DS and $\pm 0.45^\circ$ in LS-DS. An analysis of covariance (ANCOVA) performed on the replicate tests showed that the failure envelopes were not statistically different for both SS-DS and LS-DS.
4. Friction angles measured on the same sand in SS-DS and LS-DS differed by no more than 4.0° , and in most cases differed by less than 2° . A paired t-test performed at the 5% significance level showed no significant difference between ϕ' obtained with SS-DS and LS-DS for gravel contents ranging from 0 to 30%. Similarly, no statistically significant difference existed between failure envelopes and friction angles measured on four of the sands using TC, SS-DS, and LS-DS. This suggests that the friction angle of compacted granular backfills can be measured in SS-DS, LS-DS, or TC with comparable accuracy, and that tests on material where gravel is excluded can be used to define the shear strength of granular backfills having a gravel content $< 30\%$.

A-8. REFERENCES

- Bishop, A.W. 1948. A large shear box for testing sands and gravels. *In* Proceedings from the 2nd International Conference on Soil Mechanics and Foundation Engineering, Balkema, Rotterdam, 1, pp. 207-211.
- Elias, V., Christopher, B.R., and Berg, R.R. 2001. Mechanically stabilized earth walls and reinforces soil slopes design and construction guidelines. US Department of Transportation Federal Highway Administration, Publ. No. FHWA-NHI-00-043, Washington, DC.
- Fragaszy, R.J., Su., J., Siddiqi, F.H., and Ho, C.L. 1992. Modeling strength of sandy gravel. *Journal of Geotechnical Engineering*, **118**(6), 920-935.
- Jewell, R. A. (1989) "Direct Shear Tests on Sands," *Géotechnique*, 39(2): 309-322.
- Krumbein, W.C. 1941. Measurement and geological significance of shape and roundness of sedimentary particles. *Journal of Sedimentary Petrology*, **11**(2): 64-72.
- Liu, S.H. 2006. Simulating a direct shear box test by DEM. *Canadian Geotechnical Journal*, **43**: 155-168.

- Lowry, R. 2006. Concepts and applications of inferential statistics. Vassar College, available from <http://faculty.vassar.edu/lowry/webtext.html>.
- Nash, K.L. 1953. The shearing resistance of a fine closely graded sand. *In* Proceedings from the 3rd International Conference on Soil Mechanics and Foundation Engineering, Balkema, Rotterdam, 1, pp. 160-164.
- Palmeira, E.M. and Milligan, G.W.E. 1989. Scale effects in direct shear tests on sand. *In* Proceedings from the 12th International Conference on Soil Mechanics and Foundation Engineering, Balkema, Rotterdam, 1, pp. 739-742.
- Pells, P.J.N., Maurenbrechner, P.M., and Elges, H.F.W.K. 1973. Validity of results from the direct shear test. *In* Proceedings from the 8th International Conference on Soil Mechanics and Foundation Engineering, Balkema, Rotterdam, 1, pp. 333-338.
- Rowe, P.W. 1969. The relation between the shear strength of sands in triaxial compression, plain strain and direct shear. *Géotechnique*, **19**(1), 75-86.
- Simoni, A. and Houlsby, G.T. 2006. The direct shear strength and dilatancy of sand-gravel mixtures. *Geotechnical and Geological Engineering*, **24**, 523-549.
- Taylor, D.W., and Leps, T.M. 1938. Shearing properties of Ottawa standard sand as determined by the M.I.T. strain-controlled direct shearing machine. *In* Record of Proceedings of Conference on Soils and Foundations, Corps of Engineers, U.S.A., Boston, MA.
- Taylor, D.W. 1939. A comparison of results of direct shear and cylindrical compression tests. *In* Proceedings ASTM, Philadelphia, PA, pp. 1058-1070.

A-9. TABLES AND FIGURES

Table A-1. Physical parameters of sands used for shear strength testing.

Sample	C _u	C _c	% Fines	% Gravel	G _s	e _{max}	e _{min}	γ_{d-max} (kN/m ³)	Roundness	USCS Symbol
P1-S1	1.86	1.12	0.78	0.0	2.64	0.76	0.48	17.36	0.50	SP
P1-S2	2.18	1.03	0.41	2.0	2.63	0.67	0.42	17.92	0.61	SP
P1-S3	2.33	0.92	0.84	0.0	2.66	0.83	0.50	17.08	0.40	SP
P1-S4	2.67	0.95	1.03	5.7	2.65	0.70	0.40	18.30	0.59	SP
P1-S5	2.63	1.01	0.15	1.8	2.65	0.76	0.43	18.15	0.62	SP
P1-S6	2.35	1.15	0.79	1.8	2.63	0.69	0.43	17.59	0.62	SP
P1-S7	2.03	0.96	0.65	0.0	2.66	0.81	0.52	16.88	0.42	SP
P2-S1	1.88	0.97	1.12	1.0	2.68	0.80	0.51	16.98	0.31	SP
P2-S2	2.10	1.20	0.85	0.0	2.67	0.83	0.56	16.51	0.29	SP
P2-S3	2.27	0.86	12.63	10.2	2.68	0.96	0.58	16.02	0.24	SM
P2-S4	5.30	1.92	9.75	17.8	2.68	0.68	0.39	18.46	0.40	SP-SC
P2-S5	2.82	0.84	0.46	8.3	2.76	0.69	0.44	18.02	0.33	SP
P2-S6	2.82	1.06	3.52	0.4	2.75	0.76	0.46	17.86	0.25	SP
P2-S7	3.15	1.32	14.44	0.0	2.75	0.86	0.52	17.69	0.22	SM
P2-S8	3.05	0.81	1.24	6.7	2.71	0.64	0.4	18.30	0.37	SP
P2-S9	4.16	0.68	0.53	22.1	2.67	0.56	0.33	18.11	0.43	SP
P2-S10	2.33	1.35	4.98	0.7	2.7	0.75	0.46	17.51	0.31	SP
P2-S11	34.07	0.14	0.75	47.8	2.71	0.43	0.26	18.58	0.52	SW
TS	3.06	0.85	1.55	2.2	2.7	0.64	0.39	18.64	0.42	SP
P3-S1	3.20	0.82	1.11	10.0	2.72	0.58	0.35	18.68	0.50	SP
P3-S2	4.77	1.04	5.70	12.1	2.72	0.7	0.39	19.08	0.48	SP-SM
P3-S3	2.48	0.92	0.55	0.3	2.66	0.64	0.37	18.39	0.59	SP
P3-S4	2.86	1.00	0.40	4.3	2.69	0.60	0.37	18.77	0.52	SP
P3-S5	3.00	0.89	0.77	4.9	2.65	0.62	0.38	18.54	0.56	SP
P3-S6	2.07	1.04	0.79	0.0	2.65	0.77	0.5	17.12	0.36	SP
P3-S7	1.79	0.96	0.61	0.0	2.66	0.80	0.51	16.98	0.46	SP

Table A-1. Physical parameters of sands used for shear strength testing (Continued).

Sample	C_u	C_c	% Fines	% Gravel	G_s	e_{max}	e_{min}	γ_{d-max} (kN/m ³)	Roundness	USCS Symbol
P4-S1	2.00	1.10	0.14	3.3	2.69	0.84	0.56	16.67	0.42	SP
P4-S2	2.86	0.81	2.32	3.3	2.71	0.72	0.44	17.52	0.31	SP
P4-S3	6.50	0.59	1.74	13.2	2.74	0.62	0.33	18.97	0.35	SP
P5-S1	5.28	0.76	5.17	16.6	2.67	0.55	0.31	18.84	0.38	SP-SM

Note: Particle size analysis conducted following ASTM D 422, G_s determined by ASTM D 854 for particles < 4.75 mm and by ASTM C 127 for particles > 4.75 mm, e_{min} determined by ASTM D 4253, e_{max} determined by ASTM D 4254, γ_{d-max} determined by AASHTO T 99 (Standard Proctor), Roundness determined by procedures in Krumbein (1941), and Unified Soil Classification determined by ASTM D 2487.

Table A-2. Shear strength parameters for repeatability tests conducted on Sand TS using small-scale (SS) and large-scale (LS) direct shear tests.

Envelope	Box Size	ϕ'	c' (kPa)	R^2
SS-1	Small	42.5	2.27	0.999
SS-2	Small	42.8	1.12	0.998
SS-3	Small	42.5	1.80	0.999
SS-4	Small	42.5	1.79	0.999
SS-5	Small	42.6	2.19	0.997
Average	Small	42.6	1.83	0.998
Standard Deviation	Small	0.2	0.46	0.001
LS-1	Large	40.3	14.10	0.991
LS-2	Large	40.8	8.21	0.997
LS-3	Large	40.1	13.47	0.986
LS-4	Large	40.1	13.05	0.993
LS-5	Large	41.1	13.32	0.993
Average	Large	40.5	12.43	0.992
Standard Deviation	Large	0.5	2.39	0.004

Table A-3. Shear strength parameters for small-scale direct shear and large-scale direct shear tests.

Sample	Small-Scale Direct Shear			Large-Scale Direct Shear		
	c' (kPa)	ϕ'	R ²	c' (kPa)	ϕ'	R ²
P1-S1	5.06	35.8	0.998	0.00	38.1	0.991
P1-S2	4.51	32.9	0.999	4.24	31.7	0.997
P1-S3	5.25	34.3	0.999	3.07	35.7	0.999
P1-S4	3.53	33.4	1.000	7.08	32.8	0.997
P1-S5	5.10	32.3	0.999	3.79	32.0	0.996
P1-S6	5.98	32.5	0.999	9.32	31.8	0.997
P1-S7	4.34	34.8	1.000	11.17	38.0	0.996
P2-S1	2.18	36.6	0.999	7.14	36.1	0.999
P2-S2	1.33	37.8	0.999	6.30	35.3	0.995
P2-S3	4.59	35.1	0.999	6.19	37.0	0.999
P2-S4	4.59	36.5	1.000	5.30	37.0	1.000
P2-S5	5.60	40.9	1.000	12.06	41.3	0.998
P2-S6	0.82	40.5	1.000	5.97	41.7	0.993
P2-S7	0.00	39.6	1.000	12.97	38.9	0.992
P2-S8	0.62	41.5	0.998	8.43	40.1	0.998
P2-S9	7.96	38.5	0.998	13.35	36.6	0.991
P2-S10	4.14	36.4	0.999	5.18	37.7	0.994
P2-S11	5.58	38.7	0.998	24.43	42.8	0.990
TS*	1.83	42.6	0.998	12.43	40.5	0.992
P3-S1	4.10	39.2	0.997	6.58	37.6	0.999
P3-S2	0.60	36.9	0.998	0.32	35.0	0.997
P3-S3	6.66	35.4	0.998	3.24	34.7	0.992
P3-S4	2.93	40.3	0.998	5.91	40.9	1.000
P3-S5	2.57	36.4	0.998	7.00	35.0	0.997
P3-S6	4.27	34.5	0.999	5.08	35.2	0.999
P3-S7	2.77	35.4	0.999	2.59	36.4	0.995
P4-S1	2.00	36.7	0.999	1.57	35.3	0.998
P4-S2	2.55	40.7	0.998	0.00	43.7	0.993
P4-S3	3.82	42.4	0.999	7.15	41.9	0.994
P5-S1	2.87	39.1	1.000	4.97	39.3	0.999

*Averaged values from repeatability tests

Table A-4. Friction Angles and ANCOVA Statistics for Sands P1-S1, P1-S6, P2-S2, and P2-S6 for Small-Scale Direct Shear (SS-DS), Large-Scale Direct Shear (LS-DS), and Triaxial Compression (TC).

Test Type	P1-S1	P1-S6	P2-S9	TC
SS-DS	35.8	32.5	38.5	42.6
LS-DS	38.1	31.8	36.6	40.5
TC	34.8	34.3	39.7	42.1
ANCOVA p-value	0.70	0.07	0.09	0.45

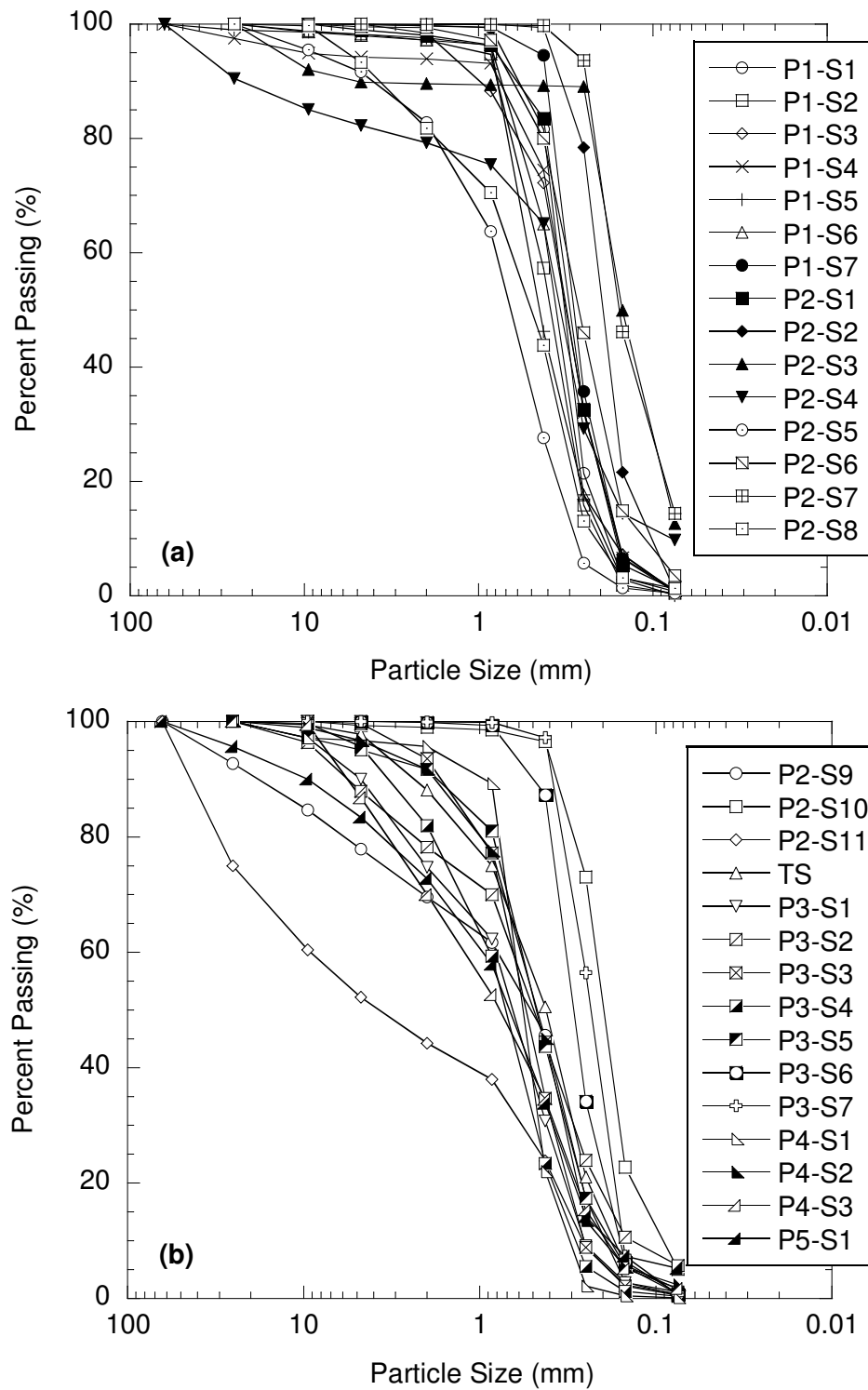


Fig. A-1 Particle size distribution curves for backfill materials used in study.

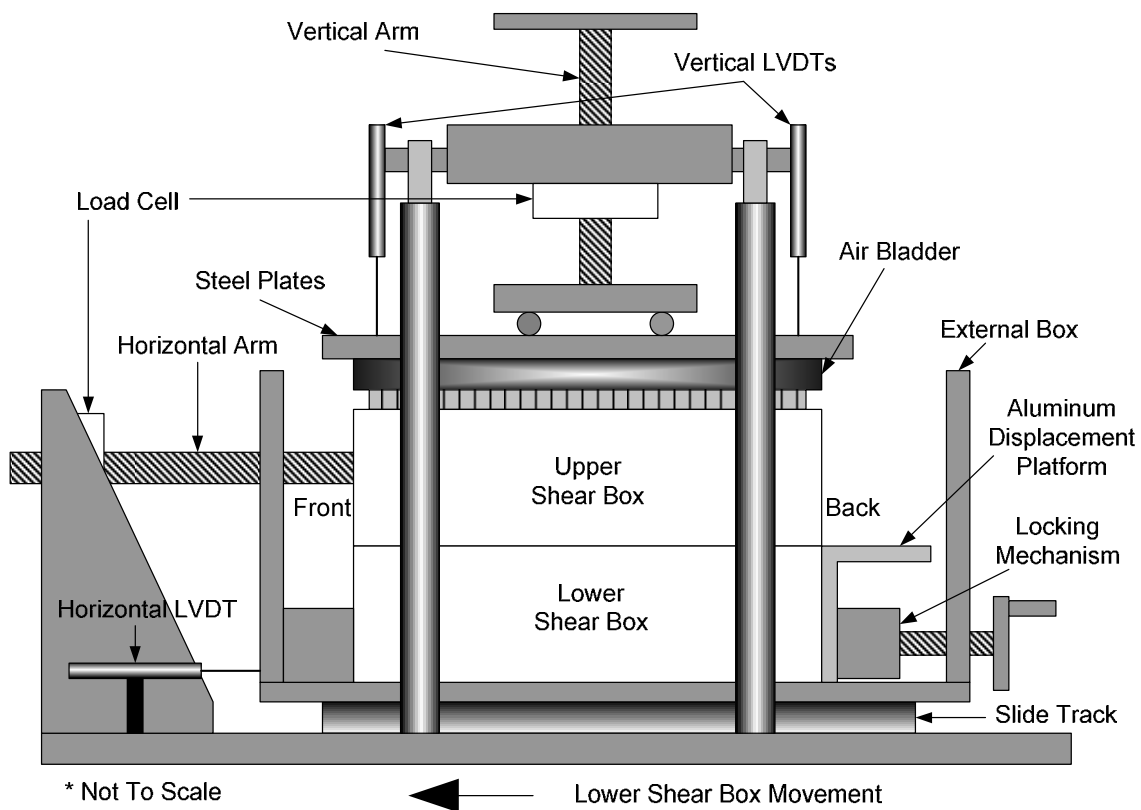


Fig. A-2 Schematic of large-scale direct shear machine.

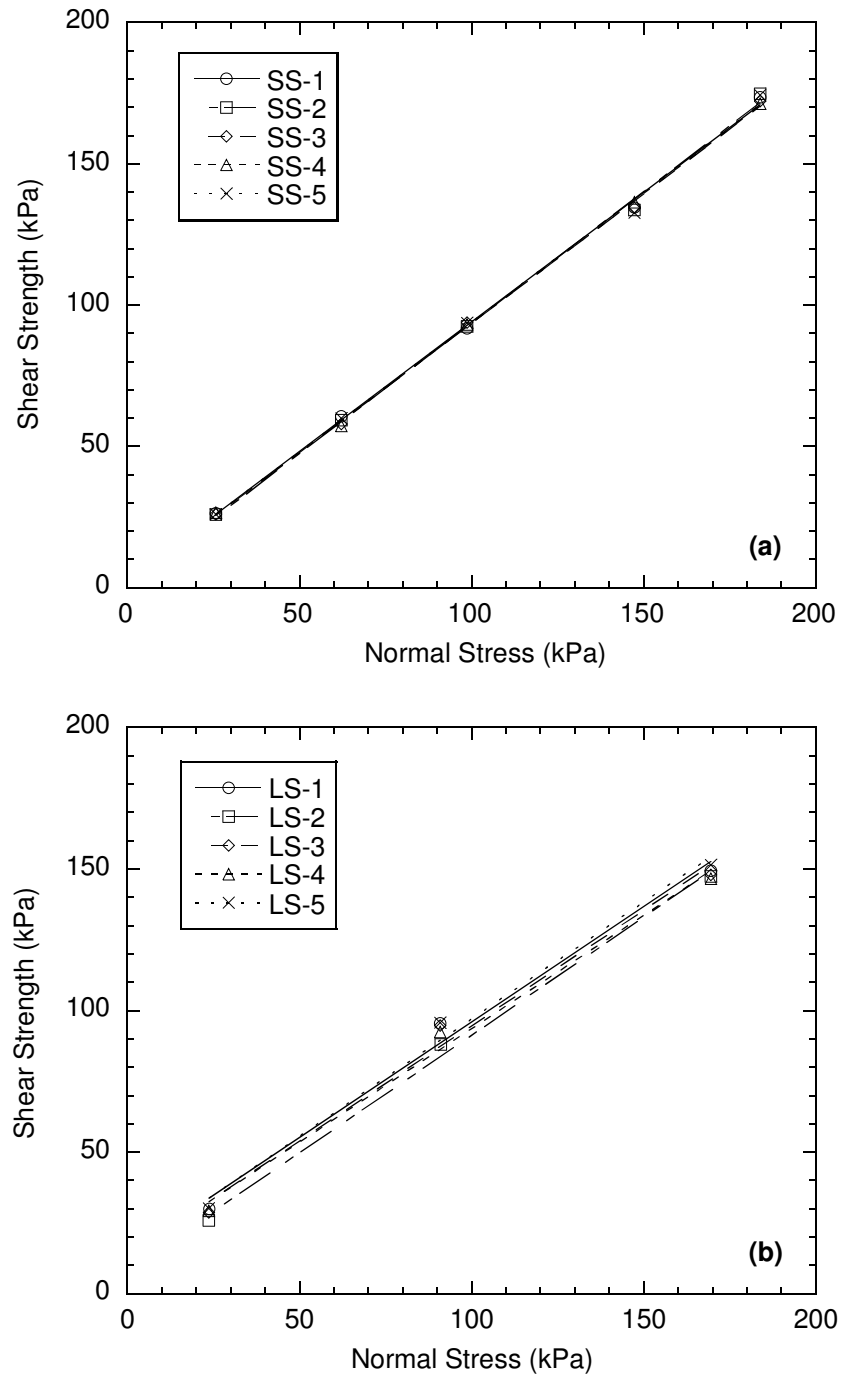


Fig. A-3. Failure envelopes for repeatability tests: (a) small-scale direct shear and (b) large-scale direct shear. All tests conducted with Sand TS while inundated using displacement rate of 0.24 mm/min.

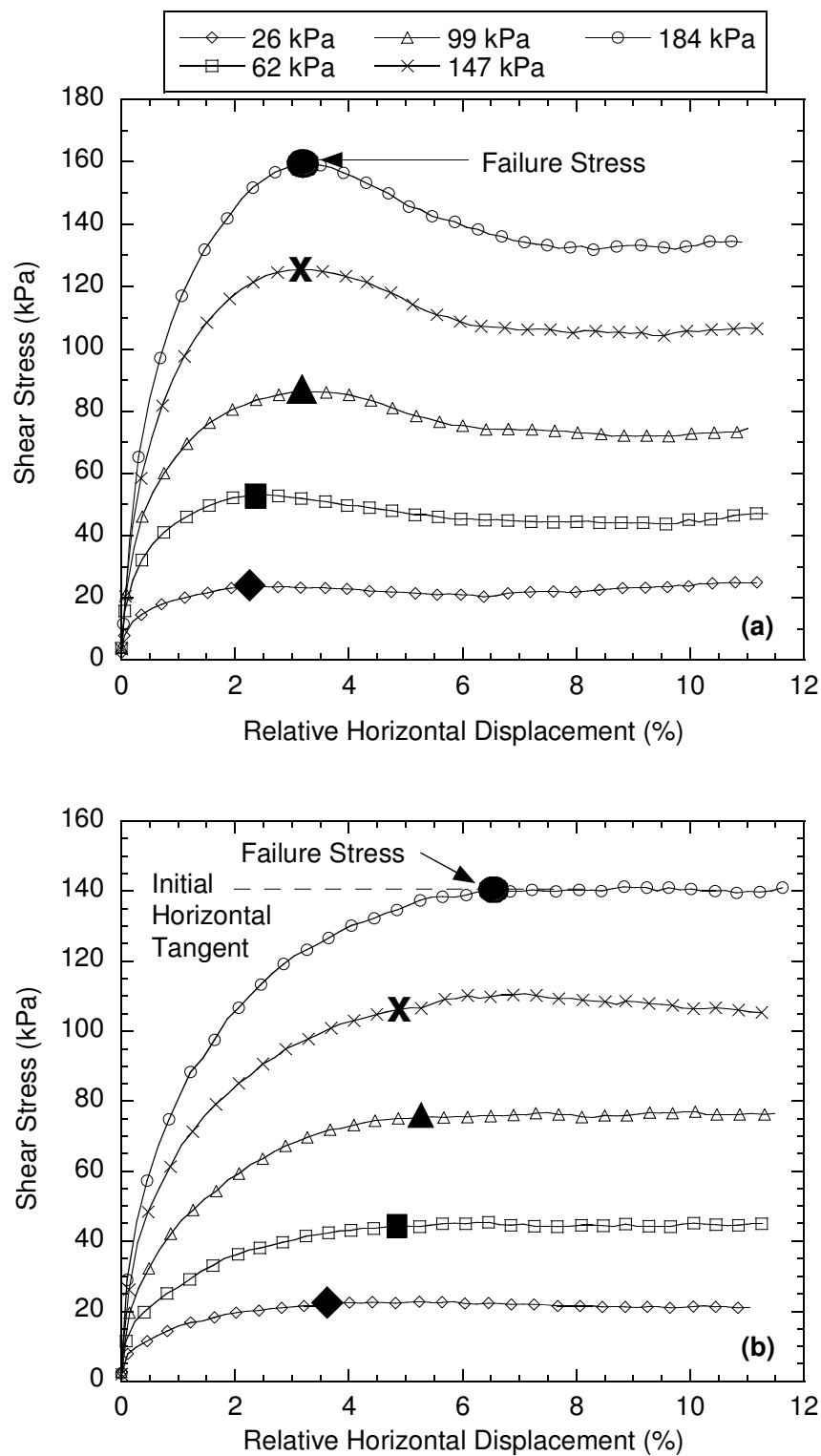


Fig. A-4. Shear stress versus relative horizontal displacement measured in small-scale direct shear with failure stress defined by (a) peak stress (Sand P2-S6) and (b) initial horizontal tangent (Sand P3-S2).

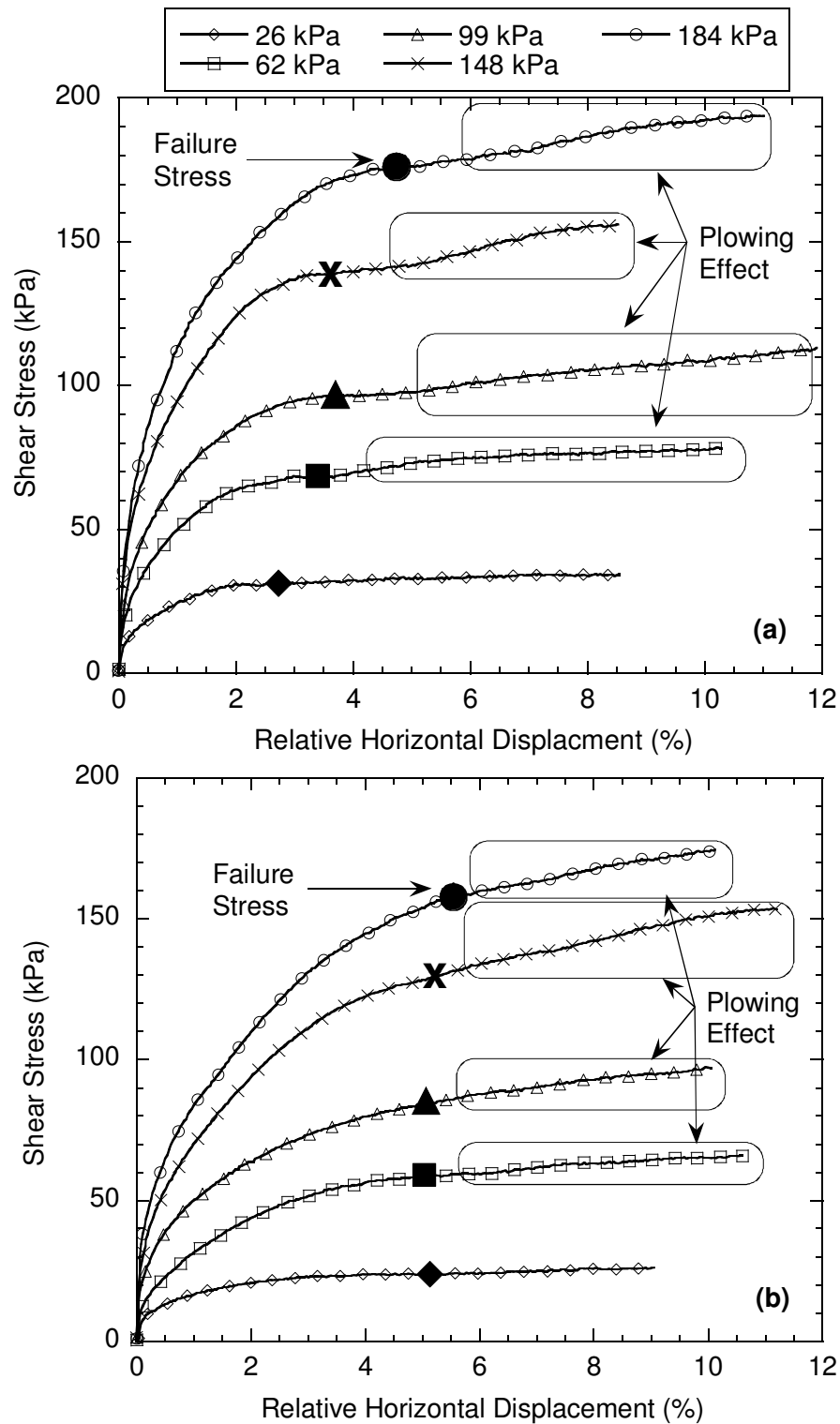


Fig. A-5. Shear-displacement curves for LS-DS tests showing failure stress for cases with (a) initial horizontal tangent followed by plowing (Sand P3-S1) and (b) shear stress increase at the same rate with additional horizontal displacement (Sand P3-S2).

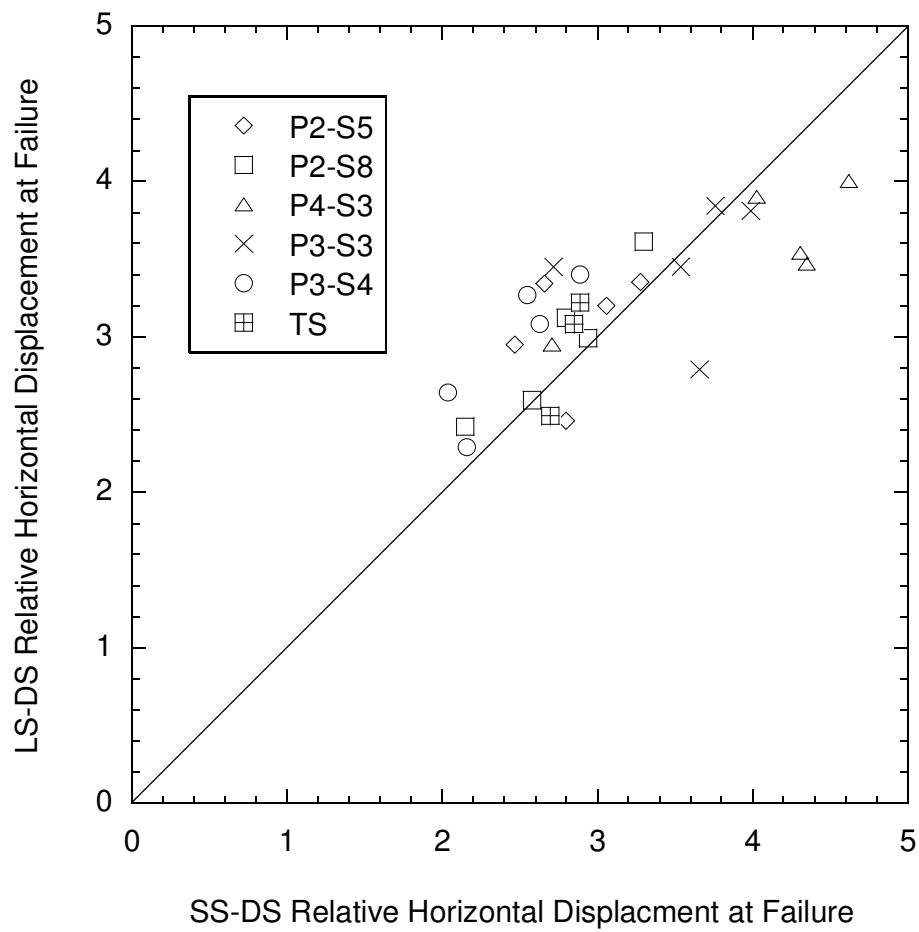


Fig. A-6. Relative horizontal displacement at failure in large-scale direct shear (LS-DS) vs. relative horizontal displacement at failure in small-scale direct shear (SS-DS) for sands exhibiting a peak stress.

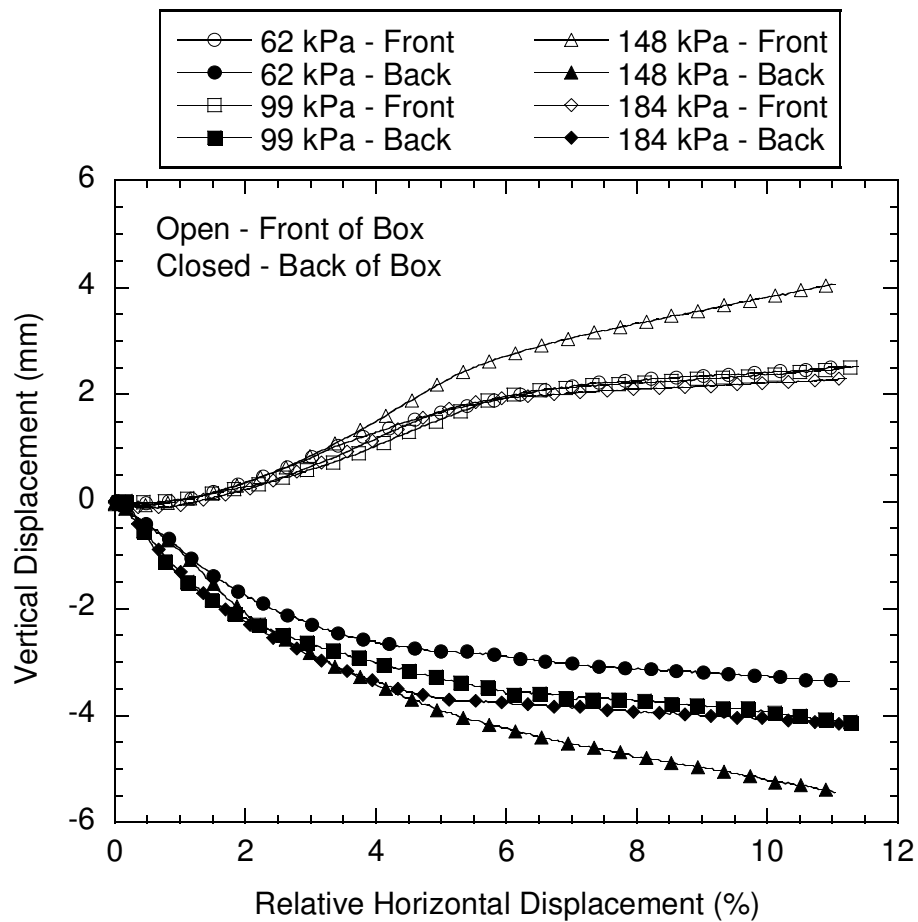


Fig. A-7. Vertical displacement at front and rear of the large-scale direct shear box vs. relative horizontal displacement for Sand P2-S4, which exhibited “plowing” behavior for normal stresses between 62 and 184 kPa inclusive.

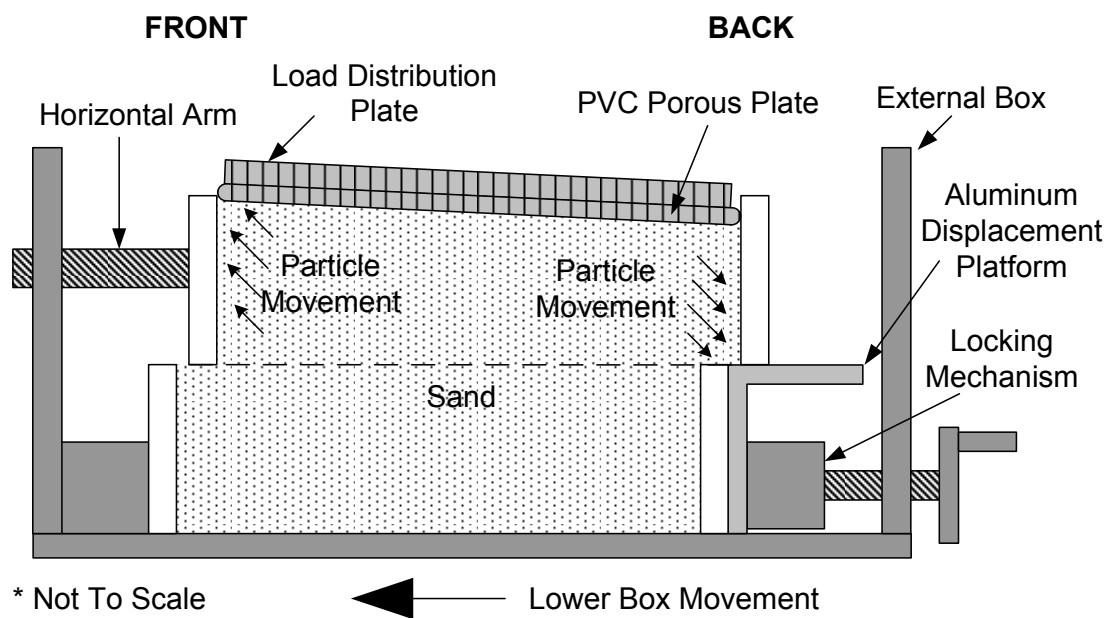


Fig. A-8. Schematic of particle movements during shearing in large-scale direct shear.

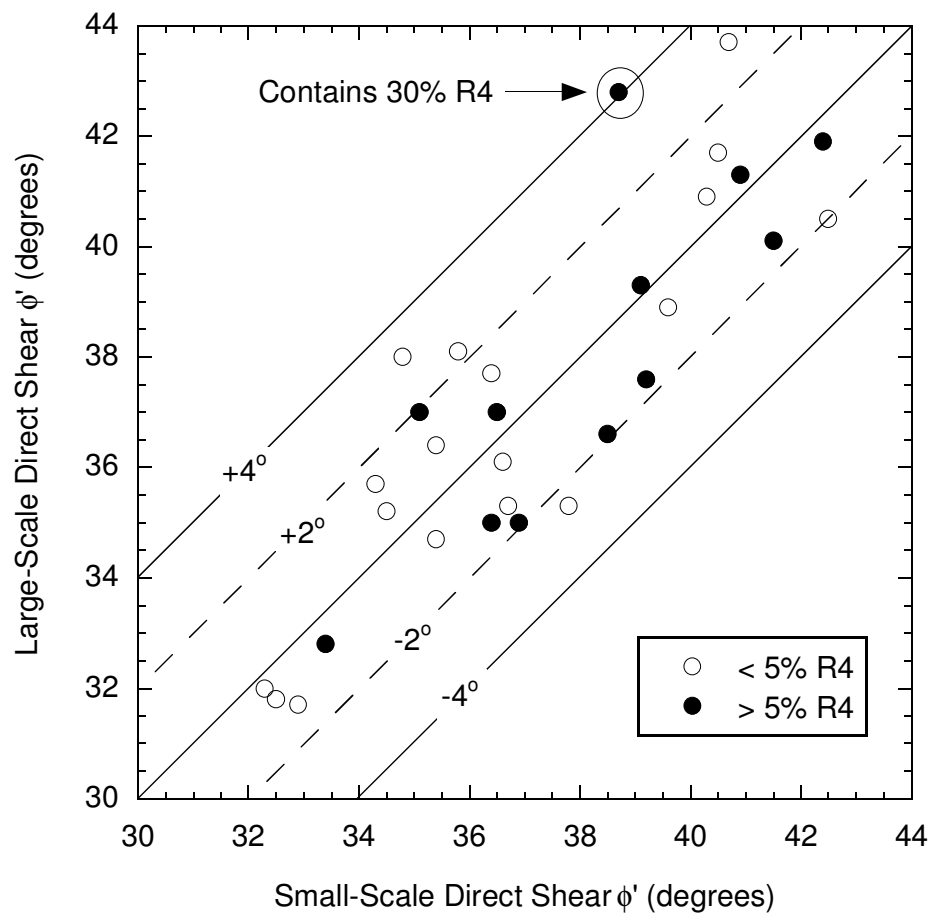


Fig. A-9. Friction angles obtained from large-scale direct shear (LS-DS) tests versus friction angles obtained from small-scale direct shear (SS-DS) tests.

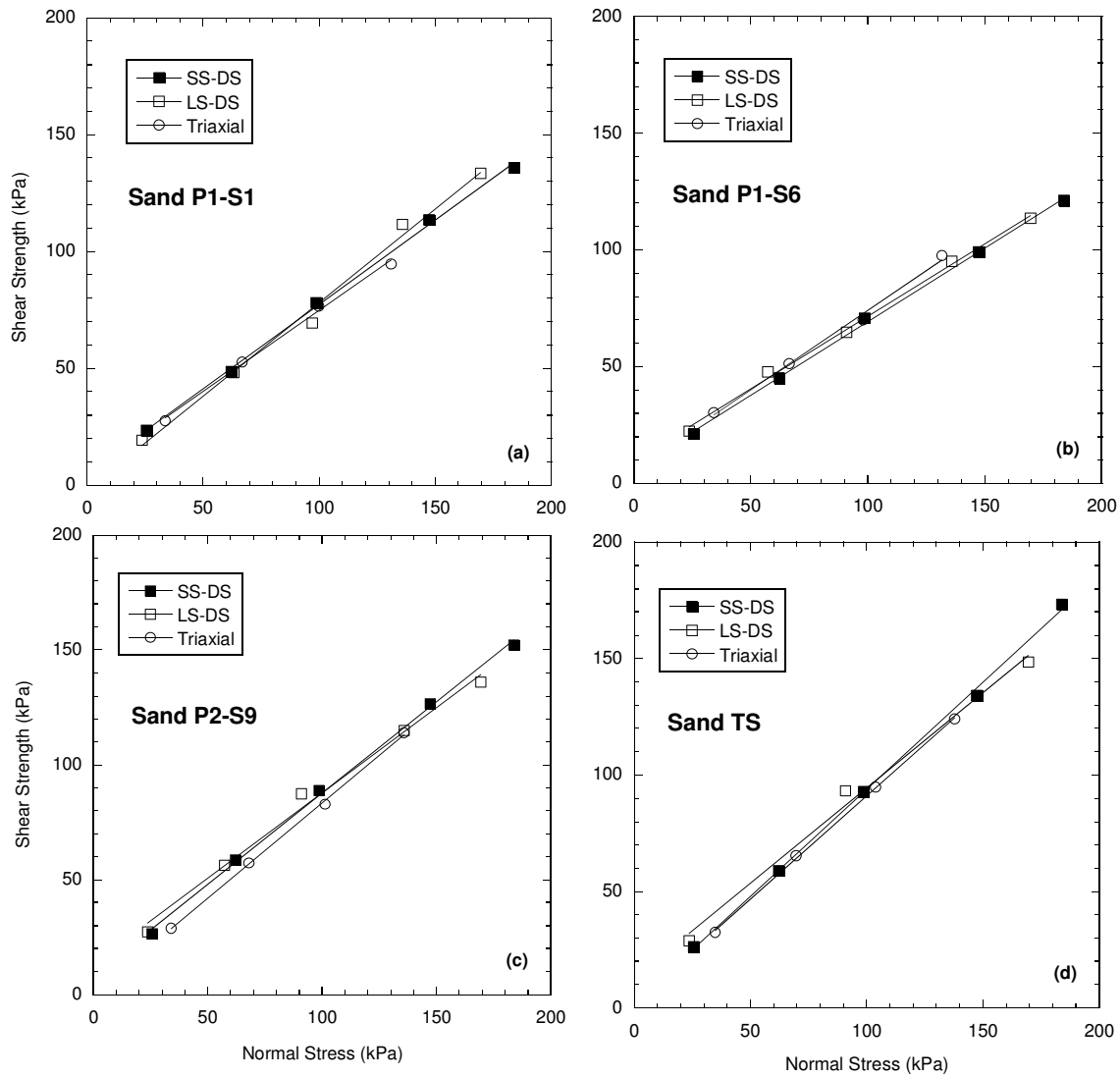


Fig. A-10. Failure envelopes obtained from small-scale direct shear (SS-DS), large-scale direct shear (LS-DS), and triaxial compression (TC) tests: (a) Sand P1-S1, (b) Sand P1-S6, (c) Sand P2-S9, and (d) Sand TS.

APPENDIX A1

A1. NORMAL FORCE TRANSFER

Tests were conducted to evaluate the normal force transmitted to the shear plane in the LS-DS and SS-DS devices. A schematic representation of the apparatus is shown in Fig. A1. The apparatus consists of the upper half of the LS-DS box supported on a lower box of the same size that is mounted on a table. Sand in the lower box was replaced by a 13-mm-thick PVC lower plate and 19-mm-thick aluminum support plate. The support plate was free to move within the boxes and the upper surface of the lower plate was flush with the bottom surface of the upper shear box.

The support plate was supported by screws while sand was compacted in the upper box. After compaction, a 12-mm-thick steel surcharge plate was placed on top of the specimen to distribute the applied normal force, the load cell was raised until contacting the support plate, and the screws supporting the plate were lowered (Fig. A1-1). Normal forces similar to those used in the LS-DS tests were then applied to the top of the specimen and the force transferred to the shear plane was measured. Force applied to the top of the specimen and force transferred to the bottom of the specimen were measured with load cells (upper: Revere Transducers Model 363-D3-5K-20P1, 22.2 ± 0.0015 kN; lower: Interface Model 1210AF-5K, 22.2 ± 0.005 kN) and recorded using a personal computer equipped with a Validyne data acquisition card (UPC601-U) and LABView software.

Four air-dried sands (P1-S1, P1-S6, P2-S2, and P2-S6) representing friction angles ranging from 32° to 42° were used in the load transfer tests. Each sand was compacted in two layers using a tamper, with the number of tamps per layer adjusted to achieve the same densities used in the direct shear tests. Sands with different friction angles were used to determine if the force transfer was affected by the shear strength of the sand.

The correspondence between the applied and measured normal force in the LS-DS apparatus is shown in Fig. A1-2a. The line marked 'no sand' illustrates that the normal force is transferred completely when no sand is present, which is expected. When sand is present, the normal force transferred to the shear plane is lower than the normal force applied to the surface of the sand. Linear regression through the data showed that the normal force on the shear plane ranged between 90.7% and 93.6% of the applied normal force, with an average of 92.0%. This average scale factor was applied when reducing the data from the LS-DS tests.

Identical experiments were conducted with the SS-DS apparatus. The correspondence between the applied and measured normal force in the SS-DS apparatus is shown in Fig. A1-2b. Linear regression through the data showed that the normal force on the shear plane ranged between 99.1% and 100.0% of the applied normal force, with an average of 99.7%. Thus, no scale factor was applied when reducing the data from the SS-DS tests.

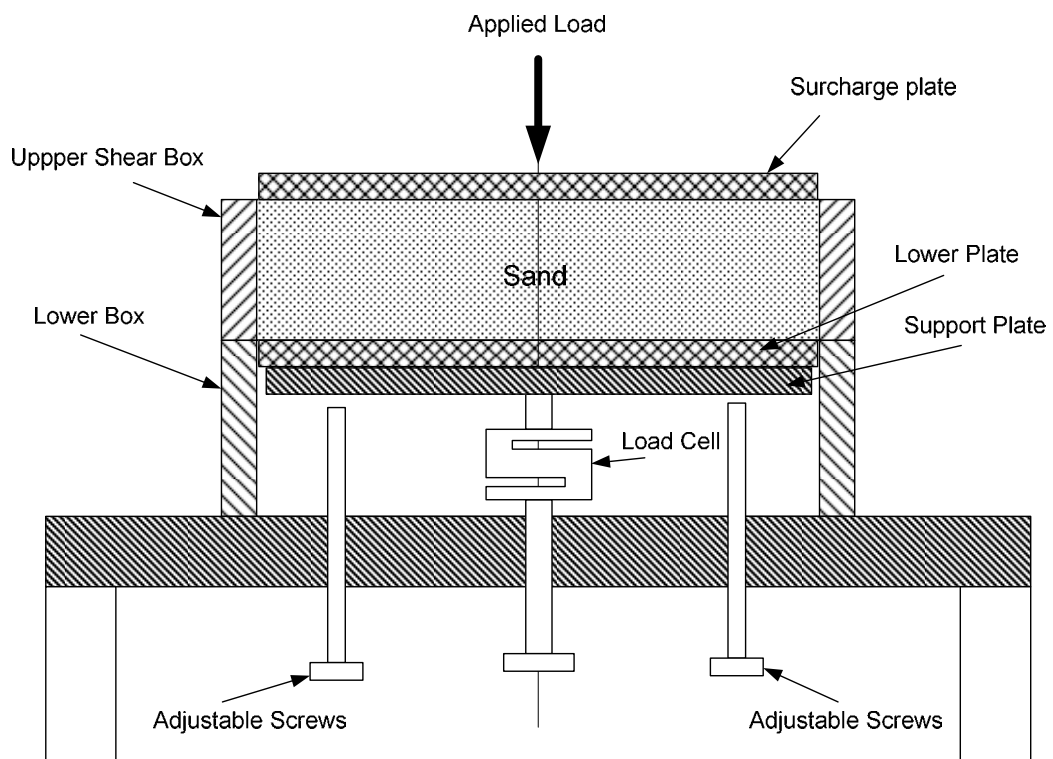


Fig. A1-1. Setup of load transfer test for large-scale direct-shear tests.

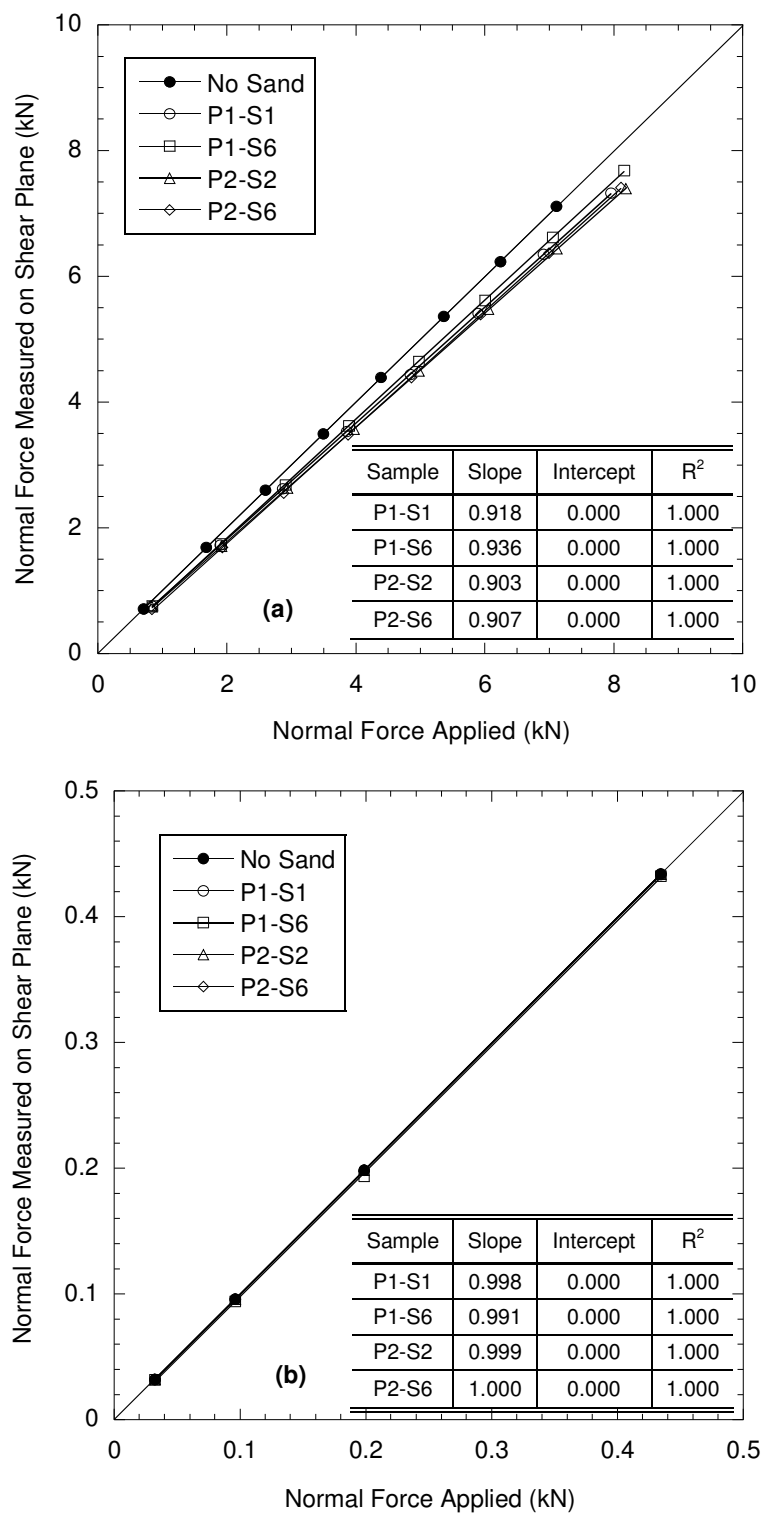


Fig. A1-2. Comparison of normal force measured on the shear plane to normal force applied on the surface: (a) large-scale direct shear and (b) small-scale direct shear.

APPENDIX A2

A2. BOX FRICTION CORRECTION PROCEDURE

Box Interface Friction

The coefficient of friction of the shear box interface was determined by performing LS-DS tests without soil in the box. Tests were conducted with the box inundated at displacement rate of 0.24 mm/min. Surcharge weights were placed on the upper shear box to apply the normal force at the box interface. Shear force was measured with a load cell (Sensotec 89 \pm 0.15 kN load cell model 41/0573-05) and horizontal displacement was measured with a linear variable displacement transducer (LVDT) (Solartron model M920002A721-01, 100 \pm 0.01 mm). A personal computer equipped with a Validyne data acquisition card (UPC601-U) and LABView software was used to record the data.

Five box friction tests were performed at interface normal forces ranging from 0.3 to 1.5 kN. Plots relating frictional force and relative horizontal displacement (RHD) are shown in Fig. A2-1. Except for Test 5 the frictional force is nearly constant during box displacement. For all tests an average frictional force was calculated from measurements between RHD of 1% and 6%. The range of RHD from 1% to 6% corresponds to the range in which the majority of sands tested in large-scale direct shear (LS-DS) achieved failure stress conditions. The relationship between average frictional force and normal force on the shear box interface is shown in Fig. A2-2. Linear regression of data in Fig. A2-2 was used to obtain a box interface coefficient of friction of 0.404.

Box Friction Equations

The shear force (F_s) measured during LS-DS testing is a combination of shear resistance in the soil specimen and shear resistance due to box friction (Eq. A2.1).

$$F_S = F_N \alpha \tan \phi' + (F_N (1 - \alpha) + W'_B) \mu_B \quad (\text{A2.1})$$

where F_N is the applied normal force, α is the force transfer constant (0.9203), ϕ' is the internal angle of friction of the soil, W'_B is the effective weight of the upper shear box, and μ_B is the box interface coefficient of friction (0.404). The left term on the right-hand side of Eq. A2.1 is the shear resistance in the soil and the right term is the shear resistance due to box friction.

Areas of the soil specimen and box interface during horizontal displacement are needed to convert the shear forces in Eq. A2.1 to shear stresses. A schematic of the LS-DS box illustrating these areas is presented in Fig. A2-3. The corrected area of soil in the shear plane (A_{CS}) is:

$$A_{CS} = A_{IS} - (W \times \delta_h) \quad (\text{A2.2})$$

where A_{IS} is the initial area, W is the width of the soil specimen, and δ_h is the horizontal displacement. The corrected area of the shear box interface (A_{CB}) is obtained as:

$$A_{CB} = A_{IB} - (W \times \delta_h) \quad (\text{A3.3})$$

where A_{IB} is the initial contact area of the shear box interface. Eq. A2.3 applies until δ_h equals the thickness of the front of the upper shear box (t). For $\delta_h \geq t$, A_{CB} remains constant ($= A_{IB} - W \times t$). As the shear boxes are displaced, the upper shear box comes in contact with the soil in the shear plane. The area of contact between the upper shear box and soil specimen (A_{SB}) equals $A_{IB} - A_{CB}$. Thus, at any given horizontal displacement A_{CS} , A_{CB} , and A_{SB} can be determined based on Eq. A2.2 and Eq. A2.3.

The box friction calculation depends on the areas of contact supporting the interface normal force (A_{IB} , A_{CB} and A_{SB}) and the interface coefficient of friction (δ) between the soil and upper shear box. The shear stress due to box friction (τ_B) is calculated by:

$$\tau_B = \left[\frac{(F_N(1-\alpha) + W'_B) \left(\frac{A_{CB}}{A_{IB}} \right)}{A_{CB}} \right] \times \mu_B + \left[\frac{(F_N(1-\alpha) + W'_B) \left(\frac{A_{SB}}{A_{IB}} \right)}{A_{SB}} \right] \times \delta \quad (A2.4)$$

Box friction calculations were made using Eq. A2.4 using four different sets of assumptions regarding what contact areas (A_{IB} , A_{CB} and A_{SB}) are actually supporting the interface normal force and if the normal force is supported at A_{SB} , what magnitude of δ should be used.

- Method 1 assumed a constant box interface contact area equal to A_{IB} , which results in $A_{SB} = 0$. Thus, the second term on the right hand side of Eq. A2.4 is zero and the first term is constant ($A_{CB} = A_{IB}$).
- Method 2 assumed that (1) area corrections of A_{CB} and A_{SB} apply and the interface normal force was supported by A_{CB} and A_{SB} , (2) the interface normal force was distributed equally over A_{CB} and A_{SB} , and (3) $\delta = 2/3 \tan \phi'$, where ϕ' is the friction angle from the SS-DS tests.
- Method 3 is the same as Method 2, except δ is assumed to be 0.
- Method 4 accounted for the area corrections in A_{CB} and A_{SB} and assumed none of the interface normal force is supported by A_{SB} . Therefore, the right-hand term of Eq. A2.4 is zero and the fraction A_{CB}/A_{IB} in the left-hand term is 1.

Box Friction Method Comparison

Calculations of box friction were initially limited to sands containing less than 5% material retained on a No. 4 sieve so that comparisons of ϕ' in LS-DS and SS-DS would apply to nearly identical specimens. The best overall comparison of ϕ'_{LS-DS} to ϕ'_{SS-DS} was used as criteria for accepting a method for box friction calculation. For all tests the shear stress corrected for machine friction (τ_c) was obtained by

$$\tau_c = \left(\frac{F_s}{A_{CS}} \right) - \tau_B \quad (A2.5)$$

and the normal stress on the failure plane (σ_n) was obtained by

$$\sigma_n = \frac{F_N \alpha}{A_{IS}} \quad (A2.6)$$

Relationships between ϕ'_{LS-DS} and ϕ'_{SS-DS} are shown in Fig. A2-4 without any corrections for box friction and with corrections for box friction by Methods 1-4. In Fig. A2-4, dotted lines represent linear trendlines with an intercept and dashed lines represent linear trendlines with the intercept forced to zero.

The average and standard deviation of $\phi'_{LS-DS} - \phi'_{SS-DS}$ for no box friction correction and for box friction correction by Methods 1-4 are listed in Table A2-1. Each box friction method resulted in ϕ'_{LS-DS} being more similar to ϕ'_{SS-DS} . Although the standard deviation is slightly higher for Method 4 compared to the other methods and no box correction, Method 4 produces the best agreement between ϕ'_{LS-DS} and ϕ'_{SS-DS} based on the average $\phi'_{LS-DS} - \phi'_{SS-DS}$ (Table A2-1). Thus, Method 4 was selected for reduction of data from the LS-DS apparatus.

Table A2-1. Comparison of Large-Scale Direct Shear Friction Angle ($\phi'_{\text{LS-DS}}$) and Small-Scale Direct Shear Friction Angle ($\phi'_{\text{SS-DS}}$) without Any Box Friction Correction and with Corrections for Methods 1-4.

	No Correction	Method 1	Method 2	Method 3	Method 4
Average ($\phi'_{\text{LS-DS}} - \phi'_{\text{SS-DS}}$)	4.8	1.9	1.6	3.1	0.4
Standard Deviation ($\phi'_{\text{LS-DS}} - \phi'_{\text{SS-DS}}$)	1.3	1.5	1.4	1.4	1.6

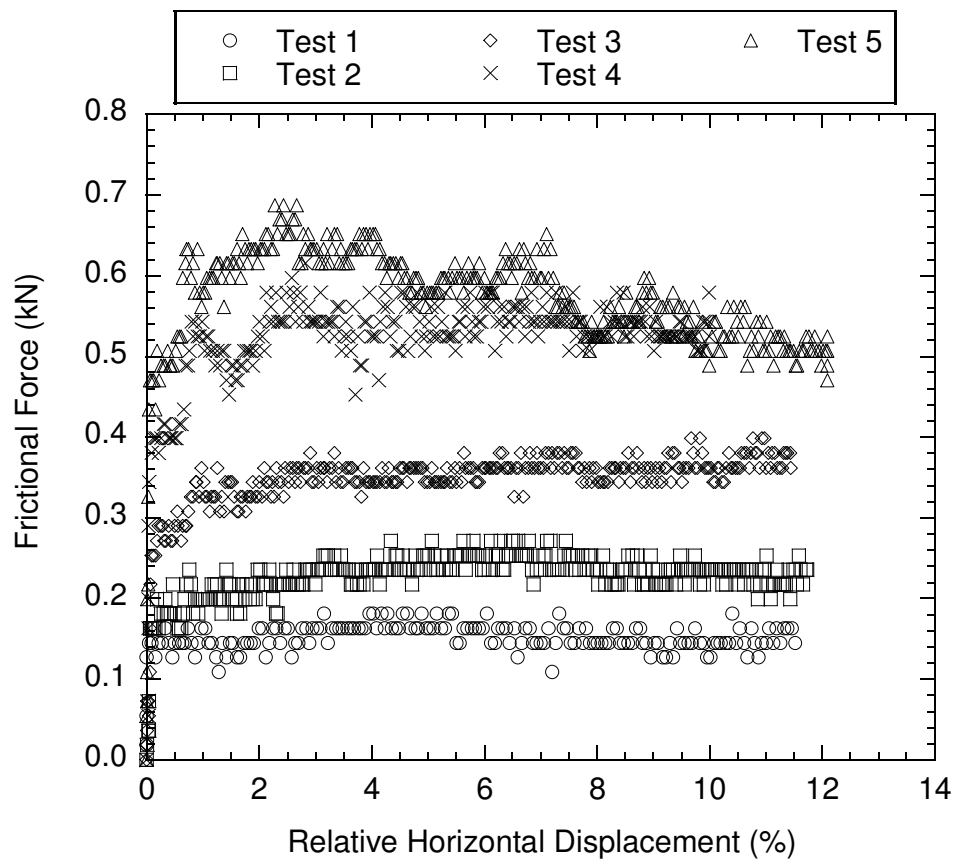


Fig. A2-1. Relationship of box interface frictional force and relative horizontal displacement for tests at interface normal forces of 0.32, 0.55, 0.81, 1.28, and 1.48 kN.

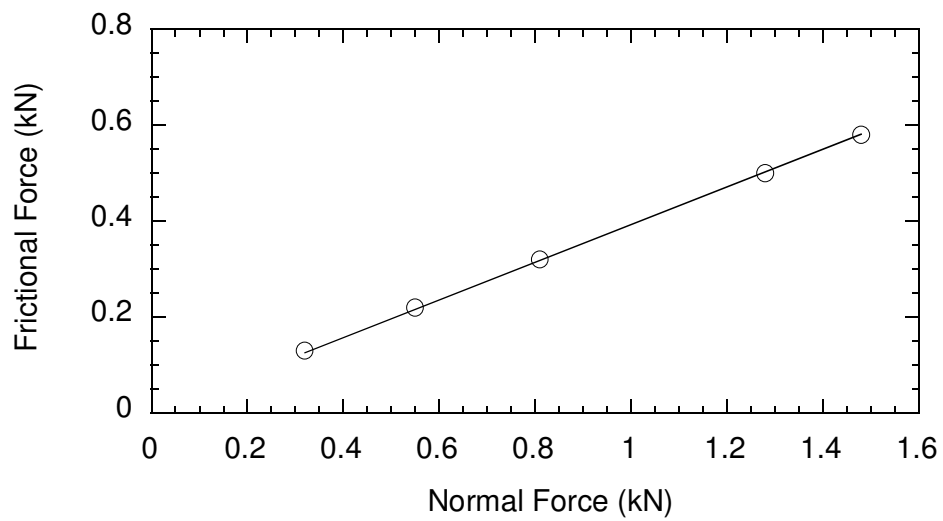


Fig. A2-2. Relationship of box interface frictional force and normal force.

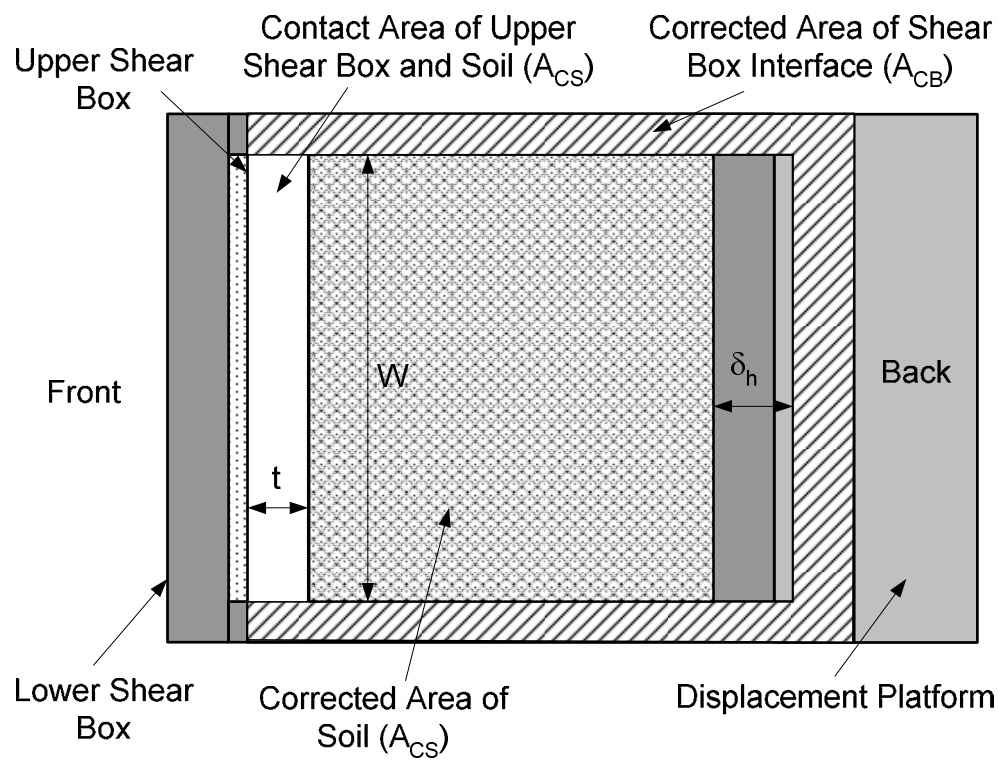


Fig. A2-3. Schematic of large-scale direct shear box identifying the corrected area of the shear box interface (A_{CB}), corrected area of soil (A_{CS}), contact area of upper shear box and soil (A_{CS}), horizontal displacement (δ_h), specimen width (W), and thickness of front of upper shear box (t).

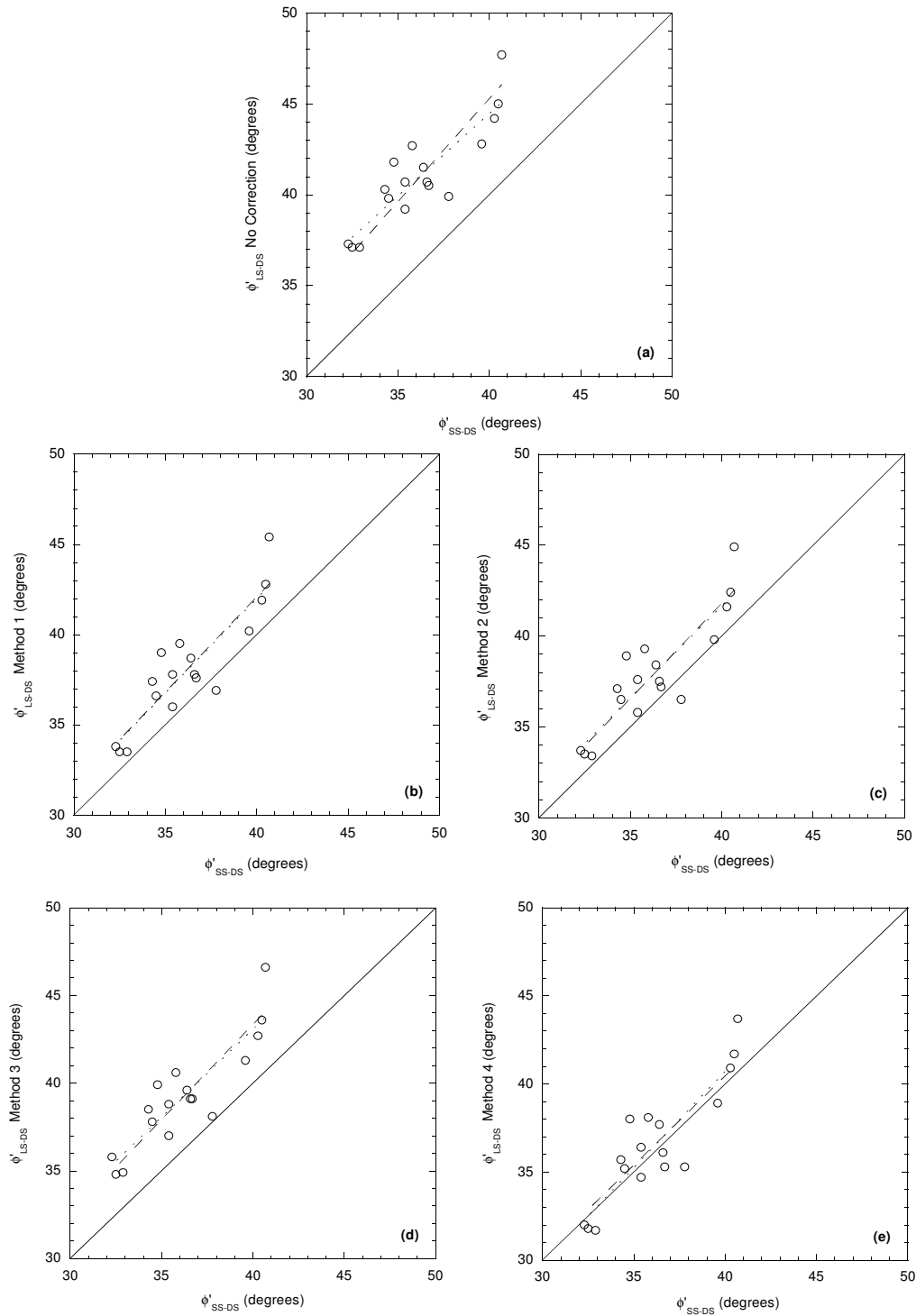


Fig. A2-4. Friction angles obtained from large-scale direct shear tests (ϕ'_{LS-DS}) versus friction angles obtained from small-scale direct shear tests (ϕ'_{SS-DS}): (a) no box friction correction applies, (b) box friction Method 1, (c) box friction Method 2, (d) box friction Method 3, and (e) box friction Method 4.

APPENDIX A3

A3. LARGE-SCALE DIRECT SHEAR SPECIMEN DENSITY

The specimens tested in small-scale direct shear (SS-DS) only contained particles passing the No. 4 sieve (P4) (maximum diameter of 4.75 mm). The specimens tested in the large-scale direct shear (LS-DS) contained particles retained on the No. 4 sieve (R4) and had a maximum diameter of 25.4 mm. To fairly compare the shear strength measured in SS-DS and LS-DS, the density of the P4 material was kept the same in both SS-DS and LS-DS.

Equations were developed to define the mass of P4 (M_{P4}) and R4 (M_{R4}) solids to be included in a LS-DS specimen so that the P4 would have the same density as that in SS-DS. Two assumptions were employed: (1) the R4 material acts as inclusions in the total specimen volume and does not contribute a void volume and (2) the particle size distribution curve (corrected to 100% passing a 25.4 mm sieve) can be used to define the percentages of P4 and R4 material based on weight. The total LS-DS specimen volume (V_T) is determined by:

$$V_T = V_{P4} + V_{VP4} + V_{R4} \quad (\text{A3.1})$$

where V_{P4} is the volume of P4 solids, V_{VP4} is the void volume of the P4 material, and V_{R4} is the volume of R4 solids. The volumes V_{P4} , V_{VP4} , and V_{R4} can be expressed in terms of their masses (M) and specific gravity of solids (G_s) as:

$$V_{P4} = \frac{M_{P4}}{G_{SP4} \times \rho_w} \quad (\text{A3.2})$$

$$V_{VP4} = e_{P4} \left(\frac{M_{P4}}{G_{SP4} \times \rho_w} \right) \quad (\text{A3.3})$$

$$V_{R4} = \frac{M_{R4}}{G_{SR4} \times \rho_w} \quad (\text{A3.4})$$

where G_{sP4} is the specific gravity of the P4 solids, G_{sR4} is the specific gravity of the R4 solids, and e_{P4} is the void ratio of the P4 material corresponding to the dry density of the P4 material (ρ_{dP4}). The void ratio e_{P4} is obtained by Eq. A3.5.

$$e_{P4} = \left(\frac{G_{sP4} \times \rho_w}{\rho_{dP4}} \right) - 1 \quad (\text{A3.5})$$

Eq. A3.1 can be written in terms of Eqs A3.2 – A3.4

$$V_T = \left(\frac{M_{P4}}{G_{SP4} \times \rho_w} \right) + e_{P4} \left(\frac{M_{P4}}{G_{SP4} \times \rho_w} \right) + \left(\frac{M_{R4}}{G_{SR4} \times \rho_w} \right) \quad (\text{A3.6})$$

and M_{P4} and M_{R4} can be related by:

$$M_{R4} = \left(\frac{\alpha}{\beta} \right) M_{P4} \quad (\text{A3.7})$$

where α is the percentage R4 material (by weight) of the total sample and β is the percentage of P4 material (by weight) of the total sample (determined from the particle size distribution curve). Combining Eq. A3.6 and Eq. A3.7, and solving for M_{P4} yields:

$$M_{P4} = \left[\frac{V_T}{\left(\frac{1}{G_{sP4} \times \rho_w} \right) + \left(\frac{e_{P4}}{G_{sP4} \times \rho_w} \right) + \left(\frac{\alpha/\beta}{G_{sR4} \times \rho_w} \right)} \right] \quad (\text{A3.8})$$

Once MP4 is known, MR4 is obtained by Eq. A3.7. These computations were used for all sands containing greater than 5% R4 material.

APPENDIX B

REPRODUCIBILITY OF DIRECT SHEAR TESTS CONDUCTED ON GRANULAR BACKFILL MATERIALS

Abstract: Intra-laboratory and inter-laboratory testing was conducted to assess the bias, repeatability, and reproducibility of the shear strength of compacted granular backfill materials tested in direct shear using AASHTO T 236. Inter-laboratory testing was conducted by 10 laboratories using four granular backfill materials. Triaxial compression tests were also conducted on the granular backfill materials to establish a reference friction angle (ϕ') for computing bias. Comparison of failure envelopes and friction angles from the intra-laboratory study showed that the test method is highly repeatable ($\phi' \pm 0.12^\circ$) when conducted in a single laboratory by a single operator using the same equipment. In contrast, data from the inter-laboratory study showed high variability in the failure envelopes and friction angles, with ϕ' varying by as much as 18.2° for a given backfill. Analysis of the data from the inter-laboratory study showed that the reproducibility of direct shear tests on granular backfill is 8.8° . The bias in ϕ' is -2.7° when area corrections are not applied and -1.4° when area corrections are applied.

B-1. INTRODUCTION

Direct shear tests have been used to determine the shear strength of soil for more than 150 yr. A historical account of the engineering application of direct shear testing is provided by Matthews (1988). Most direct shear tests in North America are conducted in accordance with ASTM D 3080 (*Standard Test Method for Direct Shear Test of Soils Under Consolidated Drained Conditions*) or AASHTO T 236 (*Standard Method of Test for Direct Shear Test of Soils Under Consolidated Drained Conditions*). These test methods have been available for decades,

but quantitative information about the reproducibility associated with shear strengths determined by these methods is virtually non-existent.

To the authors' knowledge, only Converse (1952) has evaluated the reproducibility of direct shear testing, and this study was conducted before the ASTM and AASHTO methods were first published. Converse had seven laboratories perform direct shear tests on dry 20-30 Ottawa Sand in loose and dense states using either displacement or stress-controlled loading. The minimum, maximum, average, and standard deviation of ϕ' obtained from the tests are summarized in Table 1. A wide range in ϕ' was obtained with either method, which was attributed in part to the absence of a standardized test method and the use of a broad range of testing procedures. Based on these findings, Converse (1952) recommended that ASTM develop a standard method for direct shear testing that detailed machine specifications and testing procedures.

A common application of direct shear testing is to verify that granular backfill materials for mechanically stabilized earth (MSE) walls and reinforced soil (RS) slopes have adequate shear strength. Controversy regarding disqualification of borrow sources based on friction angles measured in direct shear has resulted in concern regarding the bias and reproducibility of the test method as it is implemented in practice. The objective of this study was to estimate the reproducibility and bias of ϕ' that is representative of US practice when testing granular backfill materials using the direct shear test procedure in T 236. Ten laboratories were requested to conduct direct shear tests on four granular backfill materials under the same conditions following the method in T 236. An intra-laboratory study was conducted at the University of Wisconsin-Madison to define the inherent repeatability of the test method. Drained triaxial compression tests were also conducted on the four materials at the University of Wisconsin-Madison to define a reference ϕ' for each material.

B-2. DEFINITIONS, MATERIALS, AND METHODS

B-2.1. DEFINITIONS

Bias, precision, repeatability, and reproducibility are used throughout this paper as defined in ASTM E 177 (*Standard Practice for Use of the Terms Precision and Bias in ASTM Methods*). Bias is defined as “the difference between the expectation of the test results and an accepted reference value.” Precision is defined as “the closeness of agreement between independent test results obtained under stipulated conditions.” Repeatability describes precision under “conditions where independent test results are obtained with the same method on identical test items in the same laboratory by the same operator using the same equipment within short intervals of time.” Reproducibility describes precision under “conditions where test results are obtained with the same method on identical test items in different laboratories with different operators using different equipment.”

B-2.2. SANDS

Four poorly graded sands labeled P1-S1, P1-S6, P2-S9, and TS were selected as granular backfill materials for the study. Each of the sands is a potential source of granular backfill for MSE walls and RS slopes in Wisconsin. Particle size distribution curves for the sands are shown in Fig. B-1 and physical characteristics of the sands are summarized in Table B-2. The sands classify as SP according to the Unified Soil Classification System (USCS), with a coefficient of uniformity (C_u) ranging from 1.86 to 4.16, median particle size (D_{50}) ranging from 0.3 to 0.5 mm, gravel content (particles > 4.8 mm) ranging from 0 to 22%, and fines content (particles less than 75 μm) ranging from 0 to 2%. The sands also differ in maximum dry unit weight (17.36 to 18.64 kN/m^3), specific gravity (2.63 to 2.7), maximum void ratio (0.56 to 0.76), minimum void ratio (0.33 to 0.48), and Krumbein roundness (0.42 to 0.62).

B-2.3. TEST METHODS

ASTM D 3080 and AASHTO T 236 are the two commonly used test methods for direct shear testing in the United States. The standards are very similar. The differences that exist between the test procedures are listed in Table B-3. With exception of the gap spacing (Table B-3), an identical direct shear test can be conducted using D 3080 or T 236. Throughout this study, T 236 was followed for all direct shear tests with stipulations mentioned subsequently. The AASHTO method was used rather than the ASTM method because the study was conducted primarily for transportation-related construction, and AASHTO standards are more common in transportation construction.

B-2.4. INTRA-LABORATORY DIRECT SHEAR TESTS

Intra-laboratory direct shear (DS) tests were conducted at the University of Wisconsin-Madison on Sand TS following the procedure in AASHTO T 236 to define the repeatability of direct shear tests conducted by a single operator using the same equipment. These tests were conducted in a Wykeham Farrance direct shear machine (Model No. 25301) using a square single shear box 64 mm wide containing a specimen 31 mm thick. Tests were conducted at normal stresses of 26, 62, 99, 147, and 184 kPa. The maximum stress is comparable to the stress expected at the bottom of a 10-m high MSE wall backfilled with dense granular fill having a unit weight of 18 kN/m³.

Sands tested in DS were sieved past a No. 4 sieve (4.75 mm) so that the dimensional criteria in T 236 would be met. The sand was compacted air dried in the shear box in three lifts of equal thickness by tamping the top of each lift with a wooden tamper. The number of tamps per layer was adjusted until the dry density equaled 95% of the maximum dry unit weight (γ_{dmax}) determined by standard Proctor compaction, which is the compaction criterion used in Wisconsin and many other states for controlling the density of granular backfill.

The specimens were inundated immediately following application of the normal stress by gradually filling the direct shear chamber with deionized (DI) water. Vertical deformation of the specimen was recorded during normal stress application and inundation. After vertical deformation ceased, the upper and lower shear boxes were separated approximately 0.25 mm as stipulated in T 236, and shearing was conducted at a constant rate of displacement of 0.24 mm/min. No grease or Teflon coating was used between the shear boxes to reduce friction.

Drainage was permitted through 9-mm-thick perforated PVC plates placed on the top and bottom of the specimen. Separation was provided by a thin non-woven heat-bonded and calendared geotextile placed between the sand and the plates. Compression of the plates and geotextiles was measured at each normal stress. The volume change on initial normal loading in each test was corrected for compression of the plates and geotextiles.

Measurements of horizontal displacement, vertical displacement, and shear force were recorded using a personal computer equipped with a Validyne data acquisition card (UPC601-U) and LABView software. Two linear variable displacement transducers (LVDTs) (Schlumberger Industries Model AG/5, 5 ± 0.003 mm) were used to measure horizontal and vertical displacements and a load cell (Revere Transducer Model 363-D3-500-20P1, 2.2 ± 0.00015 kN) was used to measure shear force.

Shear strength was defined at peak stress for all intra-laboratory direct shear tests on Sand TS. Area corrections were not applied to any of the data and Mohr-Coulomb failure envelopes were obtained by linear least-squares regression with a non-negative intercept. The failure envelopes exhibited a high degree of linearity expressed by coefficients of determination (R^2) ranging from 0.997 to 1.000. In all cases, the cohesion intercept (c') was small, ranging between 1.6 and 2.7 kPa. This cohesion intercept (c') represents friction in the shear box and machine components, and possibly non-linearity of the failure envelopes near the origin.

B-2.5. INTER-LABORATORY DIRECT SHEAR TESTS

Ten laboratories participated in the study. Seven of these laboratories were commercial laboratories providing testing services to the public. Two were laboratories operated by state departments of transportation that conduct testing to support in-house design as well as conformance during construction. One was a university research laboratory. The laboratories were located in seven states in the US.

The backfill materials used in the study were collected as large (130 kg) samples for a related study on granular backfills. Each of the large samples was air dried and then thoroughly blended to ensure uniformity. Sub-samples of the large samples were sent to the laboratories. These sub-samples were also air-dried, sieved past the No. 4 sieve, and thoroughly blended before being sent to the laboratories. Each laboratory received 1.2 kg of each backfill material and was informed that the materials had been passed through a No. 4 sieve.

Each laboratory was provided with a copy of AASHTO T 236 and the following instructions identifying stipulations to the testing procedure:

1. Soil samples were to be mixed thoroughly and spread in a thin layer to air dry for 24 hr. After air-drying, the soil was to be mixed thoroughly again.
2. All tests were to be conducted in a direct shear box (i.e., single shear plane) with displacement-controlled equipment.
3. A shear box meeting the criteria in Sections 5.3-5.5 in AASHTO T 236 was to be used. The width was to be at least 50 mm and the specimen width-to-thickness ratio was to be at least 2:1. A square shear box was to be used if available.
4. None of the contacting surfaces of the shear box were to be lubricated with grease or Teflon.
5. The porous stones were not to be dampened before preparing the test specimens.
6. Each specimen was to be compacted in three layers of equal thickness to specified target dry unit weights (Table 2). Air dry soil was to be compacted in the box and no moisture was to be added prior to compaction. An equal compactive effort was to be applied to each layer to the extent practical.
7. Fresh soil was to be used for each test.

8. Each backfill material was to be tested at normal stresses of 26, 62, 99, 147, and 184 kPa. However, normal stresses close to these target normal stresses were acceptable if the equipment being used could not apply the aforementioned normal stresses.
9. Each specimen was to be inundated after the normal stress was applied and for at least 10 min before shearing began.
10. Each specimen was to be sheared at a displacement rate of 0.24 mm/min.
11. Each specimen was to be sheared until the relative horizontal displacement (box displacement \div box length \times 100) was at least 12%.
12. Data from the tests was to be reduced and analyzed following the requirements in AASHTO T 236 and the methods employed in the laboratory's standard practice.
13. The reporting requirements in AASHTO T 236 were to be followed. The following items were to be included in the report:
 - graph of shear strength versus normal stress,
 - graph of shear stress versus horizontal displacement (or relative horizontal displacement) for each specimen tested with the point used to define failure clearly identified,
 - graph of vertical displacement versus horizontal displacement (or relative horizontal displacement) for each specimen tested,
 - a brief summary of procedures and calculations including box shape, area corrections, and deviations from the standard procedure, and
 - a digital format of all data and graphs.

All calculations were checked for accuracy when data were received in spreadsheet form. Data received in other formats were checked to the extent possible and otherwise assumed to be calculated correctly. All graphs of shear stress and vertical displacement versus horizontal displacement were examined for anomalies and to evaluate how the laboratories selected the failure stress. For all but one test, peak stress chosen by the laboratories was used as the shear strength. None of the laboratories applied area corrections, which is consistent with the absence of instructions on area corrections in T 236. Thus all data presented and discussed henceforth have no area corrections applied, unless noted otherwise.

B-2.6. TRIAXIAL COMPRESSION TESTS

Triaxial compression (TC) tests were conducted on the sands for comparison with the DS data. No standard method exists for performing consolidated drained TC tests on granular soils. Thus, a triaxial testing procedure was used that simulated, as closely as possible, conditions imposed in the DS tests.

Specimens for the TC tests were prepared in a split mold (74 mm diameter, 147 mm tall) lined with a latex membrane in a similar manner as those used for DS testing. Air-dried sand passing the No. 4 sieve was used for all specimens. The specimens were prepared to the same dry unit weight as used in the DS tests. Compaction was performed in three layers of equal thickness by tamping the top of each layer with a tamper with the number of tamps per layer adjusted to achieve the target density.

A cell pressure of 34 kPa was initially applied and water was circulated through the specimen from the bottom up using a small head differential (< 6.0 kPa). Elevated backpressure was not used and B-checks were not performed so as to simulate the inundation condition used for the DS tests. Each sand was tested at effective confining pressures of 21, 41, 62, and 83 kPa. The effective confining pressures were chosen so that normal and shear stresses at failure fell within the range of those used in the DS tests.

An axial strain rate of 0.11 mm/min was used to provide a similar displacement rate along the failure plane as was applied in the DS tests. Measurements of axial displacement, axial force, and volume change were recorded using a personal computer equipped with a National Instruments data acquisition card (Model SC-2345) and LABView software. A linear variable displacement transducer was used to measure vertical displacement (RDP LLECTRONICS Model ACTL000A, 50 ± 0.09 mm), a load cell was used for axial force measurements (Revere Transducer Model 363-D3-500-20P1, 2.2 ± 0.00015 N), and a burette equipped with a pressure transducer was used to monitor the volume of water expelled or

imbibed by the specimen (Validyne Model DP15-26 connected to a Valdyne Model CD379 digital transducer indicator).

Failure in the triaxial compression (TC) tests was defined as the peak stress from p' - q relationships. Area corrections, computed assuming the specimen deforms as a right circular cylinder during shear, were applied to all data. A p' - q diagram and the failure envelope for Sand TS are shown in Fig. B-2. All sands exhibited p' - q behavior similar to that obtained for Sand TS (Fig. B-2). Strength parameters a and ψ (Holtz and Kovacs 1981) were obtained by linear least-squares regression through the p' - q failure stresses with a non-negative intercept. The Mohr-Coulomb parameters c' and ϕ' were subsequently calculated from equations relating c' and ϕ' to a and ψ (Holtz and Kovacs 1981). Mohr-Coulomb failure envelopes for the sands are shown in Fig. B-3. Failure envelopes for all four sands exhibited a high degree of linearity ($R^2 = 0.993$ to 1.000) and small c' ($0.0 - 5.9$ kPa).

B-3. RESULTS

B-3.1 INTRA-LABORATORY TESTS

The five failure envelopes for Sand TS obtained from the tests to evaluate intra-laboratory repeatability are shown in Fig. B-4. The envelopes are essentially identical and correspond to ϕ' ranging from 41.5° to 41.8° . The average ϕ' is 41.6° and the standard deviation is 0.12° . Curves of shear stress versus relative horizontal displacement (RHD) for the five direct shear tests on Sand TS at normal stress of 147 kPa are shown in Fig. B-5a. Vertical displacement is shown in Fig. B-5b. Although some variability exists in shear-displacement curves in Fig. B-5a, the curves approach a similar peak stress occurring within $\pm 0.32\%$ RHD. The unique state of failure, irrespective of the shear-displacement curve, is represented by the nearly identical failure envelopes in Fig. B-4. The intra-laboratory direct shear tests on Sand TS

conducted at other normal stresses exhibited similar shear-displacement and dilative behavior as shown in Fig. B-4.

Analysis of covariance (ANCOVA) was conducted at a significance level of 0.05 (the significance level commonly used in hypothesis testing, Berthouex and Brown 2002) to determine if the failure envelopes are statistically similar. The analysis evaluates the similarity of slopes of regression lines (in this case $\tan \phi'$) under the null hypothesis that the slopes are identical, and returns a p-value corresponding to the probability of falsely rejecting the null hypothesis (Lowry 2006). The slopes are considered statistically similar if $p > 0.05$. The ANCOVA analysis yielded a p-value of 0.99 ($\gg 0.05$), indicating that the slopes of the failure envelopes ($\tan \phi'$) are not statistically different.

Repeatability and bias in ϕ' were assessed for the intra-laboratory study using the friction angle of Sand TS measured in TC as the reference standard ($\phi' = 42.1^\circ$, Fig. B-3). Bias was computed as the mean deviation between the ϕ' obtained for Sand TS in DS and TC. Repeatability was estimated as $\pm 2\sigma$, where σ is the standard deviation of the deviations between the ϕ' measured in DS and TC. Based on this analysis, the intra-laboratory bias of the direct shear test is -0.5° and the intra-laboratory repeatability is 0.24° . Applying area corrections to the data increased ϕ' to 42.6° , which increased the bias to 0.5° .

From a practical perspective, these findings indicate that the DS testing method in T 236 is unbiased and highly repeatable when conducted in a single laboratory by a single operator using the same equipment. Given the similarity between T 236 and ASTM D 3080, a similar inference can be made regarding the intra-laboratory bias and precision of D 3080.

B-3.2 INTER-LABORATORY DIRECT SHEAR TESTING

B-3.2.1. Failure Envelopes and Friction Angles

Failure envelopes obtained from the ten laboratories are shown in Fig. B-6 for each sand. The data points in Fig. B-6 correspond to the peak shear stresses chosen by each laboratory. However, the failure envelopes were defined by the authors using linear least-squares regression with a non-negative intercept. Friction angles and cohesion intercepts reported by each laboratory and those determined by the authors are listed in Table B-4. The ϕ' reported by the laboratories and determined by the authors differed by -0.3° , on average, with a standard deviation of 0.96° .

Visual inspection indicates that the failure envelopes vary significantly for each sand, despite each laboratory being provided with homogenized samples, the standard method, and additional stipulations intended to provide uniformity. Comparison of the failure envelopes for Sand TS obtained from the intra-laboratory (Fig. B-4) and inter-laboratory (Fig. B-6d) studies indicates that the inter-laboratory variability is much greater than the intra-laboratory variability. ANCOVA was conducted at the 5% significance level to determine if the failure envelopes obtained in the inter-laboratory study for each sand were statistically different. The p-values are summarized in Fig. B-6. In all cases, $p < 0.0001$ ($\ll 0.05$), indicating that statistically significant differences exist between the slopes of the failure envelopes for each sand.

The failure envelopes from Lab G (Fig. B-6) have noticeably greater slopes for sands P1-S1 and P1-S6 and greater intercepts for sands P2-S9 and TS compared to those from the other laboratories. Thus, the failure envelopes for Lab G were removed and the ANCOVA was conducted again using the failure envelopes from the remaining laboratories. Results of the ANCOVA analyses omitting Lab G are summarized in Table B-5. Even after omitting the data from Lab G from the ANCOVA analyses, the p-values are all $\ll 0.05$, indicating that the failure envelopes are statistically different.

The friction angles obtained by linear regression are shown in Fig. B-7. The variation in the friction angles is probably due to random and systematic errors. For example, the friction

angles from Laboratories A, B, D, I, and J consistently fall within $\pm 1\sigma$ of the average friction angle (ϕ'_a) for each sand, with exception the ϕ' for Sand TS from Laboratory I. These variations are probably natural variations in the application of the test procedure. In contrast, Laboratories C and F report lower ϕ' ($\leq \phi'_a - 1\sigma$) for three out of the four sands and Laboratory H report lower ϕ' ($\leq \phi'_a - 1\sigma$) for two out of the four sands. Similarly, Laboratories E and G report higher ϕ' ($\geq \phi'_a + 1\sigma$) for two out of the four sands, and near average ϕ' for the other two sands. The greater consistency in these high and low friction angles suggests that there is a systematic difference in how these laboratories are conducting direct shear tests compared to the other laboratories.

Some of the systematic variations may be due to variations in how the tests were conducted. Although all laboratories were instructed to follow T 236 and the additional stipulations cited previously, variations in the test method occurred. Test variables that varied between laboratories are tabulated in Table B-6. Six laboratories used a specimen thinner than 28.5 mm, even though T 236 requires that the specimen thickness be at least six times the maximum particle diameter [each sand included particles passing the No. 4 sieve (4.75 mm) and retained on the No. 10 sieve (2.0 mm), thereby establishing a maximum particle diameter of 4.75 mm]. Two laboratories did not follow the instructions in T 236 regarding gap spacing, even though gap spacing is known to affect the measured shear strength (Shibuya et. al. 1997; Lings and Dietz 2004). One laboratory used a displacement rate of 1.2 mm/min, even though the rate was specified in the additional stipulations. Identifying how the variations affected ϕ' is not possible with the data that were collected. Nevertheless, the variations in test method between laboratories probably contributed to the inter-laboratory variation in ϕ' .

B-3.2.2. Shear Deformation and Volume Change

Shear deformation and volume change behavior were examined to determine if causes for the large variability in failure envelopes and friction angles could be identified. Graphs of

shear stress versus RHD and vertical displacement versus RHD for Sand P1-S1 at a normal stress of 184 kPa are shown in Fig. B-8. Similar variability in the data was obtained for the other sands and at other stresses. The data in Fig. B-8 from Laboratory D are for tests performed at a normal stress of 177 kPa and for Laboratory I at a normal stress of 192 kPa, as these laboratories could not apply 184 kPa.

Considerable variability exists in the shear stress-displacement curves shown in Fig. B-8. A peak stress is present in some cases, whereas others exhibit only an ultimate stress. Of those tests with a distinct peak stress, the sharpness of the peak, the magnitude of the peak stress, the RHD at which the peak stress occurs, and the post-peak loss in strength vary substantially. A wide range in volume change behavior (dilative behavior to contractive) was also observed (Fig. B-8b). These large variations in shear-deformation and volume-change behavior suggest that differences in specimen preparation may have contributed to the inter-laboratory variability. However, the preparation instructions provided to the laboratories included more detail than is normally submitted for conventional testing. Thus, any variation in specimen preparation that occurred during this inter-laboratory study probably represents well-controlled conditions in practice. Even less control may exist under typical conditions in practice.

Some of the variability in peak stress can be attributed to differences in the frequency of data collection, as illustrated in Fig. B-9a using data from Sand P2-S9 tested at a normal stress of 184 kPa by Laboratories A, B, E, G, and J. Laboratories A and E used a higher sampling rate for data collection, resulting in smooth curves relating shear stress and RHD. Laboratories B, G, and J collected data less frequently, and were able to define the peak stress less precisely. To determine the sampling frequency needed to represent the peak stress, the shear stress-RHD curve obtained for Laboratory E was first fit with a polynomial (i.e., to define a continuous curve corresponding to infinite sampling frequency). This polynomial was then used to create

curves corresponding to different sampling frequencies as percentage of RHD, as shown in Fig. B-9b. At sampling frequencies $\geq 0.25\%$ RHD, the shear stress-RHD curves appear no different from the continuous function. For a square shear box that is 64 mm wide, this sampling frequency corresponds to a data point being collected every 0.16 mm of horizontal displacement during shearing.

B-3.2.3. Bias and Reproducibility

Statistics describing the variation in ϕ' are summarized in Table B-7. The inter-laboratory bias and reproducibility for each sand are also shown in Table B-7. The bias and reproducibility were computed using the same method employed for the intra-laboratory study. The bias ranges from -2.2° to -3.2° and is -2.7° , on average, and the inter-laboratory reproducibility ranges from 6.9° to 10.4° , and is 8.8° , on average. Thus, if the true friction angle of a sand was 34° , direct shear testing in practice typically would yield friction angles ranging from 23° to 40° .

Area corrections were applied to the direct shear data obtained in spreadsheet format to assess the contribution of the absence of area corrections on the bias. The corrected area (A_{CS}) in the shear plane for tests conducted with a square box was calculated as:

$$A_{CS} = A_i - (W \times \delta_h) \quad (1)$$

where A_i is the initial area, W is the width of the soil specimen, and δ_h is the horizontal displacement. The corrected area in the shear plane of tests conducted in a circular box was calculated as:

$$A_{CS} = A_i \left[\frac{1}{90} \times \cos^{-1} \left(\frac{\delta_h}{D} \right) - \frac{2}{\pi} \times \frac{\delta_h}{D} \times \sqrt{1 - \left(\frac{\delta_h}{D} \right)^2} \right] \quad (2)$$

where D is the diameter of the shear box. A comparison of friction angles obtained with and without area corrections is shown in Fig. B-10. Applying an area correction increases ϕ' by 0.4 to 2.5° (1.3° , on average) and reduces the average bias by 38%.

B-4. CONCLUSIONS

This paper has presented the findings of a study conducted to determine the bias and reproducibility of direct shear tests on compacted granular backfill materials used for MSE walls and RS slopes. AASHTO T 236 was used as the test method. Intra-laboratory repeatability was determined using data from five replicate direct shear tests conducted on one backfill material in a single laboratory by a single operator. Inter-laboratory reproducibility was determined using data from 10 laboratories that conducted direct shear tests on four backfill materials. Triaxial compression (TC) tests were also conducted on these four backfill materials to define a reference ϕ' for computing bias.

The intra-laboratory study showed that failure envelopes and friction angles are highly repeatable for direct shear tests conducted by a single operator following a detailed test procedure in a single laboratory. Comparison of five replicate tests on one backfill yielded ϕ' ranging from 41.5° to 41.8° , with an average of 41.6° and standard deviation of 0.12° .

Very different results were obtained from the inter-laboratory study. Data from the inter-laboratory study showed that ϕ' for a given backfill may range by as much as 18.2° . This large variability could not be attributed to a single factor. On average, the bias is -2.7° and the reproducibility is 8.8° . Part of the bias is due to the absence of area corrections. When area corrections are applied, the bias is reduced to -1.4° , on average.

This inter-laboratory direct shear investigation did not adhere to all of the requirements of ASTM E 691 (*Standard Practice for Conducting an Interlaboratory Study to Determine the Precision of a Test Method*) and AASHTO T 236 was used instead of ASTM D 3080. Moreover,

only granular materials were evaluated in this study, and direct shear testing is also conducted on fine-grained cohesive soils too. Thus, the findings from this study cannot be used to define a formal precision and bias statement for ASTM D 3080. Nevertheless, the aforementioned precision and bias are an indication of the precision and bias representative of practice for laboratories indicating that they conduct testing of compacted granular materials following AASHTO T 236 or ASTM D 3080.

The narrow variation in ϕ' obtained from the intra-laboratory study suggests that the test method is highly repeatable when conducted by a single operator in a single laboratory using the same equipment. In contrast, the wide variation in ϕ' obtained from the inter-laboratory study suggests that efforts are needed to improve the consistency of direct shear testing in the US. The wide variation in ϕ' from the inter-laboratory study also suggests that friction angles obtained from direct shear tests on compacted granular backfill materials may not be reliable for design or for conformance testing during construction.

B-5. ACKNOWLEDGEMENTS

The author would be greatly appreciative towards the following people for donating their time and services towards the completion of this study: Thomas F. Brokaw of the Wisconsin Department of Transportation, Derrick Dasenbrock of the Minnesota Department of Transportation, Bell DeGroff of Fugro Consultants LP, Karl A. Fletcher and James W. Fletcher of Bowser-Morner Inc., Joe Tomei and W. Allen Marr of Geo Testing Express Inc., Jeffery G. Smith and Jeffrey Miller of Wisconsin Testing Laboratories LLC, Patricia Mayfield and Henry Mock of Golder Associates Inc., William P. Quinn of STS Consultants Ltd., and John Whelan of Soil Engineering Testing, Inc.

REFERENCES

- Berthouex, P. M. and Brown, L. C. (2002) Statistics for Environmental Engineers, 2nd Ed., Lewis Publishers, Boca Raton, FL.
- Bishop, A. W. (1948) "A Large Shear Box for Testing Sands and Gravels," *Proceedings from the 2nd International Conference on Soil Mechanics and Foundation Engineering*, 1, 207-211.
- Converse, F. J. (1952) "The use of the direct shear testing machine in foundation engineering practice," *Symposium on Direct Shear Testing of Soils, ASTM STP 131*, American Society for Testing and Materials, 75-80.
- Elias, V., Christopher, B. R., and Berg, R. R. (2001) Mechanically Stabilized Earth Walls and Reinforces Soil Slopes Design and Construction Guidelines, *U. S. Department of Transportation Federal Highway Administration*, Publication No. FHWA-NHI-00-043.
- Holtz, R. D. and Kovacs, W. D. (1981) An Introduction to Geotechnical Engineering, Prentice Hall, Upper Saddle River, New Jersey.
- Lings, M. L. and Dietz, M. S. (2004) "An Improved Direct Shear Apparatus for Sand," *Géotechnique*, 54(4), 245-256.
- Lowry, R. (2006) Concepts and Applications of Inferential Statistics, Vassar College, <http://faculty.vassar.edu/lowry/webtext.html>.
- Matthews, M. C. (1988) "The Engineering Application of Direct and Simple Shear Testing," *Ground Engineering*, 21(2), 13-21.
- Palmeira, E. M. and Milligan, G. W. E. (1989) "Scale Effects in Direct Shear Tests on Sand," *Proceedings from the 12th International Conference on Soil Mechanics and Foundation Engineering*, 1, 739-742.
- Pells, P. J. N., Maurenbrechner, P. M., and Elges, H. F. W. K. (1973) "Validity of Results from the Direct Shear Test," *Proceedings from the 8th International Conference on Soil Mechanics and Foundation Engineering*, 1, 333-338.
- Rowe, P. W. (1969) "The Relation Between the Shear Strength of Sands in Triaxial Compression, Plain Strain and Direct Shear," *Géotechnique*, 19(1), 75-86.
- Shibuya, S., Mitachi, T., and Tamate, S. (1997) Interpretation of Direct Shear Box Testing of Sands as Quasi-Simple Shear, *Geotechnique*, 47(4), 769-790.
- Taylor, D. W., and Leps, T. M. (1938) "Shearing Properties of Ottawa Standard Sand as Determined by the M.I.T. Strain-Controlled Direct Shearing Machine," *Record of Proceedings of Conference on Soils and Foundations*, Corps of Engineers, U.S.A., Boston, MA.

Table B-1. Summary of shear strength testing on 20-30 dry Ottawa sand (Converse 1952).

Shear Machine	Density State	Shearing Stress	Maximum ϕ'	Minimum ϕ'	Average ϕ'	Standard Deviation ϕ'
Displacement Controlled	Loose	Ultimate	32.0	23.0	26.3	4.9
		Maximum	32.0	23.8	27.5	4.1
	Dense	Ultimate	34.8	24.0	27.8	6.1
		Maximum	43.2	29.3	36.1	6.9
Stress Controlled	Loose	Ultimate	43.7	24.0	34.7	7.6
	Dense		54.9	29.2	44.8	10.3

Table B-2. Physical characteristics of backfill materials used.

Sample	D ₅₀ (mm)	C _u	C _c	% Fines	% Gravel	G _s	e _{max}	e _{min}	γ _{dmax} (kN/m ³)	Target γ _d (kN/m ³)	Roundness	USCS Symbol
P1-S1	0.31	1.86	1.12	0.78	0.03	2.64	0.76	0.48	17.36	16.50	0.50	SP
P1-S6	0.34	2.35	1.15	0.79	1.78	2.63	0.69	0.43	17.59	16.70	0.62	SP
P2-S9	0.50	4.16	0.68	0.53	22.09	2.67	0.56	0.33	18.11	17.20	0.43	SP
TS	0.42	3.06	0.85	1.55	2.16	2.7	0.64	0.39	18.64	17.70	0.42	SP

D₅₀ = Median particle size, C_u = Coefficient of uniformity, C_c = Coefficient of curvature, % Fines = % by weight passing No. 200 sieve (0.075 mm), % Gravel = % by weight retained on No. 4 sieve (4.75 mm), G_s = Specific gravity, e_{max} = Maximum void ratio, e_{min} = Minimum void ratio, γ_{dmax} = Maximum dry unit weight.

Note: Particle size analysis conducted following ASTM D 422, G_s determined by ASTM D 854 for particles < 4.75 mm and by ASTM C 127 for particles > 4.75 mm, e_{min} determined by ASTM D 4253, e_{max} determined by ASTM D 4254, γ_{dmax} determined by AASHTO T 99 (Standard Proctor), Roundness determined by procedures in Krumbein (1941), and Unified Soil Classification determined by ASTM D 2487.

Table B-3. Summary of differences between ASTM D 3080 and AASHTO T 236 standards for direct shear testing.

Test Procedure	ASTM D 3080-04	AASHTO T 236-92
Shearing	Single shear	Single or double shear
Shear Machine	Displacement controlled	Displacement or stress controlled
Inundation	Inundation is optional	Inundation is specified
Gap Spacing	0.64 mm	0.25 mm
Data Collection Frequency ¹	Record every 2% of specimen width or diameter	Record at "convenient intervals"
Area Correction	Mentioned, no method provided	Not mentioned

¹Includes horizontal and vertical displacements and shear force

Table B-4. Friction angles and cohesion intercepts reported by laboratories and determined by authors.

Laboratory	Sample	Reported by Laboratories		Determined by Authors	
		ϕ'	c' (kPa)	ϕ'	c' (kPa)
A	P1-S1	34.6	5.03	34.6	5.03
	P1-S6	31.3	5.34	31.3	5.34
	P2-S9	37.5	8.17	37.5	8.17
	TS	41.6	2.16	41.6	2.16
B	P1-S1	33.3	2.14	33.3	2.17
	P1-S6	30.7	0.62	30.7	0.65
	P2-S9	39.7	15.79	39.7	15.76
	TS	40.9	0.97	40.9	0.93
C	P1-S1	29.0	NR	28.3	1.18
	P1-S6	30.0	NR	29.1	1.71
	P2-S9	32.0	NR	30.0	5.24
	TS	34.5	NR	35.6	0.00
D	P1-S1	31.3	0.00	31.4	0.00
	P1-S6	29.0	0.00	29.1	0.00
	P2-S9	35.2	0.00	36.0	0.00
	TS	40.6	0.00	40.8	0.00
E	P1-S1	34.3	0.00	33.7	1.54
	P1-S6	37.6	0.00	36.9	2.09
	P2-S9	42.5	0.00	43.3	0.00
	TS	39.4	0.00	39.4	1.56
F	P1-S1	24.6	27.03	24.5	24.97
	P1-S6	25.3	15.69	24.9	16.32
	P2-S9	36.4	4.10	36.2	5.46
	TS	32.7	5.34	32.3	7.86
G	P1-S1	42.9	-0.90	42.7	4.98
	P1-S6	41.6	-4.23	41.1	0.00
	P2-S9	35.4	33.80	35.3	34.05
	TS	38.0	37.25	37.8	43.01
H	P1-S1	29.0	7.18	28.7	7.26
	P1-S6	28.0	2.87	24.4	5.22
	P2-S9	32.0	12.45	31.8	12.59
	TS	40.0	2.39	39.5	2.47
I	P1-S1	31.5	12.54	32.0	11.12
	P1-S6	31.2	8.91	31.1	9.22
	P2-S9	34.4	26.33	36.5	17.98
	TS	43.6	12.92	44.1	10.50
J	P1-S1	37.2	0.00	36.4	4.59
	P1-S6	36.8	0.00	35.2	9.70
	P2-S9	42.0	0.00	39.1	19.74
	TS	42.8	0.00	42.1	8.92

NR - Not Reported

Table B-5. ANCOVA summary for inter-laboratory failure envelopes, omitting Lab G.

Sample	Variable	P-Value
P1-S1	Laboratory	0.0002
P1-S6	Laboratory	< 0.0001
P2-S9	Laboratory	< 0.0001
TS	Laboratory	< 0.0001

Table B-6. Box shape and dimensions, specimen thickness, displacement rate, and gap spacing used by laboratories in inter-laboratory direct shear testing.

Laboratory	Box Shape	Box Dimensions (mm)	Specimen Thickness	Displacement Rate (mm/min)	Gap Spacing (mm)
A	Square	63.5 x 63.5	30.5	0.24	0.25
B	Circular	63.5	NR	0.24	NR
C	Circular	71.1	19.1 to 28.6	1.2	0.787
D	Circular	63.5	25.4	0.24	NR
E	Square	60.0 x 60.0	31	0.24	NR
F	Circular	63.5	31.8	0.25	1.75 to 3.25*
G	Circular	63.1 and 73.0 ⁺	25.4	0.24	NR
H	Circular	63.5	25.0	0.22	NR
I	Circular	63.5	24.6	0.24	NR
J	Circular	63.5	25.4	0.24	NR

NR - Not Reported (assumed same as Lab A)

*Varied based on nominal maximum particle size

⁺63.1 mm box for sands P1-S1 and TS and 73.0 mm box for sands P1-S6 and P2-S9

Table B-7. Inter-Laboratory Direct Shear Statistics.

Statistic	P1-S1	P1-S6	P2-S9	TS
Minimum	24.5	24.4	30.0	32.3
Maximum	42.7	41.1	43.3	44.1
Average	32.6	31.4	36.4	39.4
Standard Deviation	5.0	5.2	3.7	3.4
Triaxial ϕ'	34.8	34.3	42	42.1
Bias	-2.2	-2.9	-5.6	-2.7
Reproducibility ($\pm 2\sigma$)	9.9	10.4	7.4	6.9

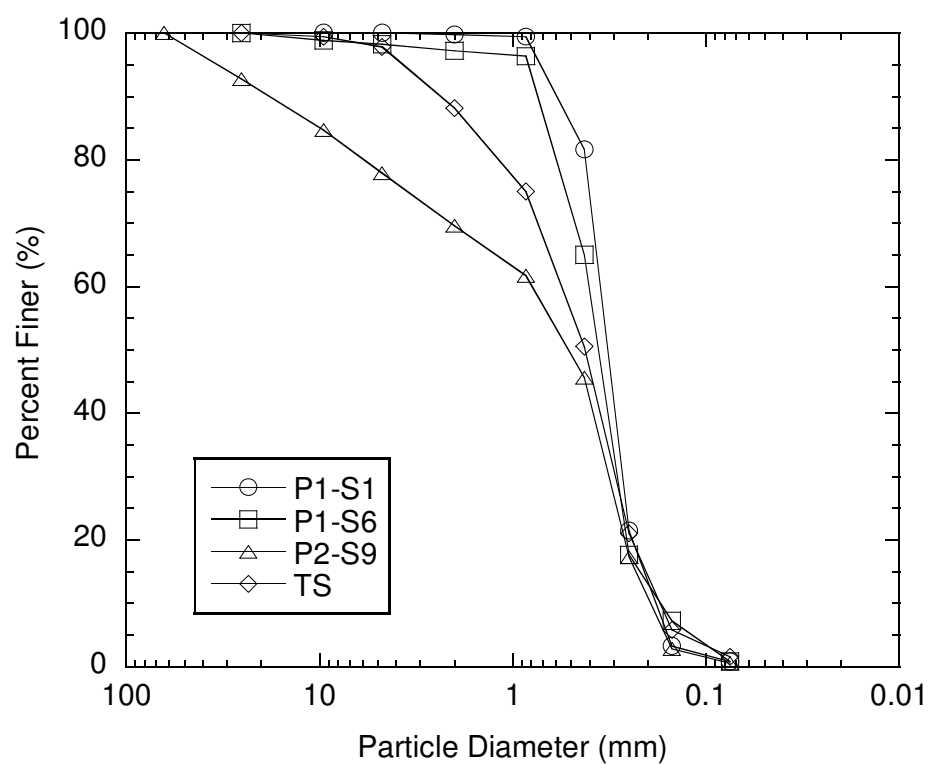


Fig. B-1. Particle size distribution curves for backfill materials used in this study.

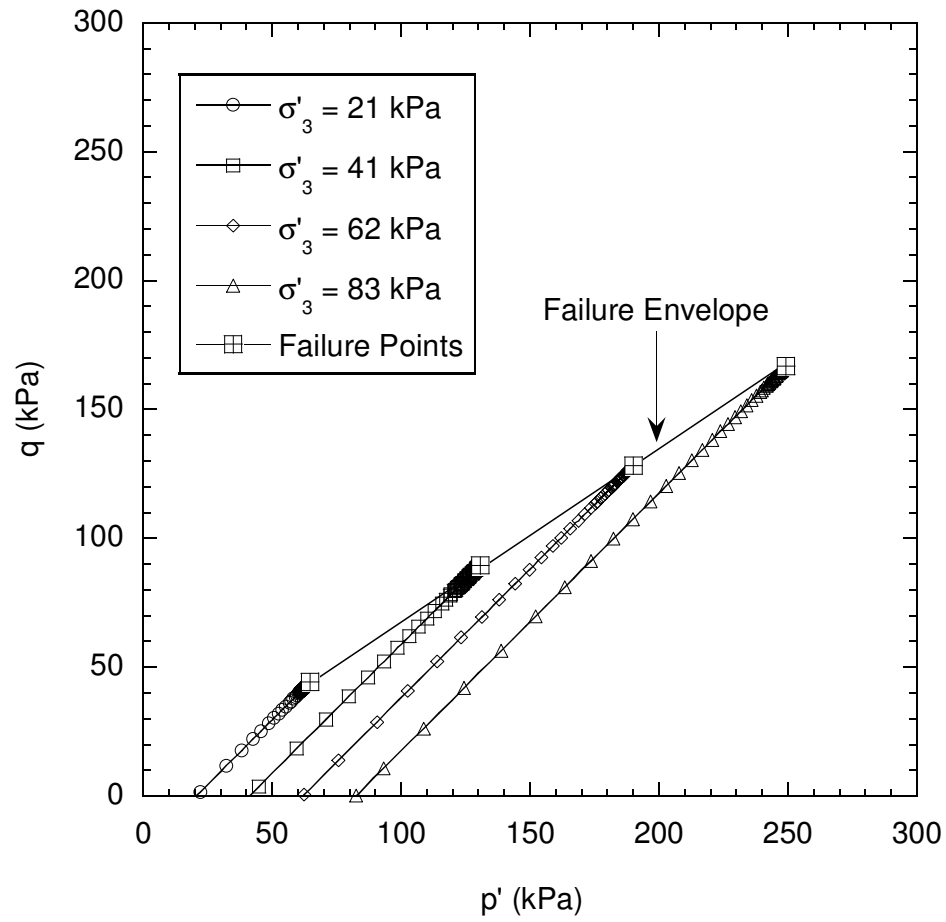


Fig. B-2. p'-q diagram for Sand TS in triaxial compression with failure envelope.

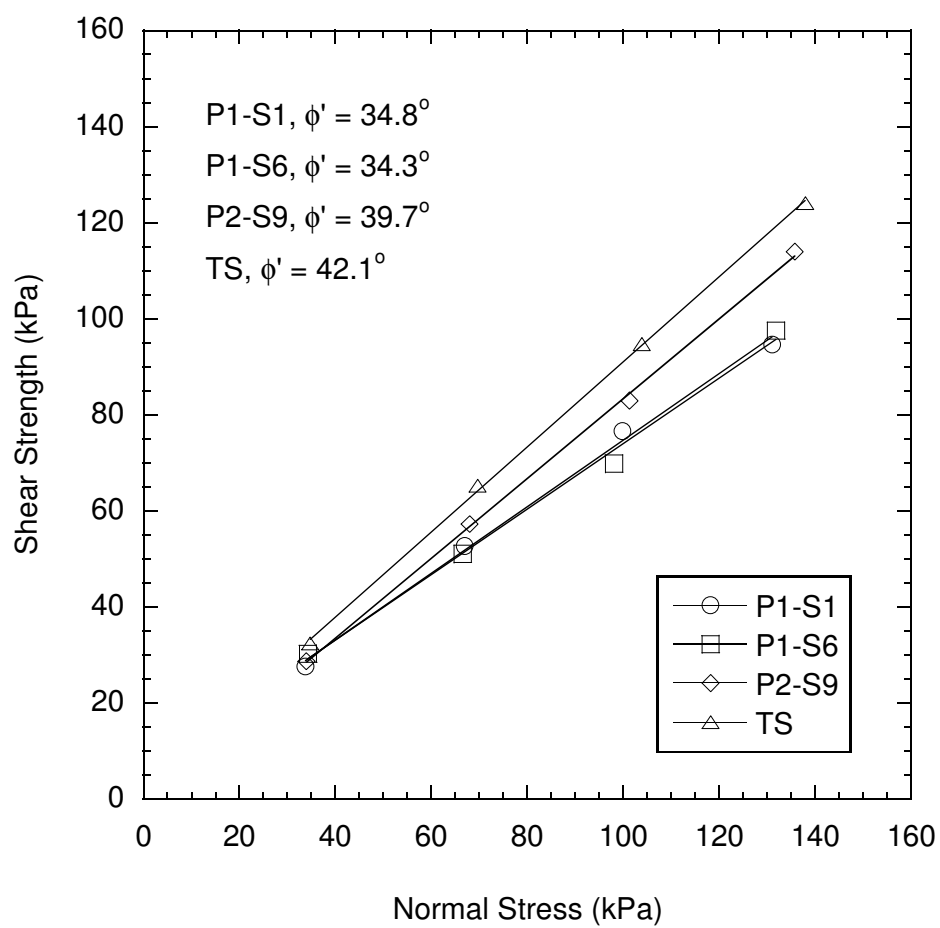


Fig. B-3. Mohr-Coulomb failure envelopes and friction angles for triaxial compression tests on P1-S1, P1-S6, P2-S9, and TS.

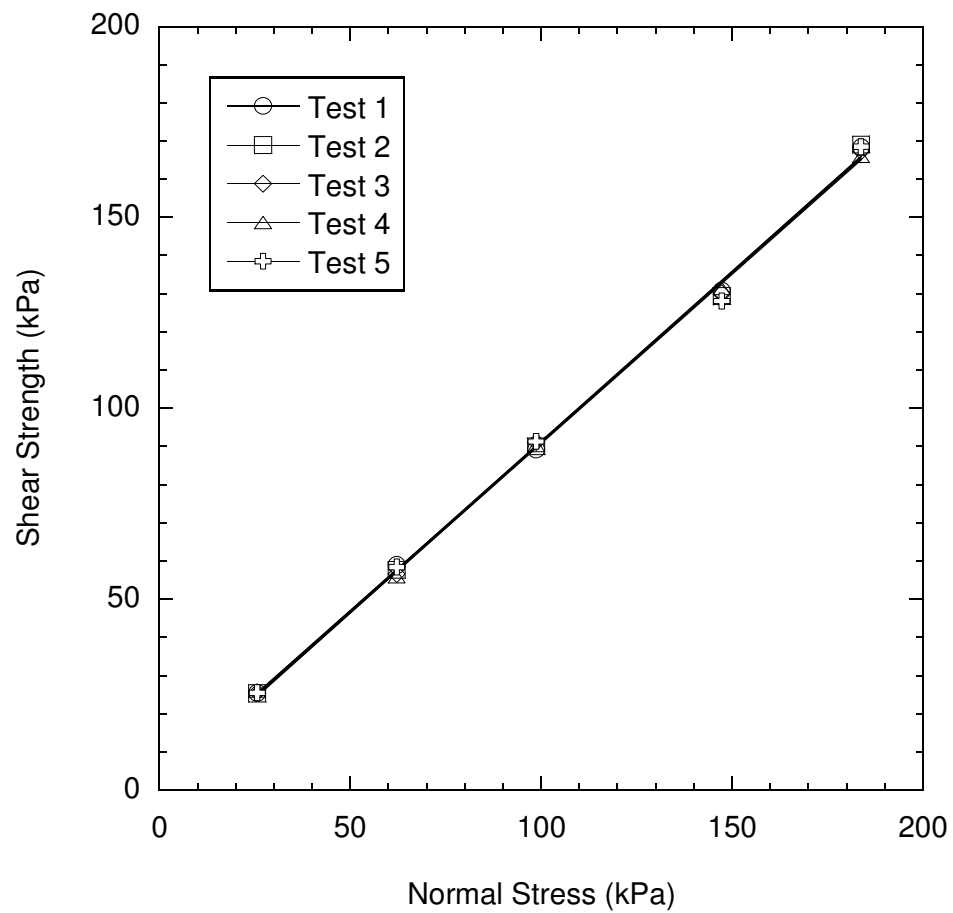


Fig. B-4. Failure envelopes for Sand TS obtained from intra-laboratory direct shear tests.

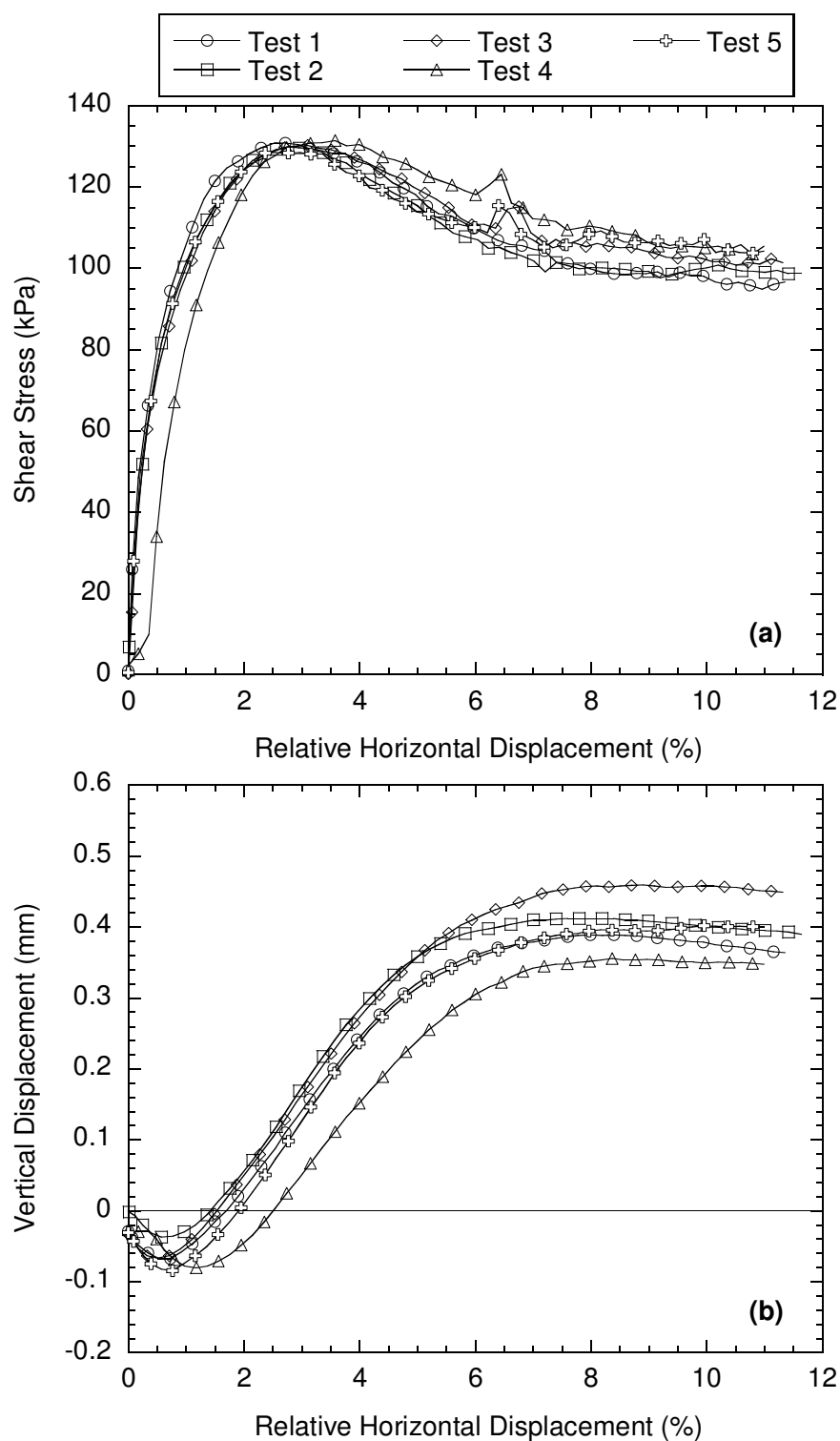


Fig. B-5. (a) Shear stress versus relative horizontal displacement and (b) vertical displacement versus relative horizontal displacement for intra-laboratory direct shear tests on Sand TS at a normal stress of 147 kPa.

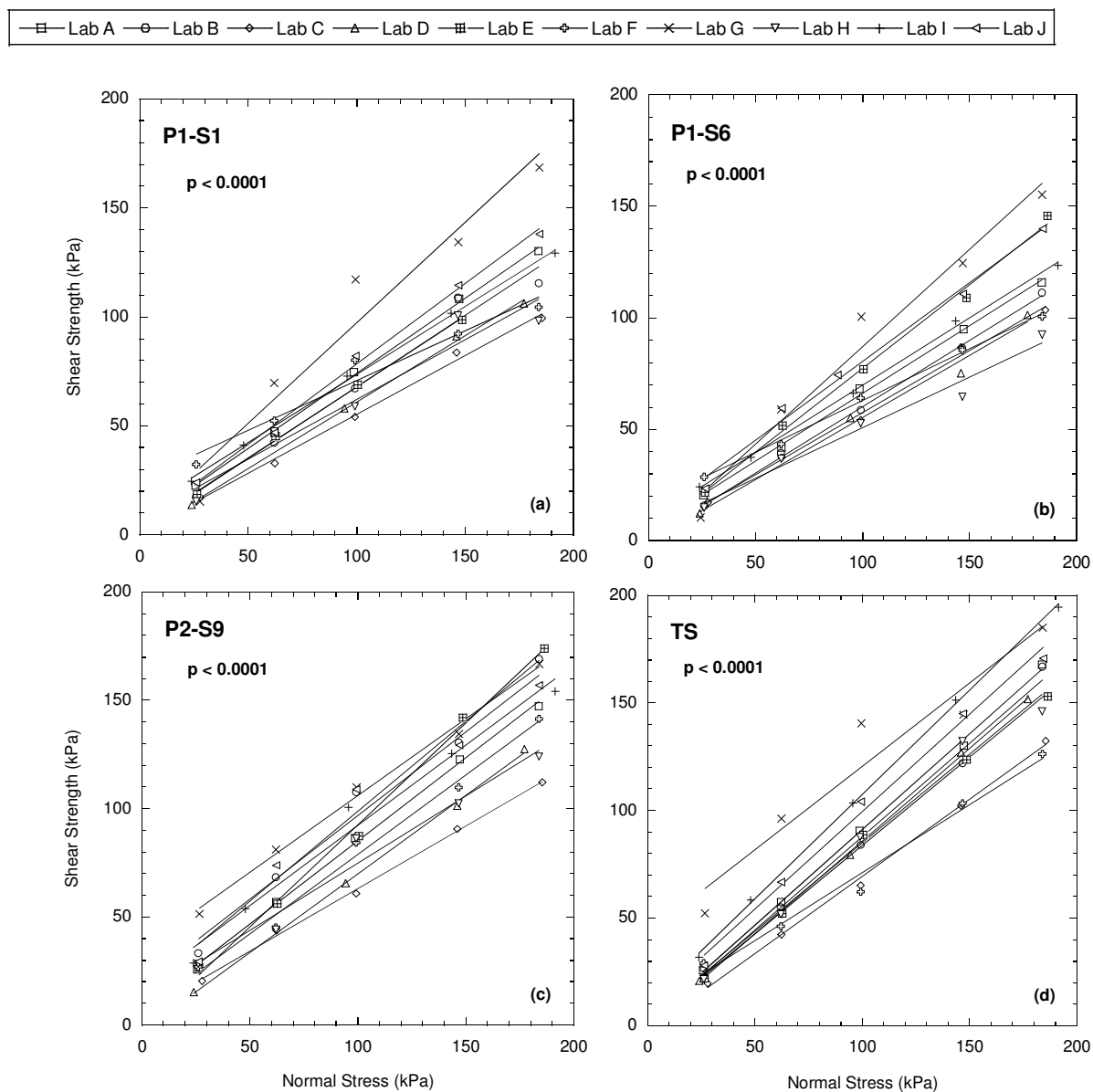


Fig. B-6. Failure envelopes from inter-laboratory direct shear tests: (a) Sand P1-S1, (b) Sand P1-S6, (c) Sand P2-S9, and (d) Sand TS.

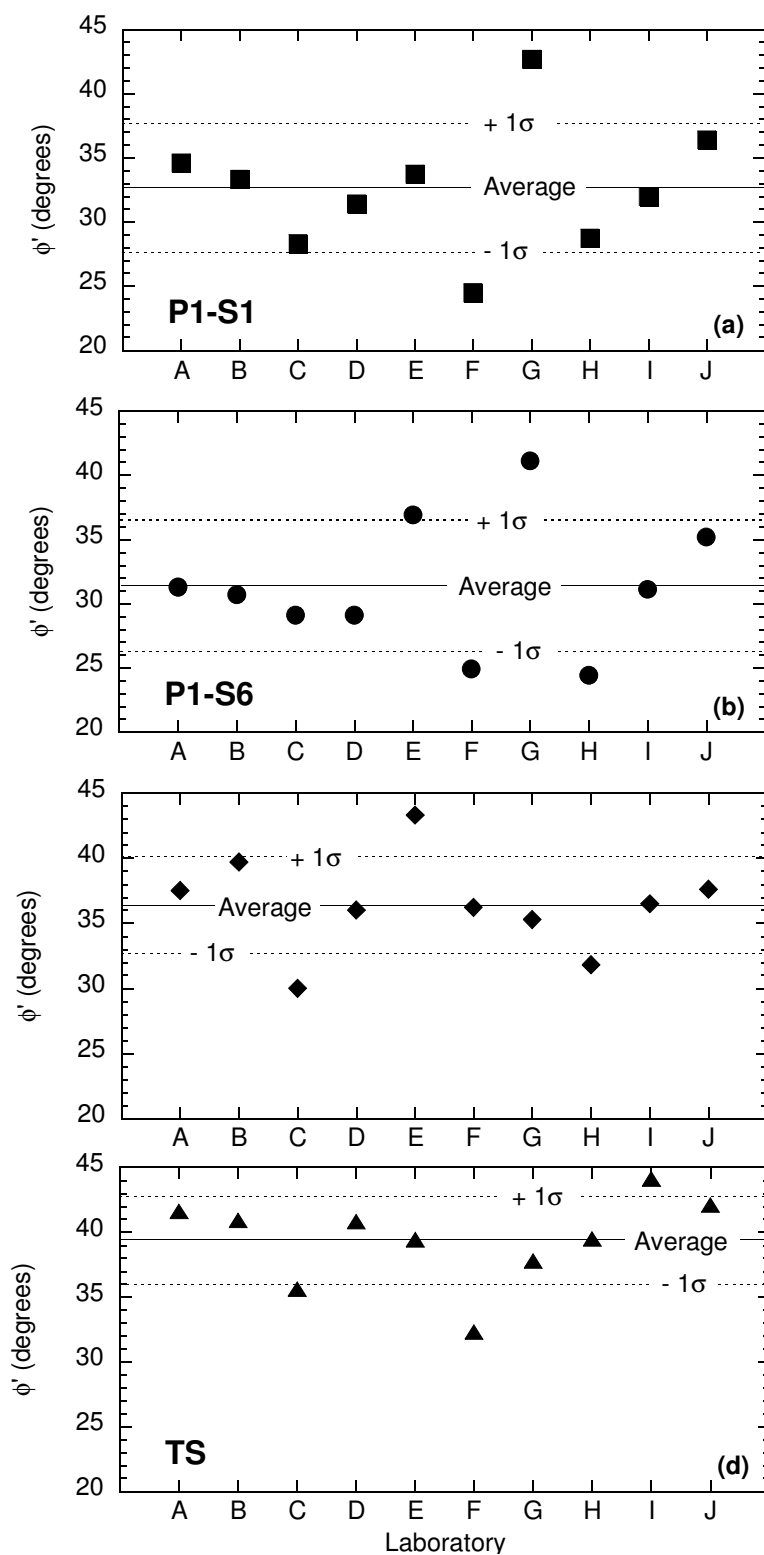


Fig. B-7. Friction angles from inter-laboratory direct shear tests (a) P1-S1, (b) P1-S6, (c) P2-S9, and (d) TS.

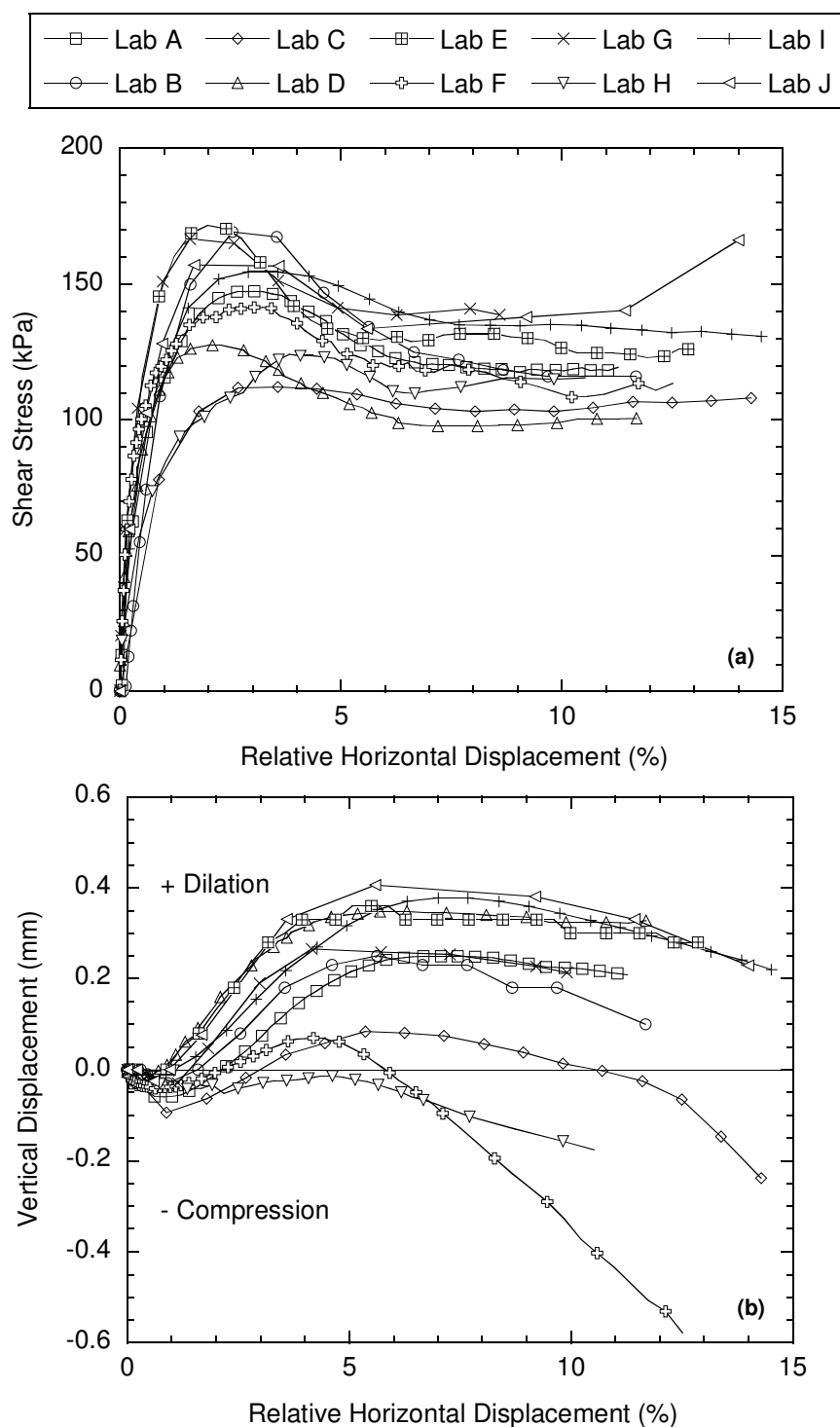


Fig. B-8. Shear stress vs. relative horizontal displacement (a) and vertical displacement vs. relative horizontal displacement (b) for Sand P1-S1 at normal stress (σ_n) of 184 kPa. Data reported for all laboratories except Lab D (tests conducted at $\sigma_n = 177$ kPa) and Lab I (tests conducted at $\sigma_n = 192$ kPa).

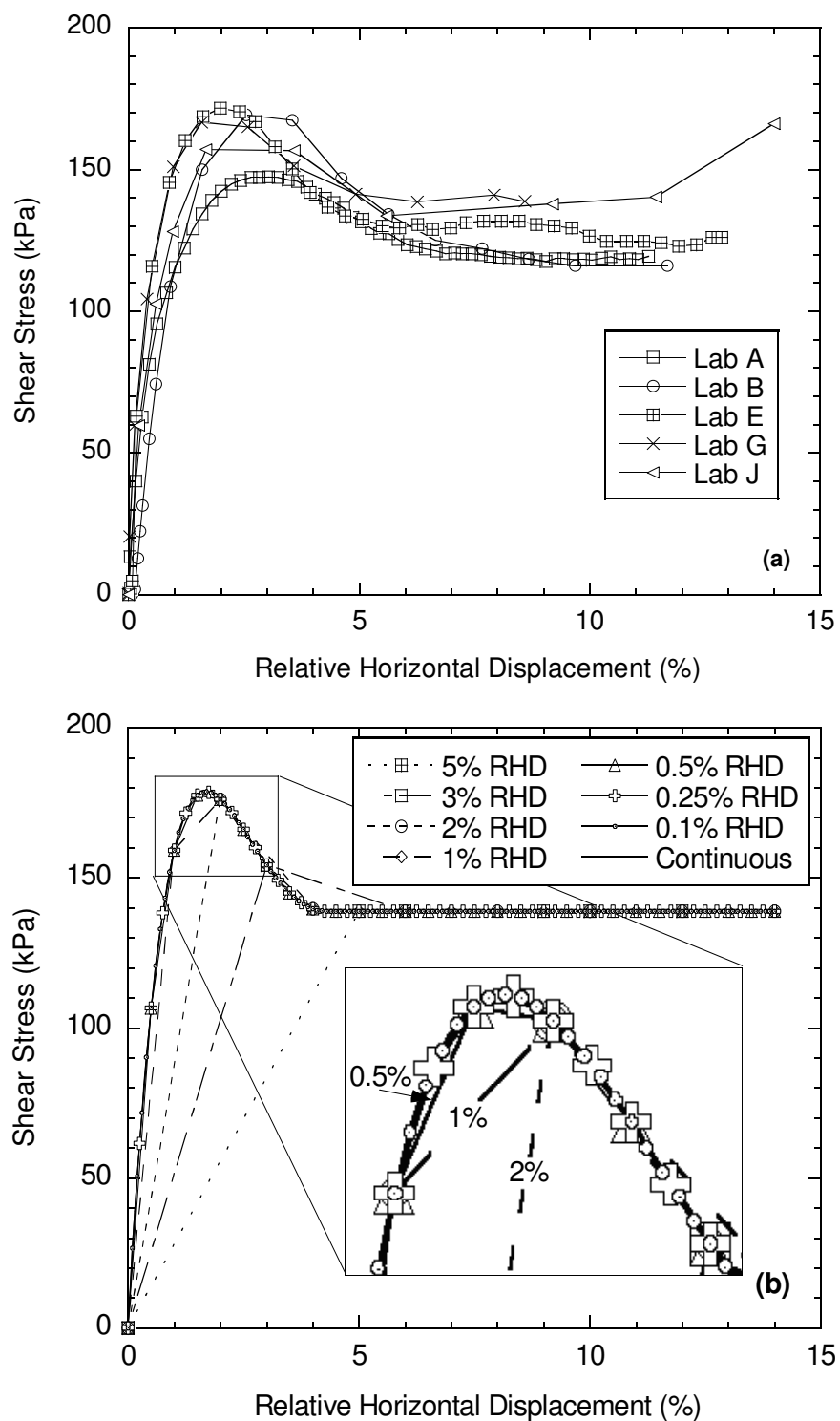


Fig. B-9. Shear stress vs. relative horizontal displacement for Sand P2-S9 at a normal as reported by Laboratories A,B,E,G and J and (a) hypothetical relationship between shear stress and relative horizontal displacement for continuous and discrete sampling.

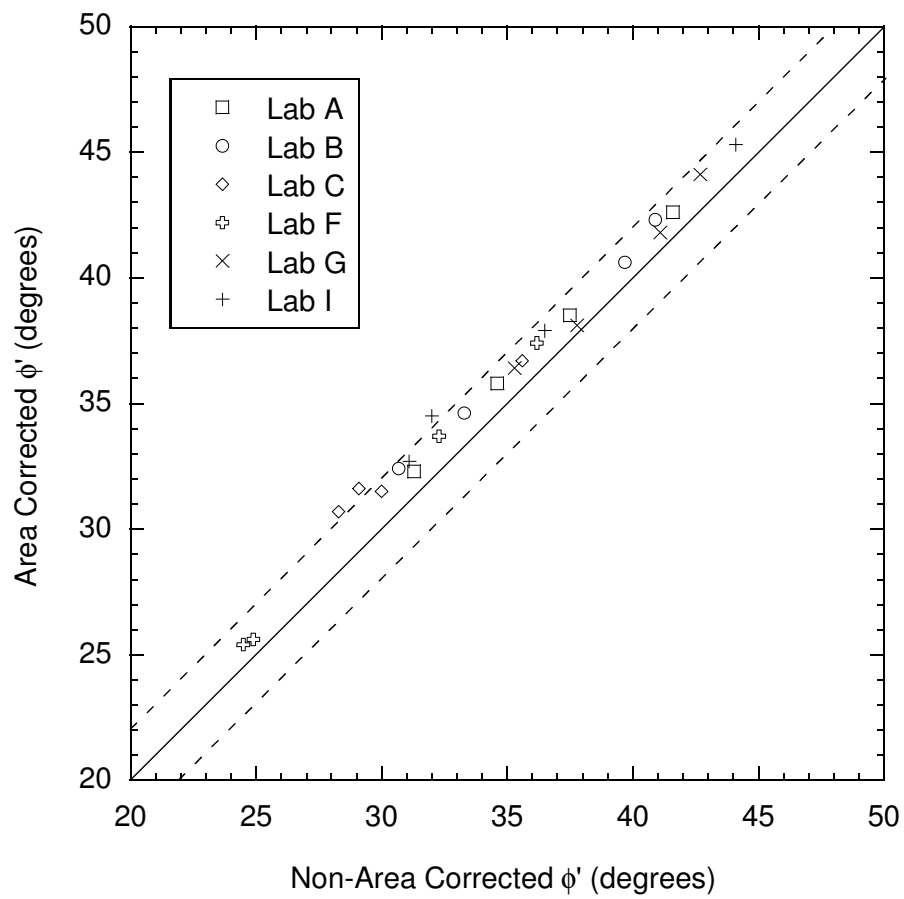


Fig. B-10. Comparison of friction angles from inter-laboratory direct shear tests with and without area correction.